Low Frequency Finite Element Modeling of Passive Noise Attenuation in Ear Defenders

By

Aamir Anwar

Thesis submitted to the Faculty of the
Virginia Polytechnic Institute and State University
in partial fulfillment of the requirements for the degree of
Masters of Science
In
Mechanical Engineering

APPROVED:

_____	_____
Robert L. West, Advisor	William R. Saunders, Committee Member

_____
Kenji Homma, Committee Member

January 12, 2005
Blacksburg, Virginia

Keywords: Ear Defenders, Noise Attenuation, Acoustics, FEA

Low Frequency Finite Element Modeling of Passive Noise Attenuation in Ear Defenders

Aamir Anwar

(ABSTRACT)

Noise levels in areas adjacent to high performance jets have increased monotonically in the past few years. When personnel are exposed to such high noise fields, the need for better hearing protection is inevitable. Adequate hearing protection may be achieved through the use of circumaural ear defenders, earplugs or both.

This thesis focuses on identifying the dominant physical phenomena, responsible for the low frequency (0 – 300 Hz) acoustic response inside the earmuffs. A large volume earcup is used with the undercut seal for the study. The significance of this research is the use of finite element methods in the area of hearing protection design. The objectives of this research are to identify the dominant physical phenomena responsible for the loss of hearing protection in the lower frequency range, and develop FE models to analyze the effects of structural and acoustic modes on the acoustic pressure response inside the earcup.

It is found that there are two phenomena, which are primarily responsible for the lower frequency acoustic response inside the earmuffs. These modes are recognized in this thesis as the piston mode and the Helmholtz mode. The piston mode occurs due to the dynamics of the earcup and seal at 150 Hz, which results in loss of hearing protection. The Helmholtz mode occurs due to the presence of leaks. The resonant frequency of the Helmholtz mode and the pressure response depends on the leak size.

Acknowledgments

I would like to express my deepest gratitude to my academic and research advisor Professor Robert L. West for his guidance and constant support in helping me to conduct and complete this work. I would also like to thank Professor William R. Saunders for his constant encouragement and expertise. In addition, I want to thank Dr. Kenji Homma of Adaptive Technologies Inc. for his efforts in conducting experiment tests and providing experimental data for use in this research and also for serving on my advisory committee. I am indebted to the Adaptive Technologies Inc. and United States Navy for funding this work and for providing research facilities.

Many thanks to all the people I have come to know in Virginia Tech and Blacksburg, whose friendship and companionship I will always enjoy. I owe my sincere appreciation to my family and relatives who have supported and encouraged me over the years. Finally, I want to extend my profound appreciation to my beloved parents for their love, affection, and invaluable support during my life and studies.

Table of Contents

List of Figures

List of Tables

CHAPTER 1
Introduction

1.1 General Overview and Statement of Need

Noise levels in the vicinity of high performance jet aircraft and modern weapon system have increased astronomically over the past few decades. As a result of increased engine power in recent jet aircraft, the noise levels in the surroundings of these jets have increased. These high noise levels have made it mandatory for personnel exposed to these noise levels to have adequate hearing protection. The hearing protection devices include earcups, earplugs or both. The use of either earcup or earplugs alone is called single hearing protection (SHP), when both are employed it's called double hearing protection (DHP). This research project is supported by the US Navy to provide state-of-the-art performance in single hearing protection and double hearing protection noise attenuating systems worn by aircraft crew and deck crew personnel. The research is conducted with collaborative efforts of Adaptive Technology Inc. and Virginia Tech.

1.2 Research Hypothesis and Goals

Through prior research literature and the experiments performed on the earcup/seal system, it is observed that there are four mechanisms that are primarily responsible for the poor performance of circumaural ear defenders. These mechanisms are:

1. Air leaks, which influence the attenuation in a broad frequency range.
2. Earcup vibration, which pumps air trapped with in the earcup into the ear canal.
3. Sound penetration of the earcup and the cushion that limits sound attenuation at frequencies above 1000 Hz.

4. Bone and tissue conduction into the outer, middle and inner ear, which limit's the sound attenuation at frequencies above 1500 Hz.

It is believed that two of these four mechanisms, air leaks and earcup vibration, are responsible for the modes that occur at frequencies below 1000 Hz. These modes are recognized in this thesis as the *Helmholtz mode* and the *Seal Piston mode.*

1.2.1 Helmholtz Mode

Due to the presence of leaks, between the earcup seal and the head, the earcup is believed to behave as a Helmholtz resonator at lower frequencies. When a slug of air present in the leak is excited by an ambient pressure source, it starts to vibrate between the inner fluid volume of the earcup and the ambient air, causing a volume change. If an ideal gas is assumed, the volume change is proportional to the pressure change in the ear cup. The volume change can be enough to cause amplification of noise within the earcup above the ambient pressure.

1.2.2 Seal Piston Mode

The seal piston mode occurs when the ambient noise field excites the earcup, such that it starts to vibrate like a piston against the earcup seal. In this case the cup acts as a rigid mass and the seal as a spring. The compression of the earcup against the seal causes a change in the inner fluid volume and thus causing pressure amplification.

1.2.3 Goals

The overall goal of the research program is to investigate the dominant physical phenomena, which are responsible for the loss of hearing protection of both SHP and DHP at low, mid and high frequency range. However, this thesis is focused on modeling and exploring the effects of low frequency modes (0 Hz -300 Hz) on the attenuation of the earmuffs. For this purpose, a large volume earcup with undercut seals will be employed in this research. Isolated study of each physical phenomenon will be performed and the effects of different parameters on the attenuation will be explored. The coupling between the fluid and structure enlightens the fact that the fluid and structure modes have

an impact on each other. Therefore, a coupled fluid-structure analysis will also be performed.

1.3 Concept For Solution

In order to achieve the desired goals of this research it is necessary to investigate the phenomena responsible for the poor performance of the circumaural ear defenders at low frequency range i.e. 0 Hz – 300 Hz. The two dominant low frequency physical phenomena are, the seal piston mode and the Helmholtz mode, modeling of these phenomena will be critical for this study.

A careful observation of these modes has lead to the conclusion that these two modes can be modeled as a single degree of freedom (SDOF) mass spring damper systems. For the case of seal piston mode, the earcup acts like a rigid mass vibrating axially on a soft spring (seal) of stiffness 'k' and damping 'c'. For the case of the Helmholtz mode the mass of the air present in the leak acts like a rigid mass, the air trapped inside the earcup provides stiffness and the damping is provided by the thermo-viscous losses and the radiation losses. The equation of motion for the seal piston mode and the Helmholtz mode can be written as,

$$m\ddot{x} + c\dot{x} + kx = F_o \tag{1.1}$$

Equation 1.1 can be used to derive the acoustic pressure response of the earcup/seal system in the lower frequency. The criterion selected to analyze the performance of the earcup is the acoustic pressure ratio P_i / P_o, where P_i is the internal acoustic pressure of the earcup and P_o is the reference acoustic pressure at the external surface of the earcup/seal system. The pressure ratio P_i / P_o, provides normalized amplitude of pressure response inside the earcup.

Although the analytical models provide a good approximation for the pressure response inside the earcup, these formulations are based on a single degree of freedom system with lumped mass assumptions. The actual earcup/seal system is a multi degree-of-freedom system with mass distributed over the volume of the earcup and the seal. It is therefore necessary to adopt a modeling and analysis tool, which better represents the physics involved in the analysis of the earcup.

Introduction of finite element modeling methods in the area of personal hearing defender design is the most significant innovation offered by this research program. The Finite Element Method has long been considered as a powerful tool for solving structural problems, acoustic problems and coupled acoustic structure problems. The evidence of FE formulations for acoustic and coupled acoustic structure problem can be found in research conducted over the past 30 years, [15, 16, and 17]. The commercial FE software programs are well equipped to perform the required analysis. The FE analysis requires that the geometry of the part be imported into or created in the FE software environment. Associated material properties are defined in the FE software program. The geometry is meshed by appropriate elements to represent the spatial domain. The boundary conditions and loads are applied on the meshed model before performing an analysis.

ABAQUS possesses very sophisticated material modeling capabilities, which are required for defining the material properties for the viscoelastic seal material. Also, it is quite versatile in its acoustic modeling capabilities. Several baseline studies are performed to verify the capabilities of the commercial FE codes and the results are correlated with the analytical results. Therefore ABAQUS was selected as the FE software of choice.

1.4 Objective of Research

An objective of this thesis is to determine the low frequency acoustic pressure response of the earcup/seal system for the purpose of identifying and examining the dominant modes, which are responsible for the poor performance of the SHP over the low frequency range (0 Hz - 300 Hz). The analysis of the earcup/seal system requires the structural and acoustics FE modeling of earcup/seal system in order to perform structural vibration analysis, acoustic leak analysis and the coupled fluid-structure analysis. The following steps are needed to achieve the desired thesis goal:

Structural Vibration Analysis

1. Import the geometry of the earcup/seal system into the FE software environment.
2. Modify the geometry to make it suitable for the FE modeling.
3. Acquire the material properties data associated with the earcup/seal system.
4. Create the FE model for structural analysis, which, includes static load analysis and structure vibration analysis i.e. mesh the geometry with appropriate elements and specify loads and boundary conditions.
5. Perform a static load analysis to predict the deflection due to headband force.
6. Perform the modal analysis to predict the vibration modes of the earcup/seal system.

Acoustic Leak Analysis

1. Create geometry of acoustic leak FE model.
2. Estimate and represent the damping associated with the Helmholtz resonator mode.
3. Create the FE model to perform acoustic leak analysis, i.e. mesh the geometry with appropriate acoustic elements and specify acoustic source and boundary conditions).
4. Perform the frequency response analysis to predict the acoustic pressure response inside the earcup due to an external harmonic pressure source.
5. Validate the FE results with the experimental and analytical results.
6. Perform the sensitivity analysis by changing the size of the leak.

Fluid-Structure Coupled Analysis

1. Create geometry for the fluid-structure coupled FE model.
2. Specify material properties associated with the earcup/seal system and air into the FE software.
3. Create the FE model to perform coupled fluid-structure analysis i.e. mesh the geometry and specify acoustics and structural loads and boundary conditions.

4. Perform the frequency response analysis to predict the acoustic pressure response inside the earcup due to an external harmonic pressure source.
5. Validate the FE results with the experimental and analytical results.
6. Perform the sensitivity analysis by changing the size of the leak.

These steps not only determine the acoustic pressure response inside the earcup but also help in studying and isolating the effects of the structural mode (seal piston mode) and the acoustic mode (Helmholtz mode) on the low frequency performance of the circumaural ear defenders. The fluid-structure coupled analysis determines the pressure response when coupling occurs between Helmholtz mode and the seal piston mode. Sensitivity analysis for different leak sizes determines the effects of leak size on the acoustic pressure response inside the earcup. In essence the steps taken in this research satisfies the desired goals of this thesis.

1.5 Scope of Thesis

This thesis is focused on the FE modeling of the large volume ear defenders for purpose of identifying and exploring the dominant physical phenomena, which are responsible for poor low frequency attenuation. The dominant modeling issues related to FE modeling of these phenomena are resolved. The material properties associated with the earcup/seal system are acquired. The damping associated with the seal piston mode and Helmholtz mode is estimated and modeled. The FE models are created and boundary conditions are specified to represent the physics involved in these two phenomena. The FE analysis is performed to obtain the acoustic pressure response inside the earcup/seal system. In order to determine the effect of leak size on the acoustic pressure response inside the earcup a sensitivity analysis is performed by employing leaks of various sizes. The earcup elastic modes and internal acoustic modes are extracted to determine their influence on the low frequency acoustic response.

1.6 Thesis Outline

This thesis consists of eight chapters including necessary background, research hypothesis and goals, concept for solution, objectives and scope of thesis in Chapter 1. Chapter 2 provides some related information and previous research done by other researchers in the same area. It includes a review of the methods adopted by other researchers to explore the attenuations limits of the earmuffs. The geometry of the earcup seal system is presented in Chapter 3. The FE modeling issues, related to the structural analysis of the earcup seal system, are discussed in Chapter 4. It also includes the development of the FE model. Chapter 5 covers the issues related to the acoustic modeling involve in the leak analysis, it also includes the development of the acoustic leak model. The FE modeling issues and the model development of coupled acoustic structure model are discussed in chapter 6. Chapter 7 includes the results from the FE analysis performed on the earcup seal system. Chapter 8 covers the summary of this thesis, the conclusion of the thesis and recommendations for future work.

Chapter 2
Literature Review

In the past fifty years researchers have explored noise attenuating characteristics of hearing protection devices and the threshold limits of hearing protection. This review will evince the fact that there is no recent literature that has been published that documents the role of certain acoustic phenomena, which impact the performance of the hearing protections devices (HPDs). Instead there is ample data describing measured performance of several HPDs.

Von Gierke and Warren (1953) [4] investigated the maximum hearing protection that can be achieved by circumaural ear defenders. The purpose of their study was to provide hearing protection developers a reliable benchmark that defines the maximum levels of protection achievable for humans exposed to noise. Their prediction was based on bone conduction thresholds derived from direct stimulation of forehead via "sound tubes", but they did not conduct the measurement with the entire body or head irradiated in a sound field. The concept of bone conduction limits implies that sound is transmitted via bony structures in the head that by-pass the normal mechanism for transmission of sound through the ear canal. Von Gierke states that hearing protection only accounted for 12 dB of noise attenuation. The conclusion of the paper was that at frequencies below 500 Hz, the maximum attenuation that could be achieved by hearing protection devices was 28 dB. Above this frequency, the best attenuation would be between 40 and 50 dB. The poor attenuation at low frequencies was attributed to the mechanical vibration of the earcup.

Zwislocki (1957) [6] performed direct measurement of bone conduction thresholds in a free sound field; he provided values that have indeed withstood the test of time. In his experiments, he measured REAT (real ear attenuation at threshold) in a free sound field on a group of six subjects wearing solid earplugs in combination with heavy circumaural ear defenders, three of those same subjects wearing only resonator earplugs

tuned to frequencies from 300 to 600 Hz, and one subjected to frequencies below 125 Hz. The bone conduction (BC) limits were determined for the resonator earplugs below 400 Hz, the better performance resonator earplugs or the dual combination from 400 to 1500 Hz, and the dual combination only above 1500Hz. The maximum attenuation was achieved for the uncovered head below 125 Hz is 52 dB; in the frequency range between 125-500Hz the attenuation is 68 dB. Due to the extreme measure employed by Zwislocki, with different types of earplugs used to acquire data at different frequencies and the type of seal he achieved in bony meatus, his data may indeed define the true BC limits with the uncovered head.

Shaw (1958) [5] was the only researcher to explore the physics of low frequency acoustic behavior of the ear defenders (earcup). He observed, "at frequencies below 1000 Hz sound reaches the ear through well fitting ear defender by setting the whole ear defender into vibration." He was the first author to develop an analogy between the earcup seal system and a spring mass damper system, he states that " If a mass-like ear defender supported by a spring like cushion and an alternating force is applied to the mass it will be set into vibration whose amplitude will depend upon frequency of the applied force." Shaw developed an analytical formula for transmission ratio as a function of frequency assuming the vibration of a spring mass system. In his paper he plotted the transmission ratio versus frequency for different values of damping, Figure 2.1.

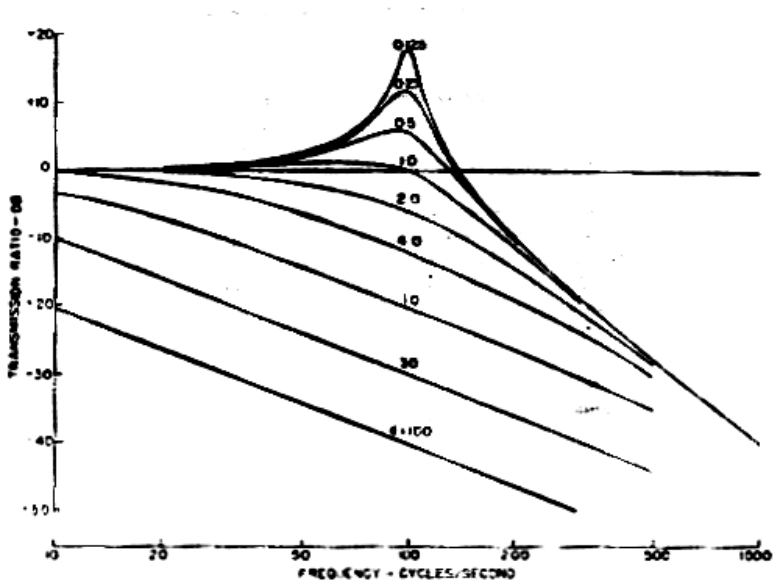

Figure 2.1 Vibration of a spring mass system as a function of frequency for different damping values. [5]

Shaw [5] then conducted his experiment on actual earmuffs having a liquid filled cushion; he obtained transmission ratios for different values of the spring constant of the cushion by changing the temperature, Figure 2.2. It is to be noted that the experimental results are similar to the results obtained by the analytical model for the vibration of spring mass system.

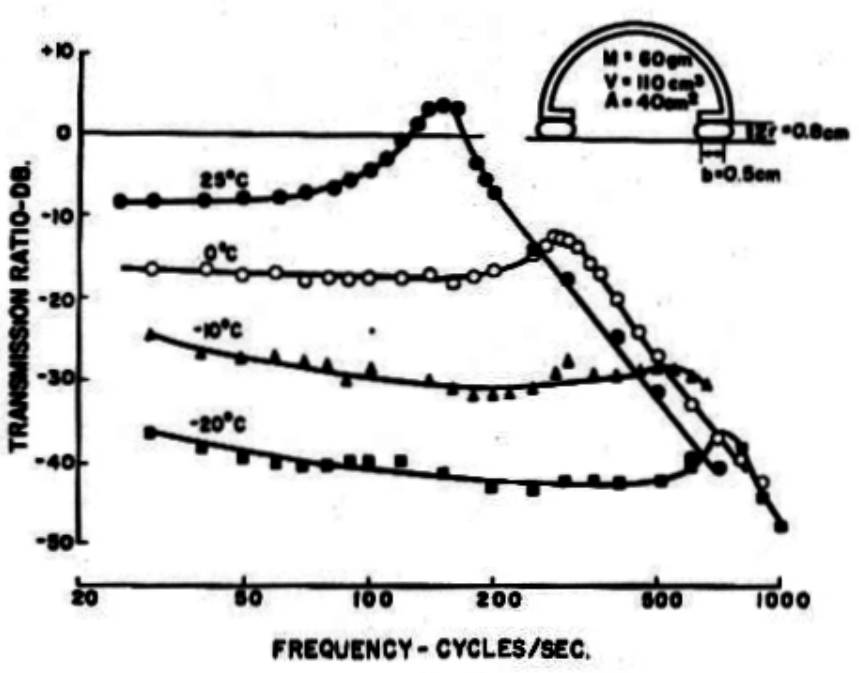

Figure 2.2 Transmission ratio of sound through ear defender for different values of the spring constant of the cushion. [5]

He also pointed out that the volume of the cup and the spring constant of the cushion including the flesh, controls the attenuation of the earcup at lower frequencies. He suggested that the vibration of the ear defenders could be minimized by means of a cushion, which uses a high Young's modulus sheath to contain high bulk modulus filler, Figure 2.3.

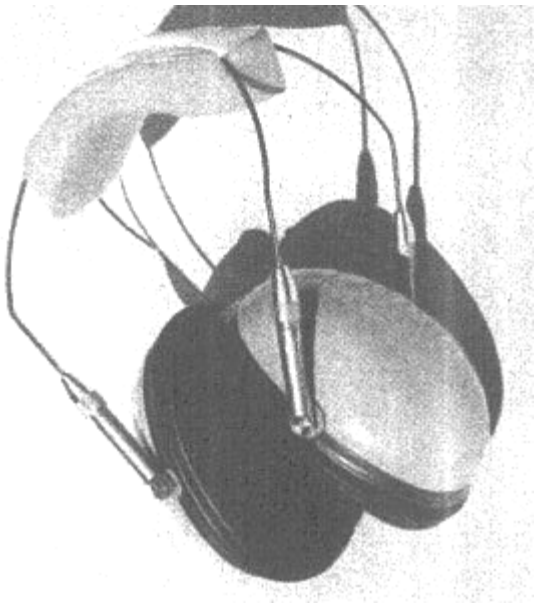

Figure 2.3 Ear defender having liquid filled cushions. [5]

By analyzing various seals (cushions) of different damping values he noticed that for reasonably low damping values there are two regions, a lower frequency region and a higher frequency region where the damping has insignificant effects, called the stiffness controlled region and the mass controlled region respectively. In the stiffness controlled region the vibration is independent of frequency and depends on the spring constant of the cushion. In the mass controlled region the vibration decrease by 12 dB per octave increase in frequency. Shaw concluded, "A suitably designed ear defender can easily provide 20 dB attenuation at 50 cps" [5].

Thiessen (1962) [7] realized that considerable attention is given to the acoustical behavior of large volume circumaural ear defenders, which is obvious from several publications on that subject. However, there were very limited publications on specific problems that arise when an electro-acoustic transducer is added into such a device. The development of louder weapon systems, more powerful aircraft jet engines and military communication have made it necessary to develop a combined circumaural ear defender and ear phone.

Theissen noticed, "When an electro-acoustic transducer is added to a circumaural ear defender the requirements of minimum sound transmission and maximum earphone sensitivity are partially incompatible." An ideal circumaural earphone would provide

maximum attenuation of extraneous noise and optimum coupling between transducer and ear. He investigated the transmission and response of simple (single cavity) and compound (two cavity) systems, Figure 2.4, and concluded "a preferred system is a rigid structure with resistive coupling between the two cavities. This system has maximum effective coupling volume at low frequencies thus providing maximum noise attenuation and a smaller effective volume at high frequencies affording increased earphone response."

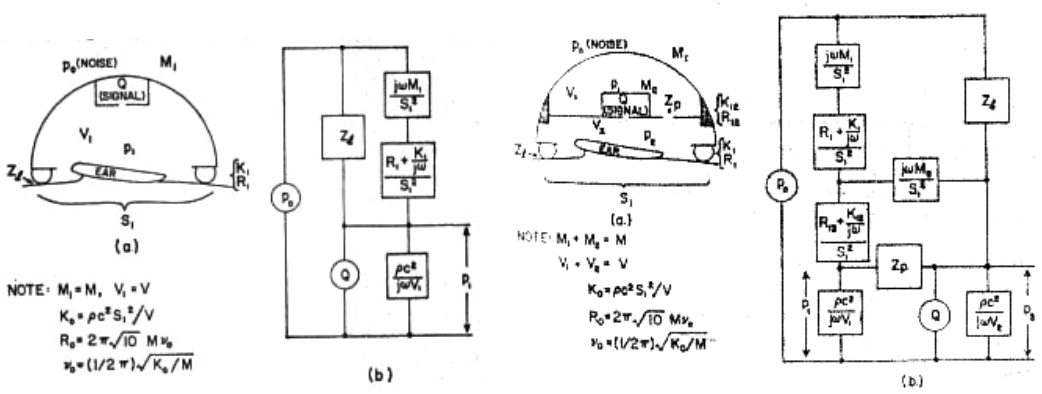

Figure 2.4. Single cavity and double cavity cushioned circumaural earphone and corresponding acoustic impedance network. [7]

Theissen also concluded that the dual cavity earcup has a constant response over a large frequency range. His theory is supported by measurements on an experimental earphone having a transducer and cavity characteristics.

Berger (1983) [8] explored various combinations of HPDs in detail and provided suggestions for the selection of each of the devices to be used in a dual protection scenario. He investigated REAT values for three earplugs and three circumaural ear defenders, which were employed both singly and in various combinations according to ANSI S3.19-1974. He used commercially available earplugs, which also include the 19 mm E·A·R® Classic® plug that was inserted partially (PI 15%-20%) of the plug in ear canal, to a standard depth (SI; about 50%-60% in the ear canal) and deeply inserted (DI; about 80%-100% in the ear canal), Figure 2.5.

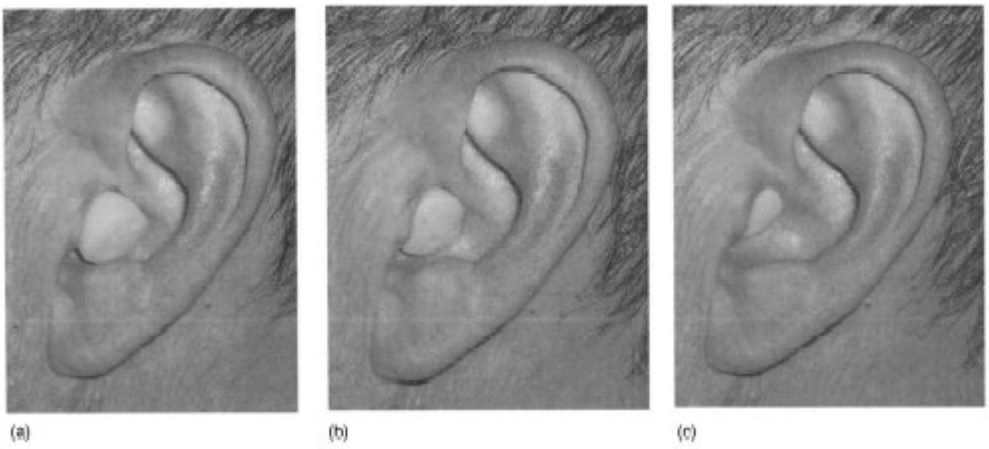

Figure 2.5 Partial (PI), standard (SI) and deep (DI) insertion of a Classic foam earplug in one subject's ear canal. [12]

Berger observed that below 1 kHz various combinations of earplugs and circumaural ear defenders provide different values of attenuation. At and above 2 kHz all combinations provide the same level of protection. He also observed that the combined protection of a circumaural ear defenders and a plug always exceed either of the individual devices at all test frequencies.

Goff (1984) [9] was interested in testing hearing protection devices for the mining industry. Personnel working in the mining industry are exposed to high ambient noise for extended periods of time. Goff performed his experiments by setting up circumaural ear defenders on several workers to test the actual noise attenuation seen in the field. He placed two microphones on each of the test subjects; one next to the ear canal, and the other on the corresponding shoulder. Time data of the microphones was then recorded on a dual track tape recorder for an extended period of time. Goff observed that better attenuation was achieved at frequency 2000 Hz and above. He also pointed out that the actual noise attenuation seen in the field was lower than predicted by NIOSH and ANSI. Goff also observed an amplification of noise between 80 and 315 Hz.

Pääkkönen (1992) [10] performed a comprehensive study to assess the effect of the cup, cushion, foam lining and headband of earmuffs on noise attenuation. In his view the noise attenuation of hearing protectors are determined not only by type of circumaural ear defenders material and by human parameters, but also by physical laws and limitations. He pointed out that sound penetrates the hearing protection devices through

four mechanisms which include, (1) air leaks (2) earcup vibration (3) sound penetration of the earcup (4) bone and tissue conduction into the outer. Pääkkönen conducted his study with a miniature microphone method in an anechoic chamber, in a low frequency chamber and with an acoustic tunnel.

He observed that "changes in cup foam lining improved attenuation as much as 10 dB, and changes in the cushion or in the dynamic stiffness and damping characteristics of the cushion improved attenuation as much as 4 dB. These changes affected the attenuation in the frequency range over 1000 Hz. However, the changes in the cup volume or the tight setting between the skin and the cushion were most effective below 1000 Hz. The spring force effect was seen at frequencies over 3000 Hz and under 250 Hz." He also analyzed the effects of defects in the earmuffs and found out that breaks in the cushion or holes in the cup deteriorated the attenuation up to 30 dB, whereas a 5mm leak between the cushion and the skin deteriorated attenuation less than 10 dB.

IMPROVEMENTS AND DETERIORATIONS IN THE ATTENUATION OF EARMUFFS IN THE EXPERIMENTS

Measures	Improvement		Deterioration		Experiment Number
	Attenuation dB	Frequency Hz	Attenuation dB	Frequency Hz	
Cup					
—Volume	3-15	63-1000	0-10	2000-6300	E1
—Mass Increase	<4	250-4000	<4	<125	E4
—Lifting Plate	3-14	125-1000	0-4	>2000	E3
Foam Lining	3-12	>1000	-		E5
Headband Force	<12	<250	<10	>3200	E7
Cushion Foam	<4		<4		E8
Vaseline between Skin and Cushion	<3	<1000	<2	>1000	E9

Figure 2.6 Summary of results obtained with various configurations for the experiments. [10]

Pääkkönen summarized his observations in a table, Figure 2.6, and concluded, " a tight setting between the skin and the cushion, an increase in spring force of the headband and the cushion, and an increase in absorption inside the cup improved the noise attenuation of the earmuffs."

Rimmer (1997) [11] proposed a new measure for hearing protection device (HPD) attenuation called BCLB (Bone Conduction Loudness Balance). Through this method Rimmer was able to measure attenuation in a 0-dB environment. He used pure tones and noise bands. He used a third octave noise band centered at 2000 Hz in order to nullify

the effect of bone conduction at the lower frequencies. It was his contention that bone conduction has the largest effects at lower frequencies and it may be a limiting factor in the low frequency attenuation of HPDs. Rimmer also mentioned that HPDs are less effective below 2000 Hz. Rimmer's results showed a 0-4 dB difference between REAT testing and his new method, BCLB.

Gauger (2003) [12] realized that military personnel are exposed to steady noise levels approaching and sometimes exceeding 150 dB and that the need for maximum hearing protection is obvious. He performed a comprehensive study and experiments to explore the limits of hearing protection and whether it can be achieved with existing technology. He used conventional hearing protection devices and compared REAT results with the experiments performed by several researchers in the past as shown in Figure 2.7.

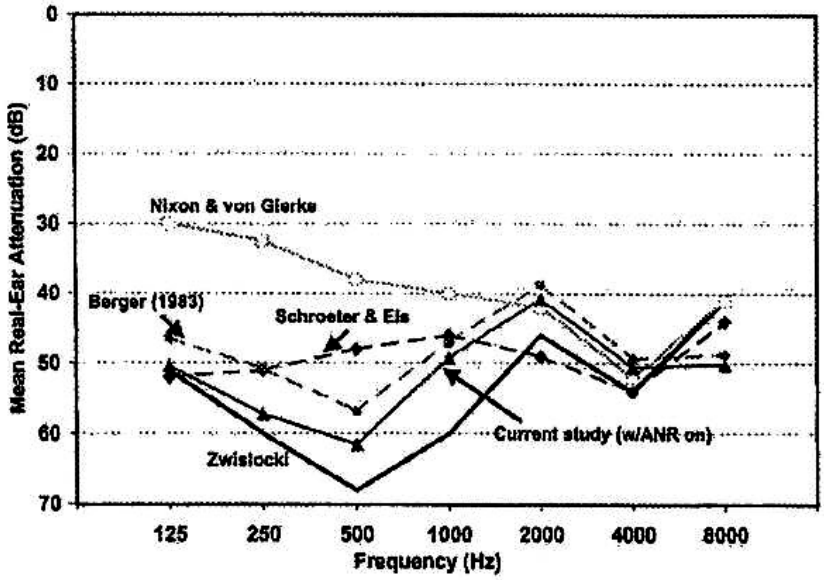

Figure 2.7 Various estimates of the BC limits to REAT attenuation with head exposed, from Gauger's study and prior literature. [12]

Gauger employed procedures similar to those used by Berger in 1983. His test method conformed to Method A of ANSI S12.6-1997. All REAT measurements were conducted in the E·A·RCAL^{SM} acoustical laboratory of Aearo company. An important feature of his experiment was the use of 24 mm long E·A·R® Classics® Plus earplug (a longer version of 19 mm classic foam ear plug) in conjunction with conventional ANR

(Active Noise Reduction) circumaural earmuffs (made by Bose) and Gentex lightweight fighter/attack aircrew helmet (HGU-55/P), Figure 2.8.

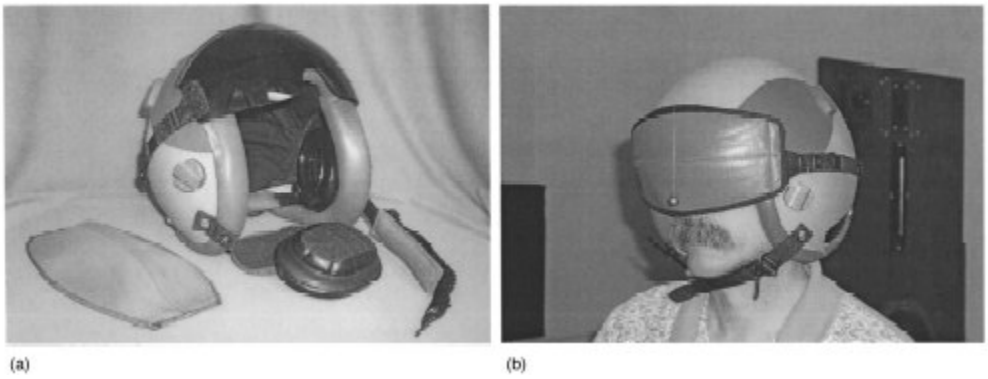

Figure 2.8 Gentex HGU-55/P flight helmet. [12]

The test signals were obtained in 1/3-octave-bands of noise spanning the range from 125 Hz to 8 kHz. Gauger observed that the attenuation values for the single HPDs increases by 2 to 4 dB with use of Classic Plus earplugs. He also observed that the flight helmet data are similar to earmuff attenuation values up through about 1 kHz, but quite different from circumaural ear defenders in the high frequency range. This is because at high frequencies, the important BC pathway has been shown to be direct transmission to the cochlea bypassing the external canal. For the case of double hearing protection, Gauger observed that the dual protection data for ANR circumaural ear defenders demonstrate values that are equal or greater than Berger's prior estimate obtained by using a lead circumaural ear defender. This is due to the fact that the earplug is an extremely important component of the dual protection system. He also observed that the DI (deep inserted) ear plug used in his study exceeds the performance of the one employed by Berger in 1983. Gauger concluded from his study that for an uncovered head, switching from single to dual hearing protection could only achieve modest gains of about 6 dB at and above 1 kHz before reaching the BC limits. However, at low frequencies gains of 10 to 15 dB are observed. He also noticed that by using the tight-fitting flight helmet with a face plate (visor) additional gains of 4 to 11 dB are possible from 1 kHz and above. The maximum attenuation achieved by dual hearing protection is 50 to 60 dB at frequencies below 1 kHz and 40 to 50 dB at frequency above 1 kHz.

Birch (2003) [13] examined the effectiveness of hearing protectors in a high amplitude impulse noise field. He designed an acoustic test fixture for the evaluation of hearing protection devices in this kind of sound field. The acoustic test fixture, referred to as ATF, consisted of a high-pressure generator, and a long tube. The system was capable of producing noise levels as high as 160 dB SPL. Birch concluded that the ATF could be used to measure HPD attenuation up to 45 dB. There was little testing conducted on the attenuation of the HPD.

In 2004, ASA work group S12/WG11 conducted experiments to develop laboratory and field procedures that yield useful estimates of hearing protection devices (HPDs) [12]. The REAT procedure was selected and tests were conducted for one earmuff and three earplugs via interlaboratory study involving five laboratories and 147 subjects. The workgroup examined the REAT distribution as a function of protector, fitting procedure and test frequency. Methodologies employed in the test were experimenter-fit, informed-user-fit, and subject-fit. It was found that the subject-fit method produced the most consistent results between the labs. Through this research, mathematical relations were derived to determine the minimum detectable difference between attenuation measurements and to determine the minimum number of test subjects to achieve that level of precision. "For a precision of 6 dB, the study found that the minimum number of subjects was 4 for the Bilsom UF-1 earmuff, 10 for the E·A·R® Classics® earplug, 31 for the Willson EP100 earplug, and 22 for the PlasMed V-51R earplug."

Summary

This literature review has adequately covered the research work that has been conducted with regard to circumaural ear defenders noise attenuation. The first ever published study of the earcup was in 1953 by Von Gierke, since then a number of scientists have conducted research that focused on modeling the cup dynamics, field testing of earmuffs, finding limits of attenuation and determining standard protocols for testing hearing protection devices. However, it is important to realize that Shaw was the only researcher to explore the theoretical acoustic behavior of earcup defenders i.e. modeling the dynamics of the earcup. All other researchers were interested in exploring the performance of several hearing protection devices (HPDs).

It is learned from the literature review that sound that there are four mechanisms that are primarily responsible for the poor performance of circumaural ear defenders. These mechanisms are:

1. Air leaks, which influence the attenuation below 1000 Hz.
2. Earcup vibration below 1000 Hz, which, pumps air trapped with in the earcup into the ear canal.
3. Sound penetration of the earcup and the cushion that limits sound attenuation at frequencies above 1000 Hz.
4. Bone and tissue conduction into the outer, middle and inner ear, which limit's the sound attenuation at frequencies above 1500 Hz.

The past research has played an important role in identifying the phenomena, which are responsible for the performance of the earcup in lower and mid frequency range. The lower frequency phenomena, air leaks and earcup vibration will be explored in this research.

CHAPTER 3
3D Modeling of the Earcup

Getting the correct geometry into the software is a fundamental step in performing finite element analysis. Once the modeling inputs are completed, analysis could be performed. Large volume circumaural ear defenders, Figure 3.1, consist of rigid earcup, soft gel seal and a stiff headband.

Figure 3.1 Large volume circumaural ear defenders

3.1 Geometry of Earcup/Seal System

The geometry used for FE modeling was obtained from the earcup supplier in IGES format. The symmetry of the earcup requires only earcup and seal to be employed in the FE model. Great efforts were made to make some modifications on the geometry, to make the given IGES CAD geometry more suitable for FE modeling; the details of the modifications will be covered in the next chapter. ANSYS modeling capabilities were

utilized to modify the geometry. The original earcup geometry and the modified ear cup geometry are shown in the Figure 3.2(a & b) respectively.

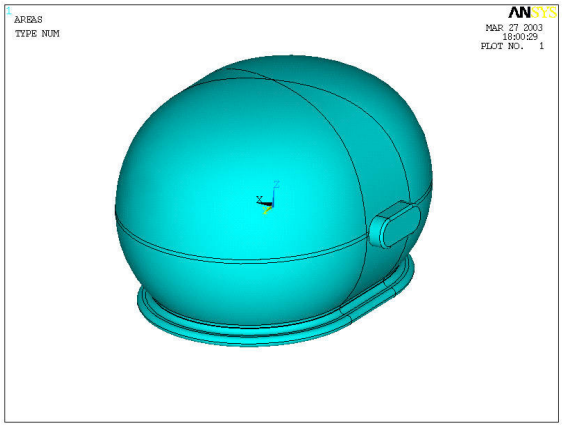

Figure 3.2 (a) Orignal earcup geometry

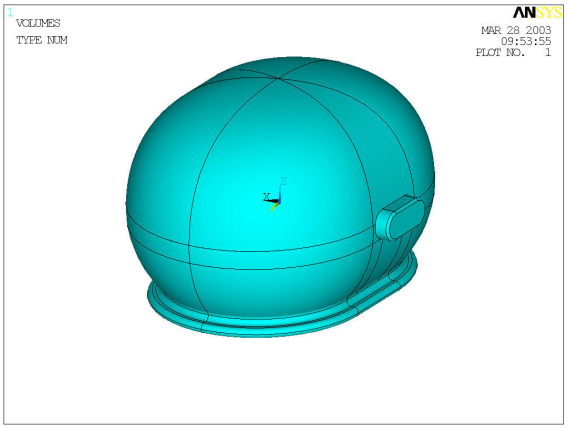

Figure 3.2 (b) Modified earcup geometry

The earcup seal was modeled by measuring the actual dimensions from the original soft gel undercut seal. Figure 3.3 shows the 3-D model for the viscoelastic foam-gel seal.

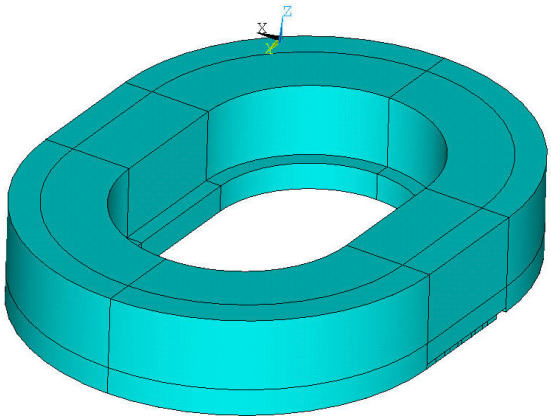

Figure 3.3 Geometry of foam-gel seal

3.2 ABAQUS Geometry

The geometry of the earcup/seal system must be imported into the ABAQUS environment to perform the FE analysis. It was quite a difficult task to get the geometry of the earcup into the ABAQUS environment. The earcup IGES file does not provide enough information for ABAQUS to import the earcup as a single entity. The lugs and the stiffeners inside the earcup had to be separated from the earcup and be imported into ABAQUS environment as separate entities. Figure 3.4 shows the geometry of the earcup/seal system after it has been modified and imported into ABAQUS.

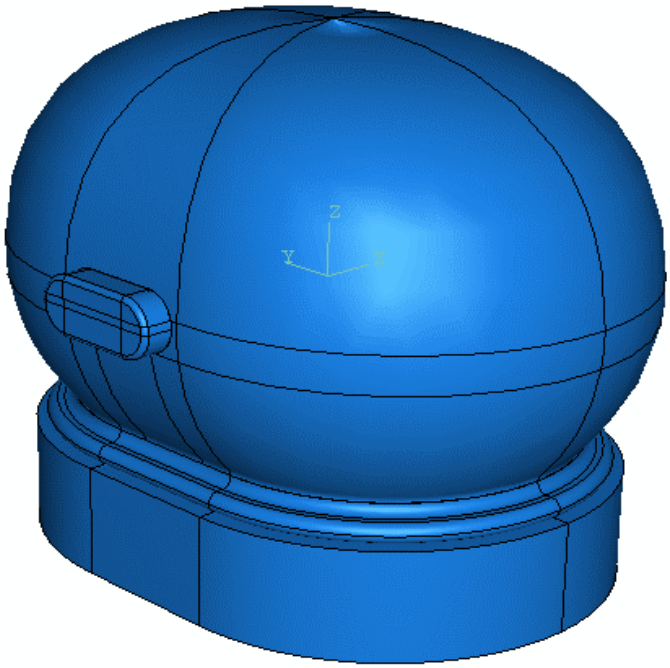

Figure 3.4 3D solid model of earcup/seal system in ABAQUS

3.3 Dimensions of the Earcup/Seal System

The overall dimensions of the large volume earcup are shown in Figure 3.5. Important overall geometric factors of the earcup are listed in Table 3.1.

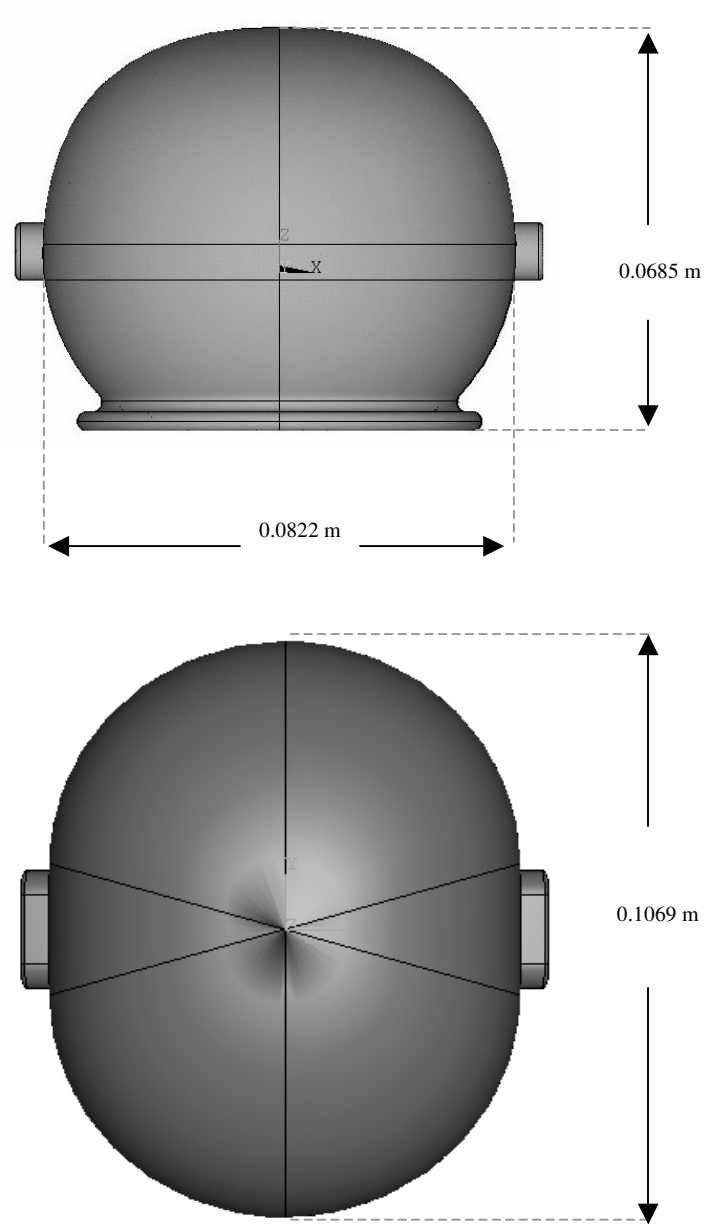

Figure 3.5 Dimensions of the Earcup

Table 3.1 Important overall Geometric Properties of the Earcup

Volume of the earcup	8.577e-5 m^3
Inner volume of the earcup	3.098e-4 m^3
Outer Surface area of the earcup	0.0245 m^2
Inner Surface area of the earcup	0.0206 m^2

The overall dimensions of the soft gel undercut seal are shown in Figure 3.6, important geometric properties of the seal are listed in Table 3.2

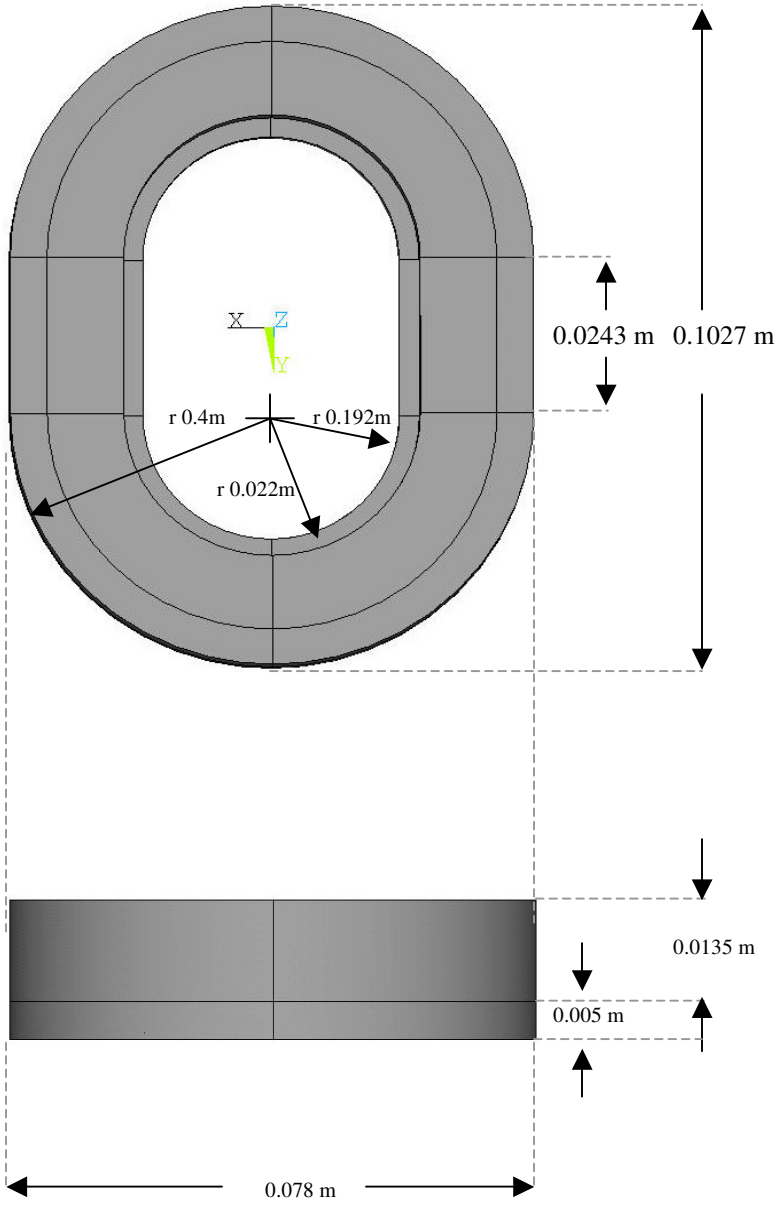

Figure 3.6 Dimensions of the viscoelastic gel seal.

Table 3.2 Important overall Geometric Properties of the Seal

Area of Cross-section of the Seal	4.107 e-3 m^2
Volume of the Seal	7.823 m^3

CHAPTER 4
Earcup Structural Vibration Modeling

The finite element modeling research effort in this project has been focused on developing models of the large volume earcup/seal system for the purpose of identifying the dominant mechanisms responsible for the acoustic response inside the earcup. The large volume earcup is made from polycarbonate material. The soft gel undercut seal is comprised of an open-celled foam and a gel enclosed in a vinyl membrane. The composition of the seal provides for comfort through compliance or low stiffness, which results in several low frequency modes. Since the earcup is directly attached to the seal, it also moves as the seal vibrates. The motion of the earcup excites the adjacent fluid particle thus causing the acoustic response. Complete understanding of the different physical phenomena causing acoustic response inside the earcup requires the isolated study of each phenomenon. The FE modeling of the earcup/seal system involves structural modeling, acoustic modeling and coupled acoustic-structure modeling. This approach will not only help in isolating the structure and acoustic phenomena but will also help in understanding the coupled acoustic-structure interaction problem. This chapter is focused on the structural dynamics modeling of the earcup/seal system.

4. 1 Mechanical Vibration of the Cup

Through prior research on the circumaural ear defenders and the experiments performed on the earcup/seal system, it is known that regardless of the seal material and cup dimensions, there is a dominant low frequency structural mode referred to as the *piston mode*. The piston mode causes the earcup to act as a rigid body sitting on a soft spring, the seal. The rigid body motion of the cup on the seal pumps air directly into the human ear, which is responsible for the loss of hearing protection. The mechanical vibration of this mode can be represented by a spring mass damper system in which case

the cup acts like a rigid mass and the seal acts like a spring of stiffness "*k*" and damper with damping "*c*". Figure 4.1 compares the earcup/seal system with a spring mass damper system,

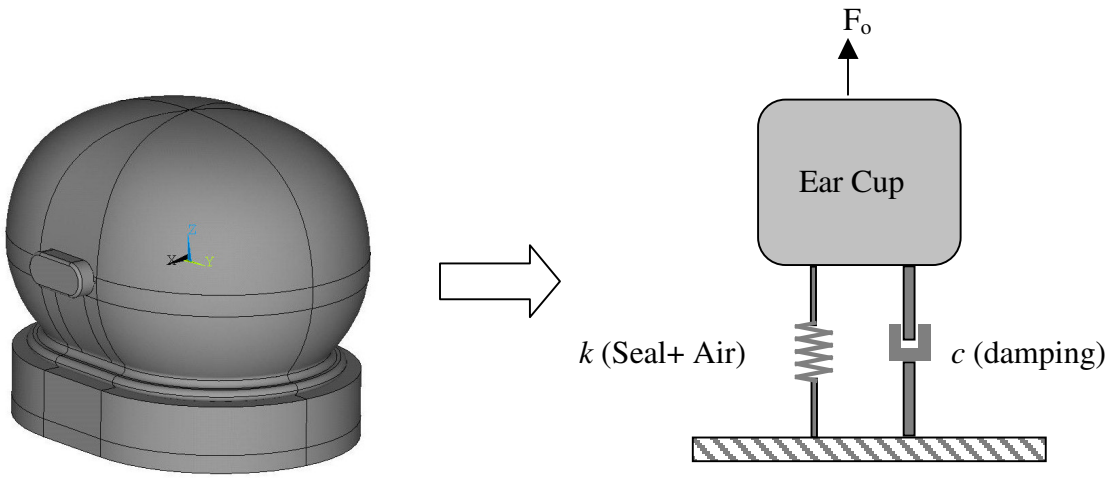

Figure 4.1 Earcup seal system is represented by a spring mass damper system.

It is important to realize that in an actual earcup seal system, some air is always trapped inside the earcup. This results in additional stiffness caused by the air spring. This stiffness is higher when the seal is perfectly fit to the head. If a leak is present, it allows some air to escape through it and hence reduces the stiffness of the air spring. However, this phase of the analysis will assume a perfect fit, i.e. the no leak case. The focus of FE modeling in this chapter will remain on the structural dynamics modeling. A free body diagram of an earcup/seal system is shown in Figure 4.2,

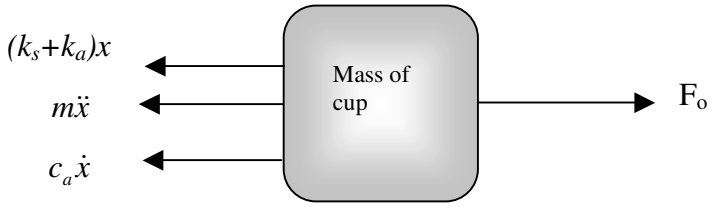

Figure 4.2 Free body diagram of earcup/seal system

The forces on the left side of the diagram are due to the stiffness of the seal, the stiffness of the air spring and the damping of the viscoelastic seal, while F_o is a function

of ambient pressure. The air spring and the seal spring are in parallel, therefore the relative stiffness are added. The equation of motion could be written as,

$$m\ddot{x} + c\dot{x} + (k_s + k_a)x + = F_o \qquad (N) \tag{4.1}$$

Where,

m = mass of the cup + the effective mass of the seal (kg)

c = damping of the seal (kg/s)

k_s = stiffness of seal (N/m)

k_a = stiffness of the air spring (N/m)

Hand Calculations for Piston Mode

For the given mass of the earcup and the seal and the stiffness of the seal and air spring, the natural frequency of the piston mode can be approximated using the equation,

$$\omega = \sqrt{\frac{k}{m}} \tag{4.2}$$

Where, ω is the natural frequency in rad/sec, m is the mass of the earcup plus the effective mass of the seal in kg and k is the stiffness of the seal plus the stiffness of the air spring.

mass of the earcup = 0.103 kg

mass of the seal = 0.046 kg

effective mass of the seal = 1/3(0.046) = 0.0153 kg

total mass = m = 0.103 + 1/3 * (0.046) = 0.1183 kg

stiffness of the seal @ 0 Hz = 1680 N/m

stiffness of the air spring = 7996 N/m

total stiffness = k = 1680 + 7996 = 9676 N/m

The estimate of the natural frequency of the earcup/seal system is,

$$\omega = \sqrt{\frac{9676}{0.118}} = 286.35 \; rad/\sec$$

$$f = 45 \; Hz$$

It is important to note that this natural frequency for the piston mode is estimated based on the value of seal stiffness at 0 Hz. The stiffness of viscoelastic seal material changes with frequency. For the case of the earcup/seal system the seal piston mode occurs in between 170 Hz to 230 Hz. However, this simple calculation provides a reasonable initial estimate for the occurrence of piston mode in the lower frequency range.

4.2 FE Modeling of Earcup/Seal System

The major concern on FE modeling of the both the structural and fluid models was model size and complexity. The time required to build, solve and interpret models of this complexity is significant. The models of the earcup/seal system were significantly large and complex. The addition of necessary model features, such as, viscoelastic material properties for the seal material resulted in longer solution times and significantly greater effort for model building. ANSYS, used as the first choice FE software, had some limitations regarding size of the model and defining viscoelastic material properties. Later on ABAQUS was used to overcome these limitations. Some of the limitations in structural vibration FE analysis are discussed in this chapter.

4.2.1 FE Modeling Issues

Model Complexity

Finite element modeling requires the meshing of part geometry with elements for solution. A very large effort was put into the earcup geometry to make it ready for meshing. Meshing 3-D parts with solid elements requires a great deal of "partitioning" of the CAD geometry definition. The smallest line of the geometry governs the size of the mesh. The original IGES earcup definition received from the supplier was reworked to remove small lines and define sub volumes so the earcup could be meshed. This was not enough; additional effort was put into the solid geometry to make it efficient for meshing. Meshing controls were placed on individual lines of the new "clean ear cup geometry" to control and produce a very effective meshing scheme for the earcup. This was significant at the initial stage of the project, being that the ANSYS Research license only allows for the use of 128,000 elements total. The effort paid off allowing the ANSYS meshing

algorithm to reduce the number of elements from over 128,000 (where the part could not be meshed at all) to 12,000 elements. Figure 4.3 (a & b) shows initially meshed model and the reduced meshed model of the earcup.

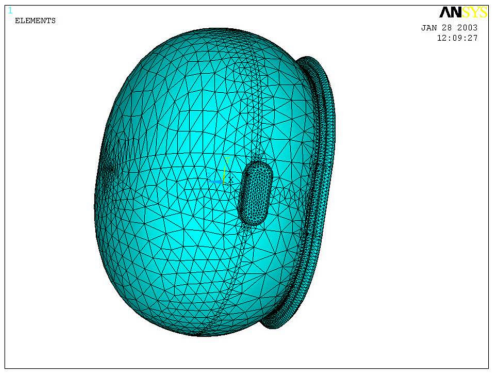

Figure 4.3 (a) Initial meshed model of the cup

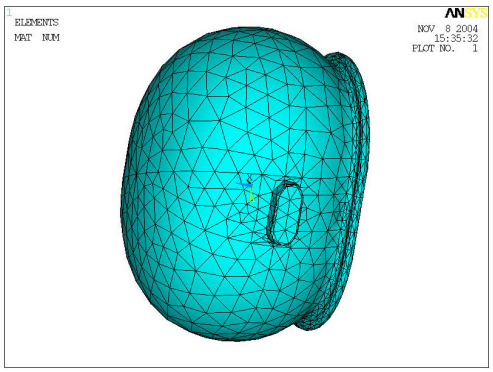

Figure 4.3 (b) Reduced meshed model.

Model Size

Because of complexity, and the approximate nature of the finite element method, the ear cup models required many nodes and elements to obtain a converged solution. This point is significant for the reason that models of this complexity require several hours for solution in addition to model preparation.

Natural Frequency Limitations

Primarily the limitation on the solutions for natural frequencies has to do with solution times required to extract the natural frequency and model shapes in the frequency range of interest. The "modal density" is relatively high for these models. Converging natural frequencies and mode shapes at the high end of the frequency range requires a greater number of nodes and elements for a given level of accuracy. Even though this study concentrated on lower frequencies associated with seal modes, getting accurate estimates of the earcup flap and shell modes was also important.

A second limitation on extracting natural frequencies and mode shapes of the earcup/seal vibration models had to do with the frequency dependent material properties of the viscoelastic seal. Standard large-scale eigen-solvers cannot include frequency dependent material properties or boundary conditions in the solution for natural frequencies. The frequency dependence of the stiffness matrix in the earcup model required the solution for natural frequencies to be broken down into several runs over a

small frequency range so that material properties of the seal could be represented as constant over the range of frequency extraction. While this approach results in reasonable estimates, the process is tedious and requires a great deal of time to extract the desired modes. Convergence of the resulting natural frequencies and mode shapes makes the process even more tedious and time consuming.

Frequency Response Limitations

Frequency resolution for the frequency response estimates is the principle limitation for the earcup/seal vibration models. The experimental frequency response estimates are regularly carried out at a frequency resolution of 1-2 Hz. The FE model size and complexity required a harmonic response solution time of 30-40 minutes per frequency on a top-end personal engineering workstation. Given the desired overall frequency range was 40 to 2000 Hz and a frequency resolution of 1-2 Hz, the solution time would have made solving the problem intractable. A modal superposition technique was also considered. However, modal superposition techniques require converged natural frequencies over the modal domain. Given the high modal density of the model, the harmonic frequency response was a much more practical approach. As a result, a frequency resolution of 5 Hz was used over a limited frequency range for the study. The frequency range used for the solutions was determined from experimental data and the extraction of natural frequencies. The time required to obtain converged solutions over the specified frequency ranges is problematic. This limitation really limits the study's ability to investigate the model at a frequency resolution comparable with the experimental data.

Viscoelastic Material Modeling

One of the most restrictive limitations at the initial stage of the project for the FE modeling had to do with ANSYS's inability to effectively handle the frequency domain solution of the viscoelastic seal material. ANSYS does not allow the viscoelastic material properties to be entered as a function of frequency. As a result a separate result file is generated for each frequency solution, making the result extraction process cumbersome and time consuming. Another issue that requires great attention is proper viscoelastic material characterization of the earcup seal. Experimental and FE results

indicate the frequency dependent nature of the seal stiffness plays a large role in the vibration and acoustic response of the earcup. Proper identification of acoustic mechanisms will require proper viscoelastic characterization of the seal.

4.2.2 FE Modeling

Great efforts were made to address the issues encountered in the FE model exploration. The software platform was replaced from ANSYS to ABAQUS standard. There are two very practical reasons for replacing the ANSYS FE code with the ABAQUS FE code. The first issue has to do with the implementation of frequency domain viscoelastic material modeling. ABAQUS naturally accommodates material properties as a function of frequency. These capabilities are effectively used within ABAQUS for harmonic frequency response. Secondly, larger models can be built and solved in ABAQUS than in ANSYS. The change to ABAQUS has enabled significantly more time for model exploration and acoustic mechanism identification.

3-D FE Model in ABAQUS

A hard fought effort was made to import the earcup geometry within the ABAQUS modeling environment in order to perform the FE analysis. The earcup geometry was divided into sub-volumes i.e. the flap, stiffeners and lugs, which are the part of the earcup, were separated out into sub-volumes. The sub-volumes of the earcup geometry are imported into ABAQUS and the adjacent surfaces were tied together by using the ABAQUS *TIE option. The creation of sub-volumes divides the complex geometry of the earcup into simplified smaller volumes, which are easy to mesh.

Meshing

Meshing is a very critical phase of a FE analysis. Mesh optimization is not only necessary for an accurate FE solution but is also important for a time efficient FE analysis. The geometry of the earcup has already been simplified to reduce the number of geometric features and hence of elements. The most critical areas to mesh were the stiffeners and lugs; this is due to the presence of small lines. Meshing controls are placed on individual lines to produce an effective mesh. The most efficient mesh is obtained by 3-D solid brick elements but the geometry of the earcup only allows the earcup to be

meshed with 3-D solid quadratic tetrahedrons. The earcup and seal system was meshed by 12,000 such elements. The 3-D meshed model is shown in Figure 4.4.

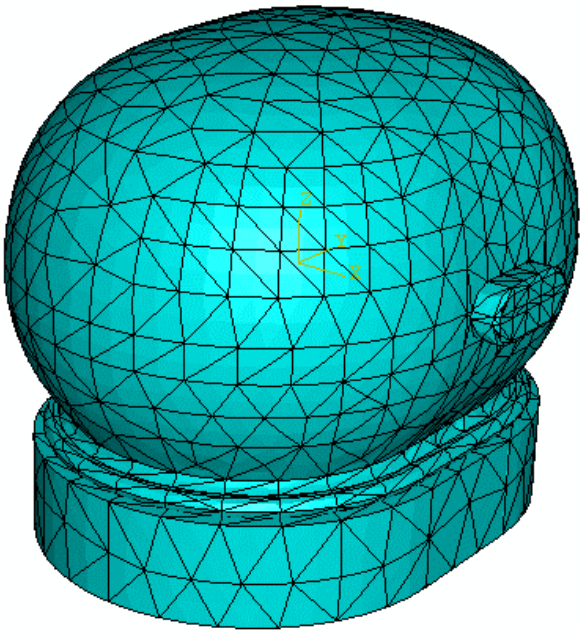

Figure 4.4 Meshed model of Earcup/Seal system in ABAQUS

4.3 Seal Material Characterization

The earcup seal plays a very important role in both the low frequency dynamic response of the earcup and in allowing acoustic energy to "leak" into the interior of the earcup, therefore, it is extremely important for the advancement of the project to characterize the seal material. A great effort was made to establish a material model, which would be appropriate for low frequency as well as the high frequency range.

During the initial stages of the project, data for storage modulus was obtained from simple load-deflection data at a few frequencies. A curve fitting technique was applied to an acceleration frequency response function (FRF) to estimate the damping values of the seal material. The FRF obtained through experiments was curve fitted using Matlab® to obtain the damping values at the resonant frequencies of the system. This simple viscoelastic material model was not adequate for more refined vibro-acoustic models. The viscoelastic material model will have to be derived from experiments on the seal over the frequency range of interest. Once a reasonable material model is established, the material behavior can be directly imported in ABAQUS for use.

4.3.1 ABAQUS Material Model

The material model in ABAQUS requires the elastic storage and loss modulus of the system to be calculated. i.e. *E'* and *E''*. Once *E'* and *E''* are obtained the bulk and shear modulus can also be calculated and inserted into the input file for the analysis. The formulae for the long-term bulk modulus K_∞, bulk storage modulus *K'*, bulk loss modulus *K"*, long-term shear modulus G_∞, shear storage modulus *G'* and shear loss modulus *G"* are given in Equation 4.3, 4.4, 4.5 and 4.6 respectively,

$$K' = \frac{E'}{3(1-2\nu)} \tag{4.3}$$

$$K'' = \frac{E''}{3(1-2\nu)} \tag{4.4}$$

$$G' = \frac{E'}{2(1+\nu)} \tag{4.5}$$

$$G'' = \frac{E''}{2(1+\nu)} \tag{4.6}$$

$$K_\infty = \frac{E_\infty}{3(1-2\nu)} \tag{4.7}$$

$$G_\infty = \frac{E_\infty}{2(1+\nu)} \tag{4.8}$$

where v is the Poisson's ratio for the seal material.

For the viscoeastic seal, these moduli are frequency dependent. ABAQUS uses bulk and storage moduli to form frequency dependent relations given in Equation 4.9, 4.10, 4.11 and 4.12.

$$m_1(f) = \frac{G''}{G_\infty} \tag{4.9}$$

$$m_2(f) = 1 - \frac{G''}{G_\infty} \tag{4.10}$$

$$m_3(f) = \frac{K''}{K_\infty} \tag{4.11}$$

$$m_4(f) = 1 - \frac{K'}{K_\infty} \tag{4.12}$$

Where, G_∞ and K_∞ are long-term shear and bulk moduli.

Hand Calculations for ABAQUS Material Model

For the known values of E_∞, E' and E'' the values for long-term bulk modulus K_∞, bulk storage modulus K', bulk loss modulus K'', long-term shear modulus G_∞, shear storage modulus G' and shear loss modulus G'' are calculated using equations 4.3-4.8, These values for ABAQUS are calculated using the data at 43 Hz.

E_∞ = 1680 N/m^2

E' @ 43 Hz = 1.892 e^5 N/m^2

E'' @ 43 Hz = 1.863 e^5 N/m^2

v = 0.4995

(4.3) => $$K' = \frac{1.892\,e^5}{3(1-2(0.4995))} = 6.3059e^7 \quad N/m^2$$

(4.4) => $$K'' = \frac{1.863\,e^5}{3(1-2(0.4995))} = 6.2099e^7 \quad N/m^2$$

(4.5) => $$G' = \frac{1.892\,e^5}{2(1+0.4995)} = 63080 \quad N/m^2$$

(4.6) => $$G'' = \frac{1.863\,e^5}{2(1+0.4995)} = 62120 \quad N/m^2$$

(4.7) => $$K_\infty = \frac{1680}{3(1-2(0.4995))} = 25193e^6 \quad N/m^2$$

(4.8) => $$G_\infty = \frac{1680}{2(1+0.4995)} = 2520 \quad N/m^2$$

Using the values of K_∞, *K', K", G_∞, G'* and *G"*, ABAQUS frequency dependent relations can be calculated from equation 4.9-4.12,

(4.9) => $$m_1(43Hz) = \frac{62120}{2520} = 24.65$$

(4.10) => $$m_2(43Hz) = 1 - \frac{63080}{2520} = -24.031$$

(4.11) => $$m_3(43Hz) = \frac{6.2099e^7}{2.5193e^6} = 24.65$$

(4.12) => $$m_4(43Hz) = 1 - \frac{6.3059e^7}{2.5193e^6} = -24.031$$

The values for entire frequency range of interest (0 to 300 Hz) are calculated and are given in Appendix B.

4.3.2 Complex Stiffness Extraction

The seal material properties currently used in this research for the lower frequency range are extracted from complex stiffness data provided by Adaptive Technology Inc. Complex stiffness associated with the soft gel undercut seal was measured using an experimental setup illustrated in Figure 4.5 below. In this setup, a wooden piece of mass, *M*, is positioned on top of the seal. The underside of the wooden mass was shaped in such a way that it resembled the way the actual earcup makes contact with the seal. A force gage and an accelerometer were installed on top of the mass for acceleration-to-force transfer function measurements. The force gage was connected to a suspended shaker. Furthermore, two coil springs are installed in order to provide an appropriate pre-loading force.

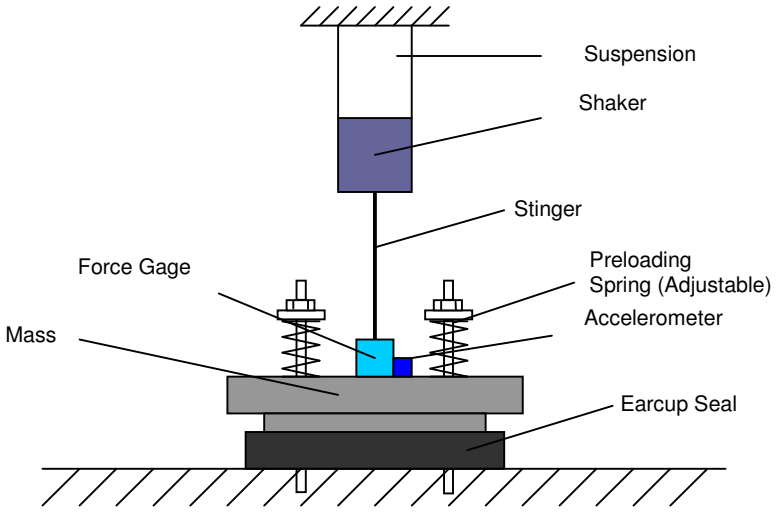

Figure 4.5 Seal complex stiffness measurement setup

The dynamics of the system shown in Figure 4.5 can be described by,

$$m\ddot{x} + \tilde{k}x + k_p x = f \tag{4.10}$$

where m is the mass of the system, k_p is the stiffness of the preloading springs and $\tilde{k}$ is the complex stiffness of the seal. The real and the imaginary part of the complex stiffness, k' and k'', (i.e. storage and loss stiffness) as a function of frequency can be obtained from measured force-to-acceleration transfer function, H_{af}, as,

$$k' = \mathrm{Re}\{\tilde{k}(\omega)\} = m\omega^2 - \mathrm{Re}\{1/H_{af}(\omega)\} \cdot \omega^2 - k_p \tag{4.11}$$

$$k'' = \mathrm{Im}\{\tilde{k}(\omega)\} = -\mathrm{Im}\{1/H_{af}(\omega)\} \cdot \omega^2 \tag{4.12}$$

The complex stiffness data obtained from the experiments is plotted versus frequency in Figure 4.6 for different levels of preload.

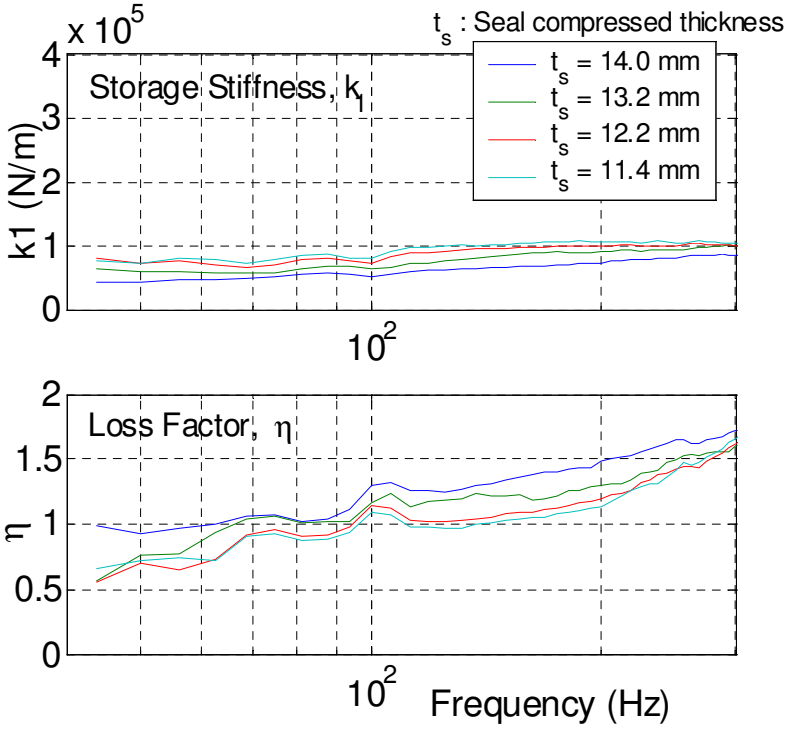

Figure 4.6 Complex stiffness experimental data for viscoelastic seal

As indicated in Equation 4.11, the calculation requires the value of system mass, m, and the preloading spring stiffness, k_p. The mass of the system m was estimated by adding the weight of the wooden mass and the effective mass of the seal, one-third of the mass of the seal.

The values of the elastic storage and loss moduli i.e. *E'* and *E"* can be estimated by,

$$E' = \frac{k'A}{L} \tag{4.13}$$

$$E'' = \frac{k''A}{L} \tag{4.14}$$

where A is the area of cross-section of the seal and L is the height of the seal. The values of the *E'* and *E"* can be used to calculate the shear and bulk moduli as described in section 4.3.1.

Hand Calculations for Elastic Moduli

For the extracted values of *k'* and *k"* from equation 4.11 and 4.12 the values of *E'* and *E"* can be calculated using equation 4.13 and 4.14.

k' @ 43 Hz = 75119 N/m
k" @ 43 Hz = 49790 N/m
$A = 4.1077e^{-3}$ m^2
$L = 0.0185$ m

(4.13) $$E' = \frac{75119 \times 4.1077e^{-3}}{0.0185} = 1.8918e^{5}\ \text{N/m}^2$$

(4.14) $$E'' = \frac{49790 \times 4.1077e^{-3}}{0.0185} = 1.863e^{5}\ \text{N/m}^2$$

These values of E' and E" are calculated at 43 Hz.

CHAPTER 5
Acoustic Modeling

Finite element modeling requires proper engineering thought given to the problem. If all the phenomena that are involved in causing an acoustic resonance inside the earcup are not accounted for in the FE model the results obtained by FE analysis could be misleading. It is therefore necessary to identify the dominant physical phenomena that are responsible for the acoustic response inside the earcup. Since the focus of this thesis is the lower frequency investigation of the circumaural ear defenders, the phenomena responsible for causing the acoustic response in the lower frequency range was modeled and explored.

5.1 Acoustic Leak and Helmholtz Resonance

As mentioned in the previous chapter, the seal of the circumaural ear defenders plays a very important role in both the low frequency dynamic response of the earcup and in allowing acoustic energy to "*leak*" into the interior of the earcup. The fact that the earcup seal fails to conform completely to the head causes leaks; the leaks also occur due to hair and eyeglasses stems etc. The leak causes the acoustic energy to seep into the earcup. Due to the presence of the leaks, the earcup is believed to behave as a Helmholtz resonator at low frequencies.

The Helmholtz resonator is a phenomenon that occurs when a slug of fluid oscillates between a rigid walled volume and the ambient surroundings. Figure 5.1 illustrates a schematic of a Helmholtz resonator. For the case of the earcup, the cup is hardly pressed against the head such that the cup acts like a rigid walled volume; the mass of the air in the leak oscillates between the cup and the ambient environment at resonant frequency. Simple harmonic motion occurs when the fluid in the neck of the resonator responds as a lumped mass, which oscillates in the neck. This condition is satisfied at low frequencies when λ (wavelength)>>L (length of the leak), $\lambda >> \forall^{1/3}$(volume of cup), and $\lambda >> A_l^{1/2}$(leak area).

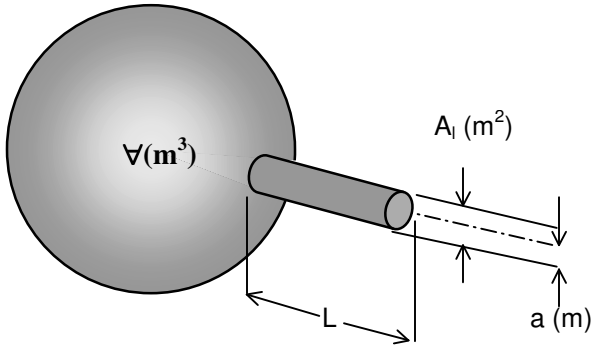

Figure 5.1The simple Helmholtz resonator

There are losses associated with the motion of the bulk fluid. These losses include radiation losses, which occur due to sound radiation through the leak opening into the ambient environment, and the thermo-viscous losses, which are caused by the resistance offered due to shear stresses between the fluid mass and neck wall. The mass of air contained in volume $\forall$ of the resonator acts as an air spring and is responsible for the stiffness of the system.

In the literature [1], the Helmholtz resonator is often modeled as a spring-mass-damper system, Figure 5.2. The slug of fluid in the neck between the large fluid volume and ambient air represents the mass. The compression of air within the rigid volume provides the stiffness of the system. The acoustic radiation losses and thermo-viscous losses provide damping to the system.

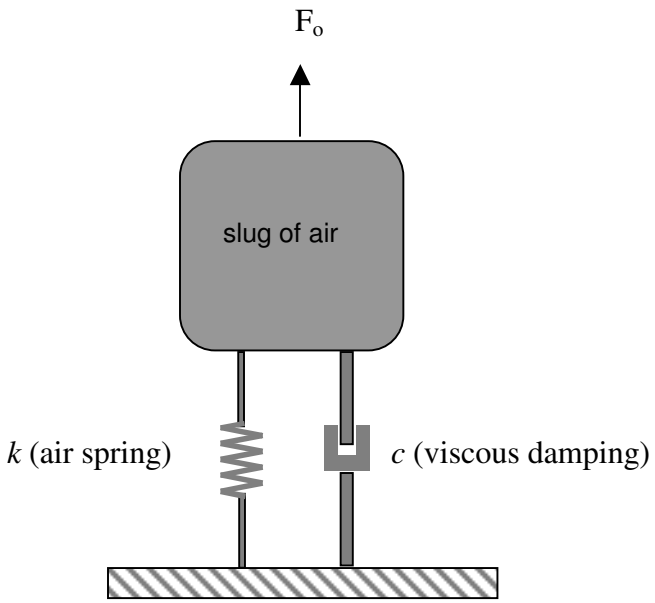

Figure 5.2 SDOF representation of Helmholtz resonator

A free body diagram of the of the spring mass damper system is shown in Figure 5.3

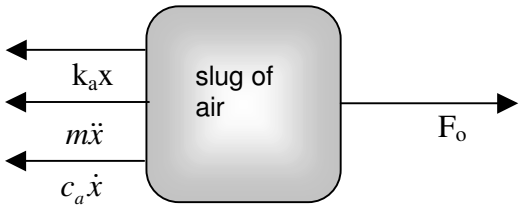

Figure 5.3 Free body diagram of the Helmholtz resonator

The equation of motion for the above system is given by,

$$m\ddot{x} + c\dot{x} + kx = F_o \tag{5.1}$$

The force F_o represents the external pressure, which is acting on the leak opening. The coefficients, *m*, *c*, and *k* are physical parameters of the system. These coefficients are defined in [1],

$$m = \rho_o A_l L' \quad (kg) \tag{5.2}$$

$$L' = L + 1.4a \quad (m) \tag{5.3}$$

m = mass of the leak fluid moving through the neck of the leak (kg)

L' = effective leak length (m)

ρ_o = density of air (kg/m^3)

A_l = area of leak (m^2)

L = length of leak (m)

a = radius of the leak (m)

For a given leak size and the internal fluid volume of the earcup, the Helmholtz resonator mode can be estimated by equation 5.4,

$$\omega = c\sqrt{\frac{A_l}{L'V}} \tag{5.4}$$

A_l = area of leak (m^2)

L' = effective leak length (m)

V = internal fluid volume of the earcup

c = speed of sound in air (m/sec)

Hand Calculations for Helmholtz Resonator Mode

The natural frequency associated with the Helmholtz resonator mode is predicted for the case of earcup using equation 5.4.

$A_l = 2.5335\text{e}^{-6}$ m^2

$L' = 0.0212$ m

$V = 3.47\text{e}^{-4}$ m^3

$c = 343$ m/sec

(5.4) => $\omega = 343\sqrt{\frac{2.5335\text{e}^{-6}}{(0.0212)(3.47\text{e}^{-4})}} = 190$ rad/sec

=> $f = 31$ Hz

5.1.1 Effective Leak Length

Effective leak length represents the effects of fluid momentum. As the slug of fluid is accelerated through the leak, it does not lose its momentum at the end of the leak. The momentum of the fluid dissipates over some length past the leak. An additional length, can be added to the physical leak length, comprises the effective leak length, to account for the radiation.

5.1.2 Damping

The damping term, *c*, is comprised of two terms, radiation resistance and thermo-viscous resistance. The radiation resistance is a representation of losses due to sound radiation into the open medium outside the leak. This component of the damping term is represented as R_r, which is given in [1] as,

$$R_r = \frac{\rho_o c k^2 A_l^2}{4\pi} \quad \left(\frac{kg}{s}\right) \tag{5.5}$$

R_r = radiation resistance (kg/s)

c = speed of sound in air at STP (m/s)

k = wavenumber (1/m)

The second component of the damping term is the thermo-viscous resistance. This term represents the losses due to viscous boundary layer effects at or near the wall. The thermo-viscous resistance, R_w is represented in equation 5.6 [1].

$$R_w = 2mc\alpha_w \quad \left(\frac{kg}{s}\right) \tag{5.6}$$

where α_w (1/m) is the absorption coefficient and is defined in Kinsler and Frey [1],

$$\alpha_w = \frac{1}{ac}\left(\frac{\eta\omega}{2\rho_o}\right)^{1/2}\left(1+\frac{\gamma-1}{\sqrt{\mathrm{Pr}}}\right) \quad \left(\frac{1}{m}\right) \tag{5.7}$$

$$\eta = \frac{1}{3}\rho_o l_m c \qquad \left(\frac{N \cdot s}{m^2}\right) \tag{5.8}$$

where,

η = viscosity (N.s/m^2)
ω = frequency (rad/s)
γ = specific heat ratio
Pr = Prandtl number
l_m = mean free path between atoms (m)
a = radius of the leak

The sum of the resistance terms yields the total resistance of the system such that,

$$c = (R_r + 5 * R_w) \tag{5.9}$$

The wall losses are multiplied by a factor of 5 in order to match the analytical results with the experimental results in [18]. This value is also used to add damping in the FE leak model.

Hand Calculations For Damping

Using the above equations the damping for the leak analysis can be calculated at a particular frequency. The material properties of air are described at Standard Temperature and Pressure, STP (0°C / 273.15 K and 1 atm/101.325 kPa).

ρ_o = 1.21 kg/m^3

γ = 1.4

η = 1.8 e^{-5} N.s/m^2

Pr = 0.75

c = 343 m/sec

The leak dimensions are,

A_l = 2.5335e^{-6} m^2

L = 0.02 m

V = 3.47e^{-4} m^3

a = 8.98e^{-4} m

Based on the above leak dimensions the mass of the air in the leak is calculated as,

$$m = \rho_o A_l L$$

$$m = (1.21).(\ 2.5335e^{-6}).(0.02) = 7.0013\ e^{-8}\ \text{Kg}$$

the wavenumber k is calculated at 43 Hz as,

$$k = \frac{\omega}{c} = \frac{2\pi f}{c} = \frac{2(3.14)(43)}{343} = 0.787$$

Radiation Resistance

For the above-calculated parameters and the material properties of air, the radiation resistance is calculated using equation 5.4,

$$R_r = \frac{(1.21).(343)(0.787)^2 (2.5335e^{-6})^2}{4\pi} = 1.31e^{-10} \quad \left(\frac{kg}{s}\right)$$

Thermo-viscous Resistance

The absorption coefficient used to calculate thermo-viscous resistance is obtained by equation 5.7,

$$\alpha_w = \frac{1}{(8.98e^{-4})(343)}\left(\frac{(1.85e^{-5})(2\pi.43)}{(2).(1.213)}\right)^{1/2}\left(1+\frac{1.4-1}{\sqrt{0.75}}\right) = 0.2074 \qquad \left(\frac{1}{m}\right)$$

using this value for absorption coefficient, the value for thermo-viscous resistance is calculated at 43 Hz ,

$$R_w = 2(7.0013e^{-8})(343)(0.2047) = 9.8315e^{-6} \quad \left(\frac{kg}{s}\right)$$

Total Damping

The total damping is the sum of thermo-viscous resistance and the radiation resistance.

$$c = 5 * 9.8315e^{-6} + 1.31e^{-10} = 4.916\ e^{-6}\ \text{Kg/sec}$$

This value of damping is calculated at 43 Hz frequency, the values for damping for the entire frequency range of 0-300 Hz is given in Appendix B.

5.2 Acoustic FE Modeling

The lower frequency acoustic response of the earcup/seal system is dominated by the leak phenomenon, which causes the earcup to behave like a Helmholtz resonator. In order to capture the Helmholtz resonance phenomenon in FE analysis it is required to model an external acoustic pressure source emitting a spherical pressure wave that travels in an infinite medium, the pressure wave reaches the internal fluid volume of the cup through the leak. The acoustic modeling of the earcup requires the 3-D geometry of external fluid (air) domain, the internal fluid volume of the earcup and the leak are to be imported into the FE software environment. The leak connects the external air domain to internal fluid volume of the earcup. ABAQUS, which is appropriate for the structural part of the problem, is also versatile in acoustic modeling; therefore it is used for the acoustic analysis as well. ABAQUS not only has a quadratic acoustic element but also have built-in radiation boundary conditions for specified geometric shapes, which is necessary for the creation of an infinite acoustic medium.

In order to understand completely the Helmholtz resonator phenomenon, it is initially necessary to isolate the structural effects that are caused by the dynamics of the earcup/seal system. This means that for acoustic only analysis it is not necessary to model the structural components of the earcup (cup and the seal) in the FE model, only fluid volumes are required. Once the isolated structural and acoustic effects are analyzed the structural components will be added to the problem for a coupled fluid structure analysis. This approach will greatly simplify the FE modeling efforts by eliminating the ambiguities that are caused by the viscoelastic seal material. Since the structural components are not modeled initially, the acoustic FE analysis will only consist of fluid elements, which will significantly reduce the model size and complexity. Some of the issues related to the acoustic modeling of the earcup are discussed in the following section.

5.2.1 FE Modeling Issues

Infinite Medium

The proper representation of an acoustic infinite medium is an extremely important aspect of FE analysis of the problems involving large domains such as a submarine in a sea, a car in an open atmosphere or an earmuff in a noise field, which is the case for this research. The term "infinite medium" refers to an endless domain. The FE analysis of such a domain is crucial because, simulation time increases with the size of the problem; moreover, it is impossible to represent infinite domains in FE without specifying appropriate boundary conditions which leave the same effect of a domain on infinite extent. Fortunately, the commercial FE software programs allow users to specify such conditions at the boundaries of a finite acoustic domain, which allows the acoustic waves to pass through and not reflect back into the computational domain and hence represent an infinite domain. In ABAQUS, an infinite medium can be modeled in two different ways, by meshing the boundary with infinite acoustics elements or by specifying radiation boundary conditions at the boundary of the acoustics domain. ABAQUS allows to specify a built in radiation boundary condition e.g. for a spherical domain, a plane wave domain, as well as user defined radiation boundary for shapes that are not regular. For simplicity, the built-in radiation boundary condition for spherical air domain is employed in this research. The next question arises, how much acoustic domain has to be modeled for an accurate FE analysis? The ABAQUS theory manual [3] recommends modeling a layer of the acoustic medium using finite elements, to a thickness of 1/3 to a full wavelength, out to a "radiating" boundary surface for the lowest frequency to be used in the analysis. A condition is then imposed on this surface to allow the acoustic waves to pass through and not reflect back into the computational domain.

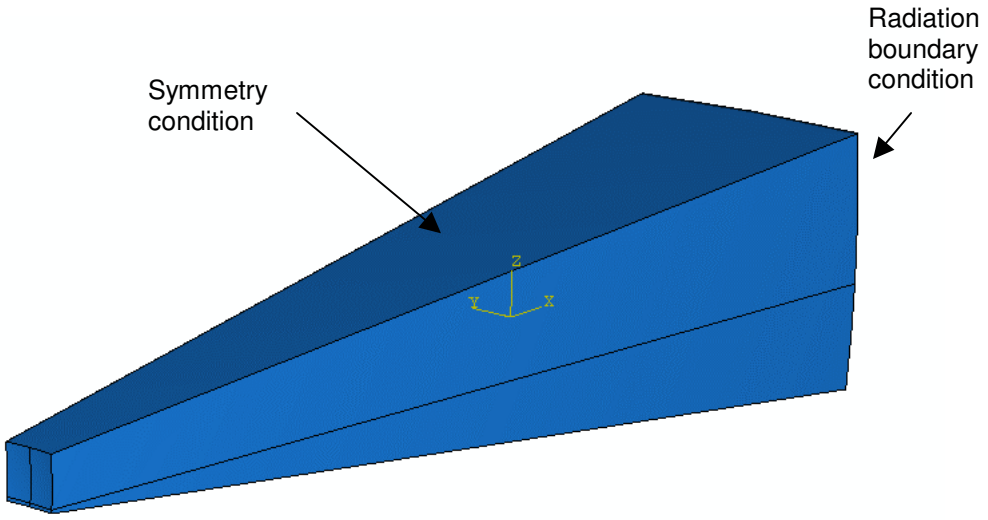

Figure 5.4. External air domain (infinite medium)

The geometry of the external air domain is shown in Figure 5.4. In order to minimize the number of degrees of freedom (DOF) in the FE model, the symmetric boundary condition option is employed which allows modeling a portion of sphere instead of modeling a full sphere to get the same effects as modeling a full sphere. The lowest frequency of interest for this analysis is 50 Hz; in order to get accurate results from the FE analysis, the radius of the acoustic medium has to be 1/3 of the lowest wavelength, which in this case is 2.5 m. Radiation boundary conditions are then applied at the boundary of the sphere.

Acoustic Source Representation

Acoustic source representation is another important aspect of the FE modeling. The sound waves emitted from an acoustic spherical source in an ambient environment travel in the form of spherical waves. A simple point source generating spherical waves could be employed into FE model. However, the real issue is, what is the best way to represent a point source in the FE model. The point source can be represented in the FE model by specifying pressure at a single node. However, this is a singularity in the acoustic formulation, which requires a highly refined mesh around the source to properly inject the energy from that node into the entire fluid domain. This highly refined mesh will result in very large number of nodes and elements, which will result in large simulation time. A better way to represent a point source is to expand the surface area

upon which the acoustic source acts such that the acoustic source strength remains the same as it is for the case of pressure acting on a point. Figure 5.5 (a & b) show two different representations of a point source.

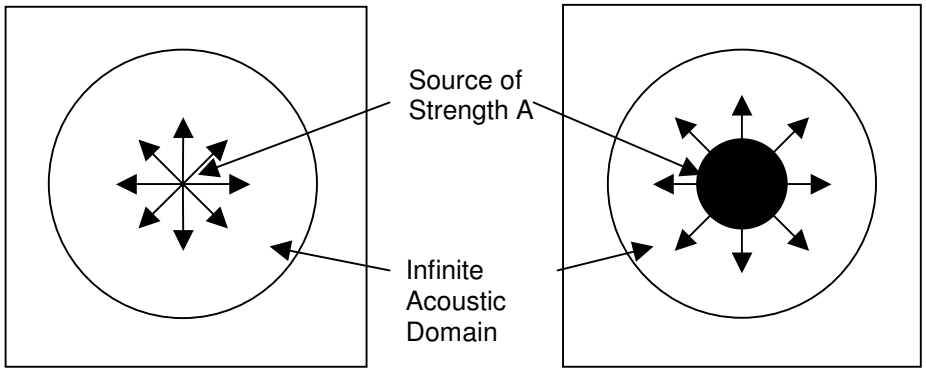

Figure 5.5 (a) Pressure radiation from a point Figure 5.5 (b) Pressure radiation from a surface

The geometry of the external air domain is truncated at 0.5 m from the origin of the sphere. Acoustic pressure is applied at the truncated area. Expanding the surface area of the source will significantly reduce the number of elements required near the source to propagate the pressure wave effectively into the entire fluid domain. This approach is used in modeling the source in FE model.

Spherical Source in an Infinite Domain

The pressure emitted by a point source in an infinite domain at a distance *'r'* is given by equation 5.10 [1],

$$P(r,t) = \left(A/r\right)e^{i(\omega t - kr)} \tag{5.10}$$

where,

A = source strength (N/m)

r = radial distance from source (m)

k = wavenumber

ω = frequency (rad/sec)

t = time (sec)

The spatial component of the emitted pressure wave is given by,

$$P(r) = \left(A/r\right)e^{i(-kr)} \tag{5.11}$$

Hand Calculations for Spherical Source in an Infinite Domain

A spherical acoustic source of radius 0.5 m is emitting pressure in an infinite domain. The source strength is 3502.66 N/m. The pressure amplitude can be calculated at some distance from the source using equation 5.11.

$$P(1.756) = \left(3502 \big/ 1.756\right) = 2\ e^3 \text{ Pa}$$

The infinite domain FE model shown in Figure 5.4, gives the same results for pressure amplitude at a distance of 1.756 m from the source.

Damping

Damping plays an important role in determining the accurate response of the system; therefore, it is necessary to get the correct damping estimates into the FE model. In ABAQUS the damping of an acoustic medium is introduced in the analysis by specifying a frequency dependent volumetric drag. ABAQUS uses the equilibrium equation for small motions of a compressible, adiabatic fluid with velocity-dependent momentum losses to solve for an acoustic problem. It is important to realize that the velocity is higher where the momentum is high i.e. the leak. Therefore in the FE solution it will make only a slight difference whether the damping is spread out to the complete acoustic domain or if it is lumped over the leak volume. For lower frequency analysis the damping is calculated from the Equation 5-8 derived in Kinsler and Frey [1] and as described in section 5.1. These damping values are entered in ABAQUS as volumetric drag after slight modification as described in section 5.2.1.

5.2.2 Acoustic Leak Model in ABAQUS

The major issues regarding the acoustic modeling are resolved. However, an effective meshing scheme is key to finite element analysis. In order to create an effective mesh, partitioning has to be performed on the geometry of the fluid domain. The 3-D solid geometry of the external fluid domain, the leak and the internal fluid domain are brought into the ABAQUS environment in order to mesh and conduct the FE analysis. The geometry of the external fluid domain is complicated because the volume of the earcup has to be subtracted from it, which leaves lots of curved surfaces that are causing

problems in meshing. The initial mesh of the external fluid domain, the internal fluid volume and the leak volume consisted of more than 90,000 3-D quadratic acoustic elements, which was not appropriate for a time effective FE analysis. In order to have more mesh control and to add versatility to the model, a cubic fluid volume is created at a point, where the earcup is placed in the field, this box has plane outer boundaries but inner boundaries assumed the external shape of the earcup and seal (Figure 5.6).

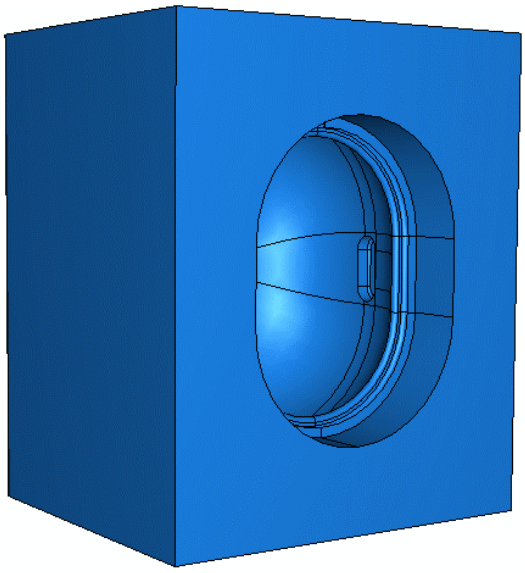

Figure 5.6 Fluid box created in the external domain

Using the earcup's internal surface area easily creates the inner fluid volume of the cup. Figure 5.7 displays the inner fluid volume of the earcup.

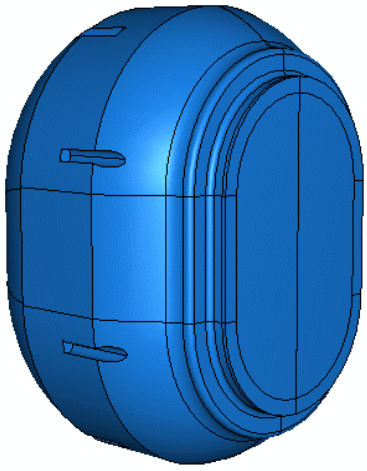

Figure 5.7 Internal fluid volume of the earcup

The internal fluid volume of the earcup is connected to the external fluid domain through the leak (Figure 5.8). The leak is defined by an air volume the surfaces of which are tied to the internal and external fluid volume using ABAQUS *TIE option. The leak sizes were selected to match the leak sizes used in the experiments performed for the analysis.

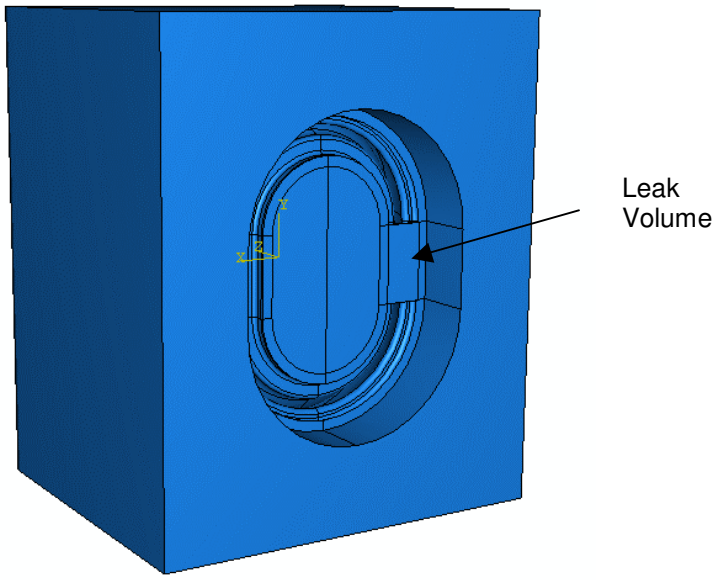

Figure 5.8 Leak connects the internal fluid volume of the earcup and external fluid box

The external fluid volume is partitioned to accommodate the fluid box. The outer boundaries of the fluid box are tied to the external fluid volume using ABAQUS *TIE option (Figure 5.9). The remaining portion of the external fluid domain is added to obtain a symmetric external fluid domain as shown in Figure 5.4

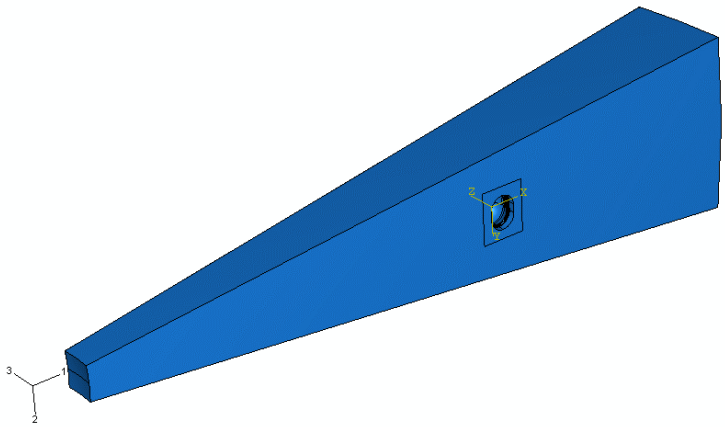

Figure 5.9 The box of fluid volume is added to the rest of the external fluid domain

Mesh controls are placed on lines to mesh the external fluid volume, the leak volume and inner fluid volume by 45,000 3-D quadratic acoustic elements, hence, reducing the size of the model by 50 percent. The meshed volumes of the external fluid volume, box fluid, leak and the inner fluid volume are shown in Figure 5.9.

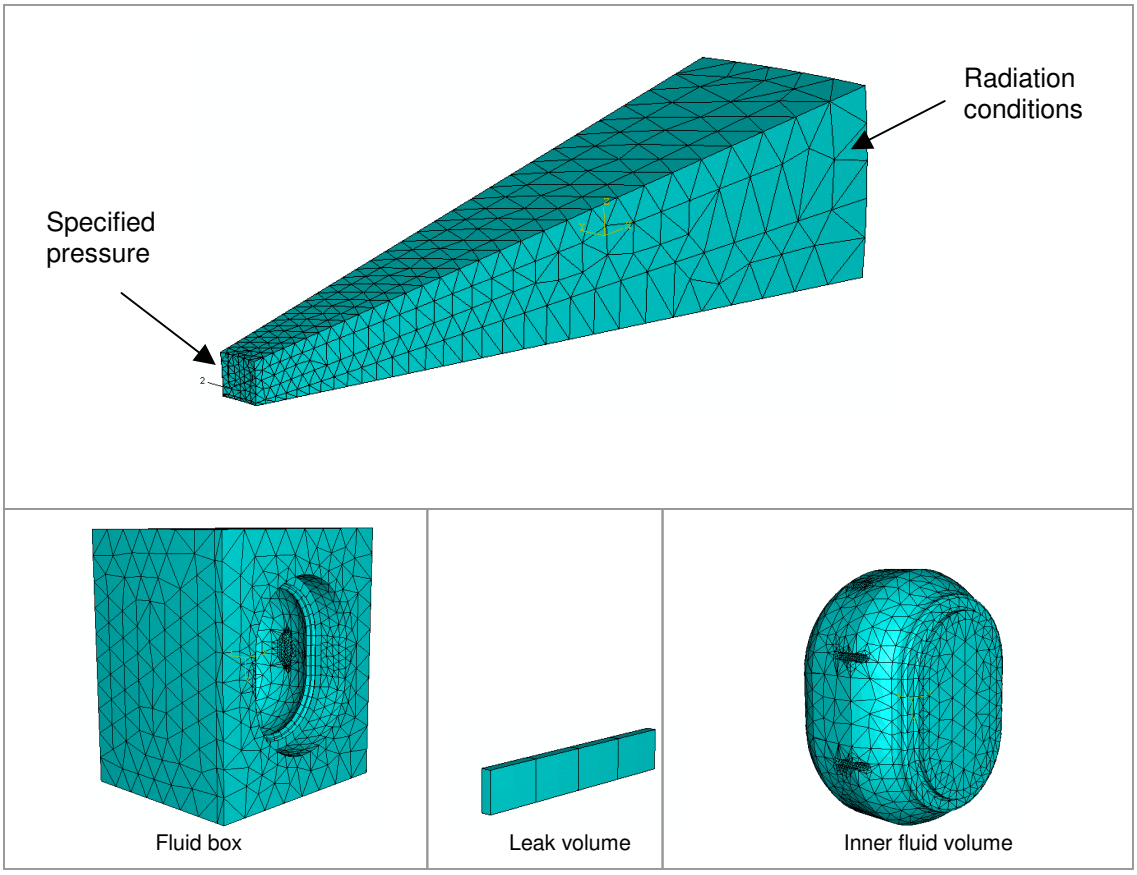

Figure 5.9 Meshed components of the acoustic leak model.

Chapter 6
Coupled Modeling

The FE models created for the structure and acoustics allow the isolated study of the acoustics and structural phenomena and the factors affecting these phenomena in addition to the reduction in size and complexity of the FE model. The reduction in size and complexity of the FE model allow for better exploration of the model. However, it is important to realize that if an acoustic medium is adjacent to a structure, fluid-structure coupling occurs, such coupling is also present in the actual earcup seal system. The acoustic and structural modes of the earcup are coupled i.e. the acoustic modes have an impact on the structural modes of the earcup, and vice-versa.

6.1 Coupled Mode

For the case of earmuffs two main phenomena (Piston mode and Helmholtz mode) are identified which are responsible for low frequency acoustic response inside the earcup. However, it is important to realize that these phenomena are not mutually exclusive. The pressure wave approaches the earcup/seal system and excites the earcup structure and the fluid present in the leak (Figure 6.1).

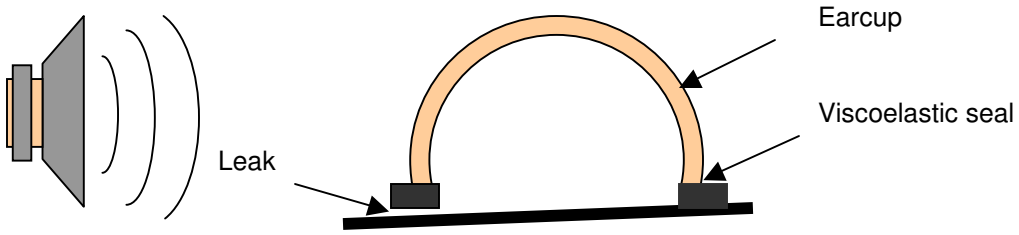

Figure 6.1 Earcup/seal system and leak excited by a pressure wave.

Depending upon the dimensions of the leak and the seal used, these modes could occur very close to each other, in which case the pressure response could only be

predicted by a coupled model. It is therefore necessary to perform a coupled physics FE analysis of the earcup seal system.

6.2 Coupled FE Modeling

The FE model for the coupled acoustic structure response is the combination of the acoustic leak model and the earcup structure model. The issues regarding FE modeling of the coupled fluid structure problem are similar to those, which were associated with the structure and acoustic models.

6.2.1 Modeling Issues

Many of the issues related to the acoustic and the structural modeling of the earcup/seal system has already been discussed in previous chapters. These issues include model size and complexity, viscoelastic seal properties, infinite acoustic medium acoustic source and leak damping. In addition to these issues the coupled acoustic-structure modeling involve the coupling of fluid and structure meshed surfaces.

Fluid-Structure Coupling

Defining the fluid-structure coupling is the key to the coupled fluid-structure analysis of the earcup/seal system. In ABAQUS, a surface-based procedure is used to enforce this coupling. This method requires that the structural and acoustic meshes use separate nodes. The user defines surfaces on the structural and fluid geometries and defines the interaction between the two meshes using the *TIE option. The *TIE command replaces the adjacent fluid and structure elements with the interface elements. The nodes of the interface element possess both acoustic and structure degrees of freedom i.e. the pressure as well as the displacement degrees of freedom.

6.2.2 Coupled FE Model

The FE model for the acoustic structure coupled analysis, is created by importing the geometries of the earcup, seal, internal fluid volume of the earcup and seal, leak volume and the external fluid volume into the ABAQUS environment. The volumes are partitioned so that the adjacent areas could be tied using ABAQUS *TIE command. The earcup and the seal geometry are meshed by 3D solid quadratic tetrahedrons, while the fluid domains are meshed with 3D acoustic quadratic tetrahedrons. The initial FE model consists of more than 140,000 elements. The geometries of the internal and external fluid domain were partitioned and meshing controls were specified on lines in order to reduce the mesh size to 55,000 elements. The reduction in mesh size reduces the simulation time and enables model exploration.

An acoustic source is specified at the inner radius of the sphere and the radiation boundary conditions are specified at the outer radius of the sphere. The meshed coupled FE model and all the components are shown in Figure 6.2.

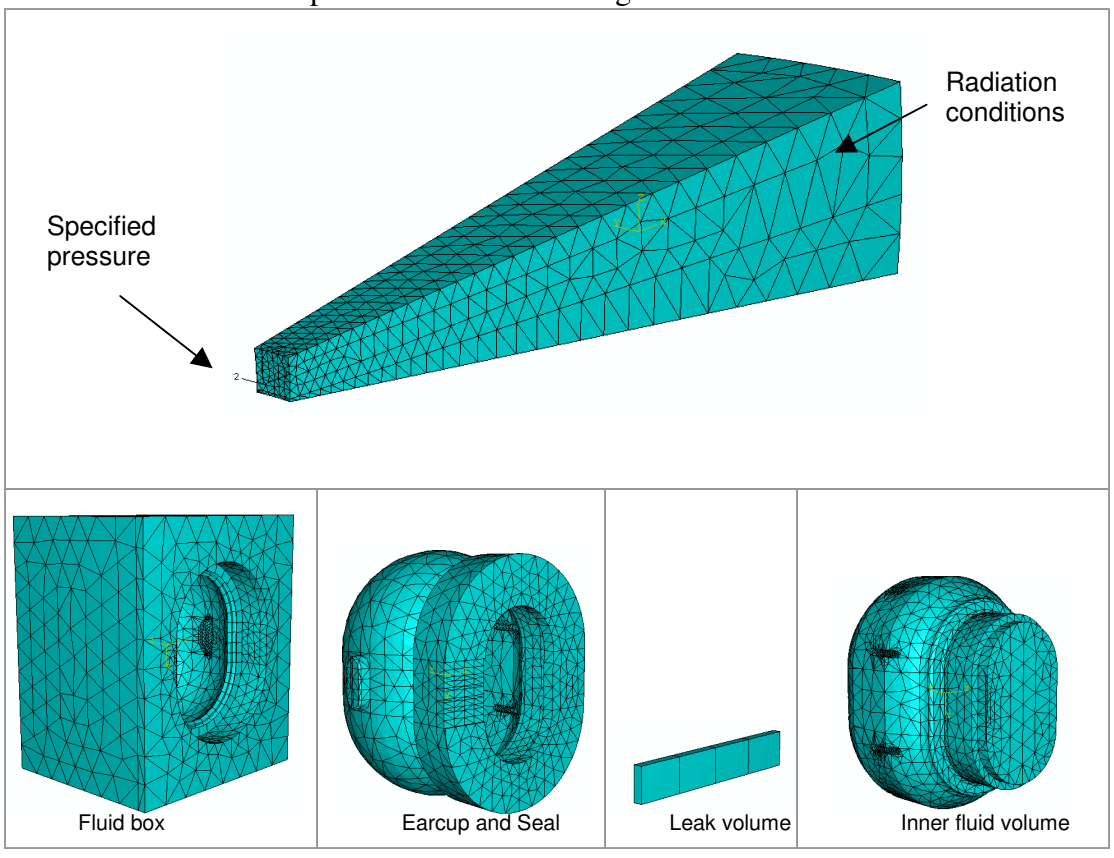

Figure 6.2 Acoustic structure coupled FE model components

CHAPTER 7
ANALYSIS and RESULTS

The objective of the FE analysis in this research work is to investigate the lower frequency structural and acoustic phenomena, which are responsible for the acoustic response inside the earcup. FE modeling efforts were focused on two main phenomena, the seal piston mode and the acoustic response due to the presence of acoustic leaks. The FE models created for the investigation of the above-mentioned phenomenon are meshed and major modeling issues are resolved. The FE analysis is performed on the meshed models.

7.1 FE Analysis Formulations

The analysis of the earcup/seal system involves steady-state dynamic analysis as well as modal analysis. In steady-state dynamic analysis, a harmonic force excites the cup or the acoustic medium and the response of the system is examined. Modal analysis is important because it provides information about the various structural and acoustics modes. However, it is extremely important to correlate these analyses in order to understand which structural and acoustic modes are responsible for causing large resonance and hence, greater acoustic response inside the earcup. The formulations associated with these analyses are described below,

Steady-state Response Analysis

For objects subjected to continuous harmonic excitation, ABAQUS/Standard offers a "direct" steady-state dynamic analysis procedure. The formulation for this procedure is based on the dynamic virtual work equation [3],

$$\int_v \rho.\delta u.\ddot{u}dV + \int_v \rho\alpha_c.\delta u.\dot{u}dV + \int_v \delta\varepsilon : \sigma dV - \int_S \delta u.tdS = 0 \tag{7.1}$$

where $\dot{u}$ and $\ddot{u}$ are the velocity and the acceleration fields, ρ is the density of the material, α_c is the mass proportional damping factor, σ is the stress, *t* is the surface traction, and $\delta\varepsilon$ is the strain variation that is compatible with the displacement variation δu. The same procedure can also be used for coupled acoustic-structural medium analysis, including radiation boundary conditions and infinite elements.

The direct-solution steady-state dynamic analysis procedure is the preferred solution method for acoustics in ABAQUS if volumetric drag and/or acoustic radiation are significant. If these effects are not significant, the mode-based procedure is preferred because of its efficiency.

All model degrees of freedom and loads are assumed harmonic at an angular frequency ω, therefore,

$$f = \tilde{f} \exp i\omega t \tag{7.2}$$

where $\tilde{f}$ is the constant complex amplitude of the variable *f*. Thus,

$$\dot{f} = i\omega f \tag{7.3}$$

$$\ddot{f} = -\omega^2 f \tag{7.4}$$

The equilibrium equation for small motions of a compressible, adiabatic fluid with velocity-dependent momentum losses is,

$$\frac{\partial p}{\partial x} + \gamma \dot{u}^f + \rho_f \ddot{u}^f = 0 \tag{7.5}$$

and use the harmonic time-derivative relations to obtain

$$\frac{\partial \tilde{p}}{\partial x} - \omega^2 \left(\frac{\gamma}{i\omega} + \rho_f \right) \tilde{u}^f = 0 \tag{7.6}$$

the complex density, $\ddot{\rho}$ is defined as,

$$\tilde{\rho} = \frac{\gamma}{i\omega} + \rho_f \tag{7.7}$$

thus,

$$\frac{\partial \tilde{p}}{\partial x} - \omega^2 \left(\rho_f \right) \tilde{u}^f = 0 \tag{7.8}$$

Divide equation 7.8 by $\ddot{\rho}$ and combine it with the second time derivative of the constitutive law equation 7.9 to obtain equation 7.10.

$$p = -K_f(x,\theta_i)\frac{\partial}{\partial x}u^f \tag{7.9}$$

where K_f is the bulk modulus and p is the pressure,

$$-\omega^2 \frac{1}{K_f}\tilde{p} - \frac{\partial}{\partial x}\left(\frac{1}{\tilde{\rho}}\frac{\partial \tilde{p}}{\partial x}\right) = 0 \tag{7.10}$$

The variation equation is,

$$\int_{V_f} \delta p\left[-\omega^2 \frac{1}{K_f}\tilde{p} - \frac{\partial}{\partial x}\left(\frac{1}{\tilde{\rho}}\frac{\partial \tilde{p}}{\partial x}\right)\right]dV = 0 \tag{7.11}$$

Modal Analysis

Modal analysis is the extraction of eigenvalues of the system, and hence investigate it's natural frequency of vibration. The formulation for eigenvalues extraction is given in equation 7.12,

$$\left(-\omega^2[M]+[K]\right)\{\phi\} = 0 \tag{7.12}$$

where M is the mass of the system, K is the stiffness and ϕ represent the eigenvalues.

7.2 Earcup Structure Modes

Earcup structural modes have an effect on the acoustics of the earcup. Therefore, it is necessary to investigate these modes. Also, it is necessary for the creation of a valid mesh to converge the first few modes of the earcup. Modal analysis is performed on the cup structure with free-free condition i.e. no boundary conditions were applied on the cup. This analysis is performed at the initial stages of the research therefore ANSYS is used for this analysis. The FE model of the earcup is shown in Figure 7.1.

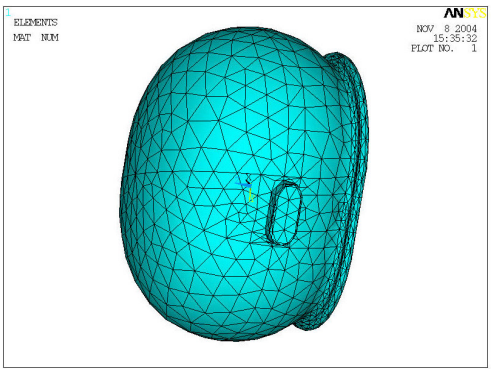

Figure 7.1 Free Free structural model

Analysis and Results

Modal analysis was performed on the earcup. The undeformed shape and first few mode shapes of the earcup are shown in Figure 7.2.

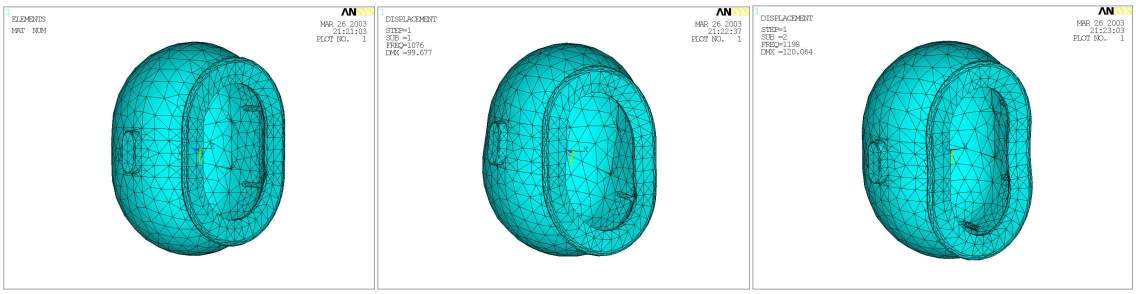

undeformed | 1st Flap mode (1083 Hz) | 2nd Flap mode (1204 Hz)

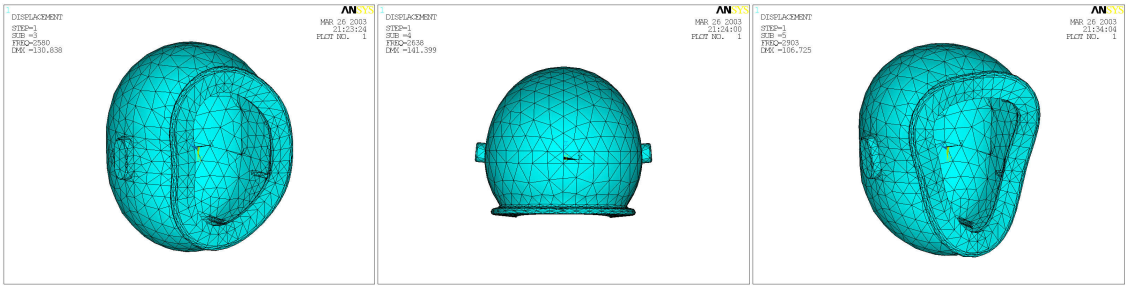

3rd Flap Mode (2592 Hz) | 1st Shell Mode (2644 Hz) | 4th Flap Mode (2915 Hz)

Figure 7.2 Structural modes of the earcup

Some modes are responsible for large deformation primarily associated with the vibration of earcup flap these modes are referred to as “Flap modes”. A mode in which the shell of the cup contracts and expands is named as “Cup piston mode”. The cup piston mode (2,638 Hz) may lead to significant loss in attenuation, especially if that mode shape couples with an internal acoustic resonance. In fact, the uncoupled acoustic

analysis indicates that there is a nearby translation acoustic resonance (one-half wave) at a similar frequency (2860 Hz).

The frequencies associated with each of the modes are compared with the experimental results in Table 7.1. The FE results show very good correlation with the experimental results. The first few modes extracted by FE are within 2% of the experimental results. However, it is important to realize that these modes are not significant for the lower frequency analysis, but have great significance in mid and higher frequency analysis.

Table 7.1 Comparison of Earcup Structural Modes

Mode	Frequency (Hz) (Experiment)	Frequency (Hz) (FE)	% Difference
1st Flap Mode	Missed	1083	-
2nd Flap Mode	≈ 1200	1204	0.33
3rd Flap Mode	2642	2592	1.8
1st Shell Mode	2692	2644	1.7
4th Flap mode	2932	2915	0.5
6	3135	3059	2.2

The percentage difference calculated in the above table is given by,

$$\%\ difference = \frac{Frequency\ FEA - Frequency\ Experiment}{Frequency\ Experiment} * 100$$

7.3 Ear Cup Internal Acoustic Modes

There are resonances associated with the internal fluid volume of the earcup. It is important to have information about the occurrence of the internal acoustic modes in the frequency range. The internal fluid volume mesh is shown in Figure 7.4.

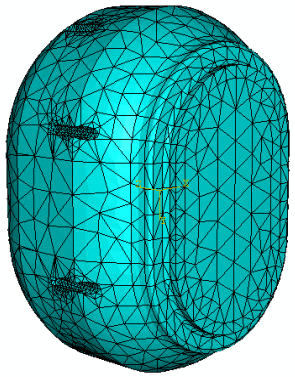

Figure 7.3 Inner fluid volume of the earcup

Analysis and Results

Modal analysis is performed on the rigid volume of the fluid. The first few acoustic modes of the internal air volume are shown in Figure 7.5.

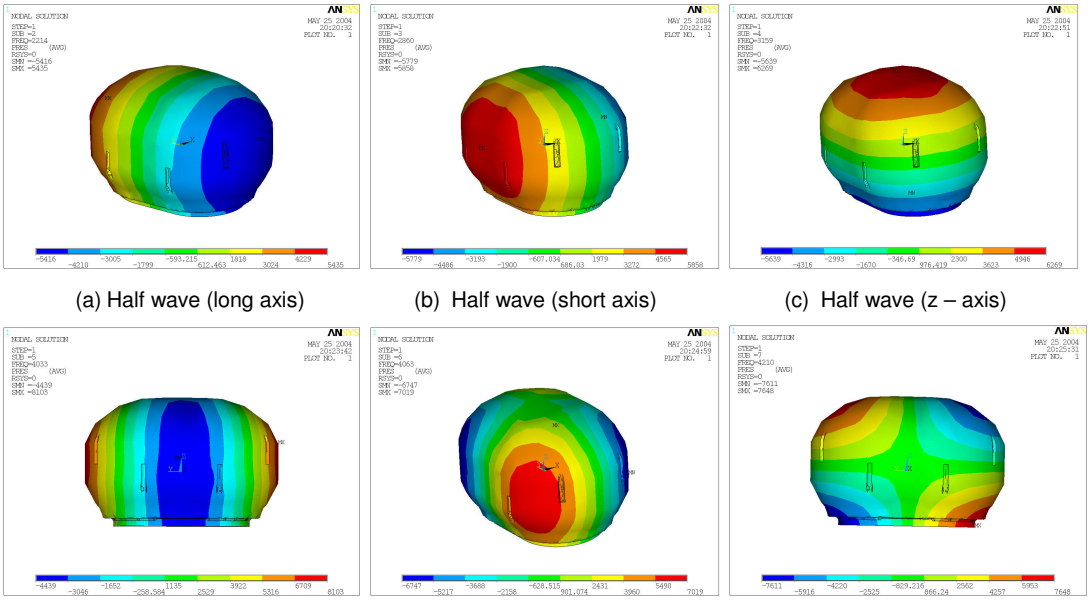

(a) Half wave (long axis) (b) Half wave (short axis) (c) Half wave (z – axis)

(d) Full wave (long axis) (e) Full wave (diagonal) (f) Full wave (diagonal)

Figure 7.4 Standing waves associated with the inner fluid volume of the earcup

The FE results predict that the first three modes are half waves that setup in three primary directions i.e. x, y and z directions. A rough estimate of half waves and full waves can also be estimated using the wavelength calculation in Equation 7.1.

$$\lambda = \frac{c}{f} \tag{7.1}$$

Where λ is the wavelength in meters, c is the speed of sound in m/s and f is the frequency in cycles/sec. First full wave is shown in Figure 7.5 (d).

Table 7.2 Comparison of Earcup Internal Acoustic Modes

Mode	Frequency Analytical (Hz)	Frequency FE (Hz)	% difference
1	1603	2201	37
2	2085	2840	38
3	2503	3152	26
4	3207	3994	25
5	-	4000	-
6	-	4151	-

The percentage difference calculated in the above table is given by,

$$\%\ difference = \frac{Frequency\ FEA - Frequency\ Analytical}{Frequency\ Analytical} * 100$$

However, it is important to important to realize that the earcup does not have three specific lengths, due to the spherical geometry of the earcup these modes could setup in directions other than x, y and z Figure 7.7 (d & e). The first internal acoustic mode appears at frequency 2214 Hz, this means that these internal acoustic modes are not significant for the lower frequency analysis.

7.4 Coupled Modal Analysis

The earcup seal plays a very important role in the low frequency dynamic response of the earcup; therefore it is essential to investigate the modes, which are considered to be responsible for the poor low frequency performance of the earcup. The meshed models of the earcup/seal system are shown in Figure 7.6. Under typical operating conditions the headband compresses the earcup to the head. This preload due to the headband results in the seal material, being stressed and deformed. It is important to account for preload because of the fact that it compresses the seal, as a result of which the stiffness of the seal is increased. The preload on the ear cup due to the headband is estimated experimentally to be 11.7 N. In order to account for preload, a structural pressure equivalent to the preload force is applied on the areas of ear cup's lugs.

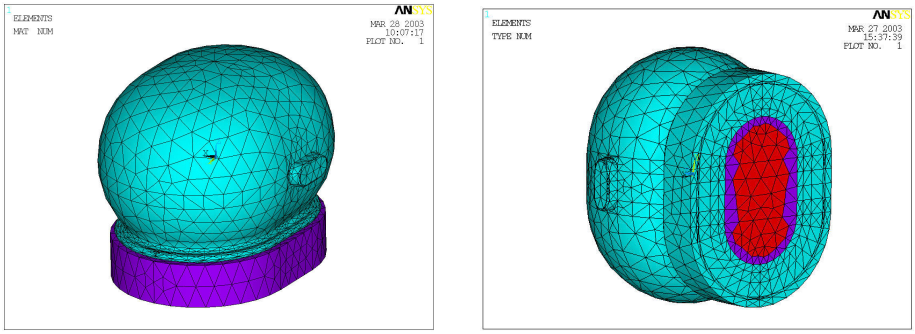

Figure 7.5 Fluid Structure coupled FE model without leak

Analysis and Results

The analysis consists of two steps; the first step is the static analysis due to the preload. The deformed shape of the earcup seal system due to the preload is shown in Figure 7.6. The actual deflection of the seal due to this preload is calculated using Equation 7.14 and is found to be 7 mm, where as FE results predict a maximum deflection of 5 mm. The difference in the FE and analytical results could be due to the shortcomings in the material model used for the extraction of the viscoelastic seal material properties.

$$F = kx \Rightarrow x = \frac{F}{k} \tag{7.14}$$

where k is the static stiffness and F is the force. The values of k and F are obtained from the experiments,

k= 1680 N/m

F= 11.7 N

Therefore,

$$x = \frac{F}{k} = \frac{11.7}{1680} = 7e^{-3}m$$

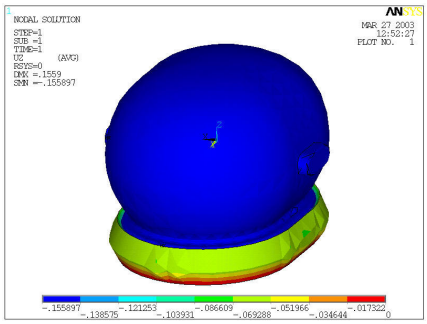

Figure 7.6 Static deflection due to preload

The second step in the solution is the modal analysis of the pre-stressed earcup/seal system. The modal density of the viscoelastic seal is very high but it was learned from the experiments performed on the earcup/seal system that the resonances occur in the frequency range of 170 Hz~230 Hz therefore modal analysis was focused in this frequency range. The natural frequencies of the seal in the frequency range from 170~230 Hz and there identities are tabulated below,

Table 7.3 Natural Frequencies of the Seal

Mode No.	Natural Frequency(Hz)	Mode Identity
1	178	Rocking (Diagonal)
2	193	Rocking (Diagonal)
3	203	Rocking (Long Axis)
4	206	Piston
5	231	Rocking(Short Axis)

The cup pumping resonance (piston mode) has long been considered to be responsible for the poor low frequency performance of an earcup defender in a SHP application. However, the rocking of the earcup may also contribute to seal lifting if the

displacements associated with either the external pressure loading or mode compliance is high enough. The lifting of the seal may lead to acoustic leaks.

7.5 Acoustic only Leak Analysis

Acoustic leaks cause the earcup to behave like a Helmholtz resonator at lower frequencies. The Helmholtz resonator acoustic response occurs when a slug of fluid undergoes harmonic oscillation between a large fluid volume and an ambient environment. Thus, it is important to analyze the effects of the leak on the performance of the earcup. In order to isolate the effects of the leak from the earcup/seal dynamics, acoustic only analysis is performed on the acoustic leak model. A schematic of the model is shown in Figure 7.7 Specifying a harmonic pressure at surface "A" generates a pressure wave that travels through the ambient air and excites the mass of air present in the leak, which also connects to the inner fluid volume of the earcup.

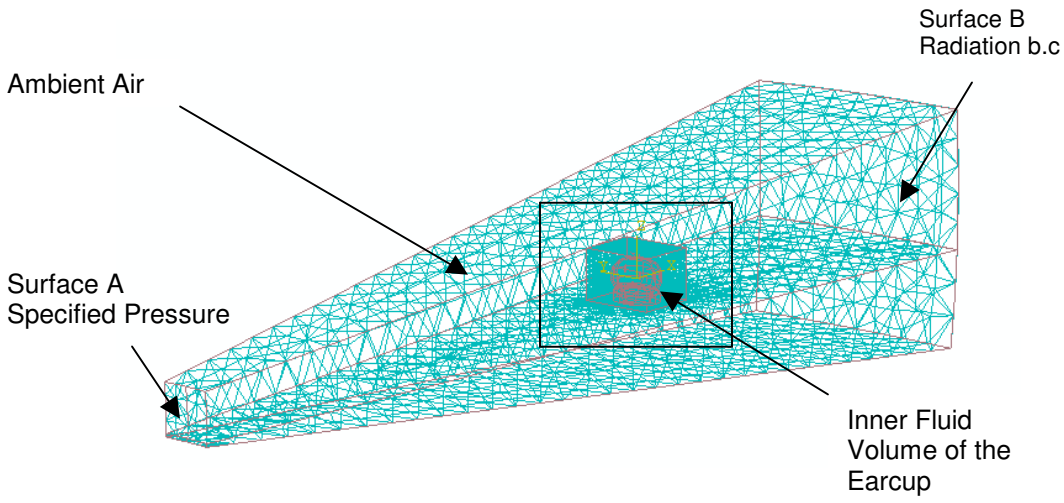

Figure 7.7 3D FE Model representing the Leak in the earcup.

The acoustic energy is carried out of the computational domain without any reflections back into the domain by specifying the radiation boundary condition at the outer boundary surface "B" of the domain.

For an actual earcup, the parameter which is most likely to change from person to person, is the leak area. This is due to the different shape of the skull around the ear, different hair pattern and use of different eye glasses stems. Therefore, FE analysis is performed for six different leak sizes and the pressure is measured at several locations inside the earcup. This pressure inside the earcup is called the internal pressure, P_i. The external pressure or the reference pressure P_o is measured at the leak opening. The ratio of internal pressure to the reference pressure, P_i / P_o is the normalized amplitude of the pressure, called the pressure ratio.

Analysis and Results

The analysis is primarily focused on the lower frequency range between 0~200 Hz where the Helmholtz resonance is believed to occur for the given leak sizes. The contour plot from FE results, Figure 7.8, shows the propagating pressure wave.

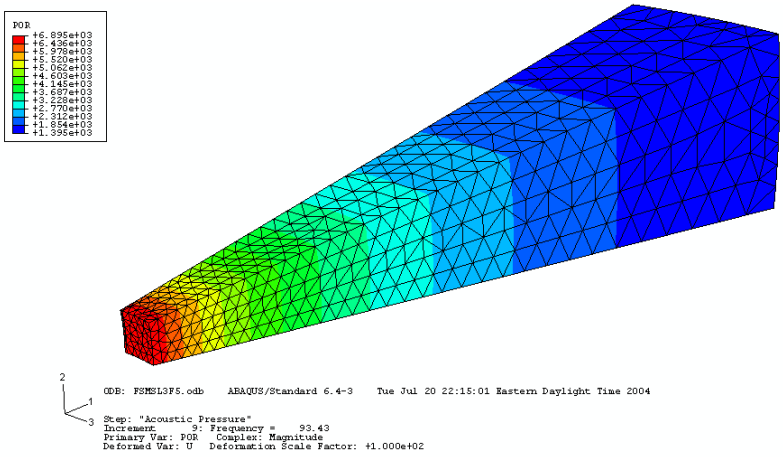

Figure 7.8 Contour plot of pressure for 1/8" leak analysis

Comparison FE versus Analytical

The FE results are plotted versus the analytical results for six different leak sizes in Figure 7.9,

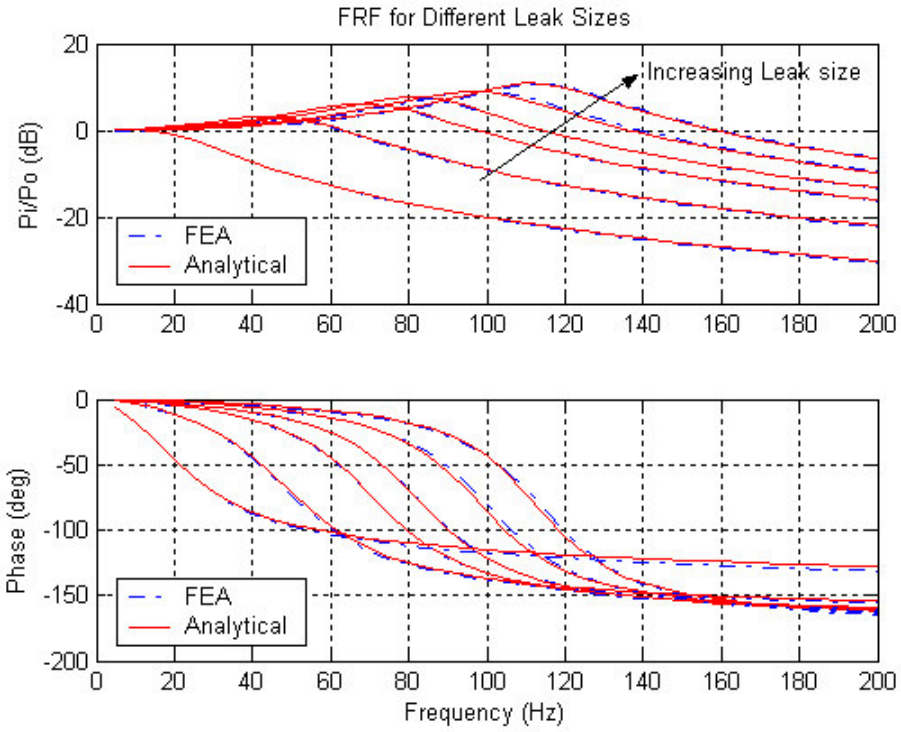

Figure 7.9 Driving point FRF for the pressure ratio P_i/P_o

The analytical solution to the problem is obtained from Jonathan Sides [18]. The transfer function for the Helmholtz resonator is given as,

$$\frac{P_i(s)}{P_o(s)} = \frac{\rho_o c^2 A_l^2}{\forall_{cup} ms^2 + \forall_{cup}(R_r + R_w)s + \rho_o c^2 A_l^2} \tag{7.15}$$

The above equation is used to model the Helmholtz trends in the ear cup. The complete derivation of can be found in "Low Frequency Modeling and Experimental Validation of Passive Noise Attenuation in Ear Defenders"[18]. It can be observed from Figure 7.9, that the FE and analytical results follow the same trend. The pressure amplitude at resonance and the resonant frequency increase with the increase in leak area,

while the damping decreases with the increase in leak area. The frequency of the Helmholtz mode and amplitude of the response are also tabulated in Table 7.3.

Table 7.4 Helmholtz Resonance and Amplitude of Pressure Ratio for Different Leak Sizes

Leak Size	Natural Frequency			Pressure Ratio		
(in)	Analytical (Hz)	FE(Hz)	% difference	Analytical (dB)	FE (dB)	% difference
1/8"	42	43	2.3	-7.9	-7.8	1.2
3/16"	56	56	0	3.2	3.2	0
3/8"	76	76	0	6.2	6.1	1.6
1/2"	86	86	0	7.8	7.6	2.5
3/4"	101	102	1	9.1	9.2	1
1"	115	116	1	10.6	10.5	1

The percentage difference calculated in the above table is given by,

$$\% \; difference = \frac{FEA - Analytical}{Analytical} * 100$$

The results obtained by FE are in good agreement with the analytical model. It can be observed from Figure 7.9, that the inner pressure response of the cup from both the solutions follows the same trend. The analytical results agree with FE results with an error of less than 3%. However, it is important to realize that the purpose of FE modeling in this research is not limited to a comparison against analytical model solution. The analytical solution is applicable for the lower frequency response but in the higher frequency range it may not be possible to derive an analytical solution for the acoustic pressure response. Therefore, this comparison can help to validate the FE model.

Comparison FE versus Experiment

The objective of FE modeling in this research effort is to predict the acoustic response and to investigate the physical phenomena, which are critical for the design of the earcup. The goal is to simulate the ambient noise field and boundary conditions, which are acting upon the earcup. Therefore it is necessary to validate the FE results with the experimental results obtained by the analysis performed on the actual earcup. The acoustic only leak analysis is performed by modeling and meshing the earcup internal fluid volume. This model implies a rigid earcup. An artificial leak was created

in a rigid seal gasket; the actual earcup seal is not used. The driving point FRF for experimental results is plotted in Figure 7.10.

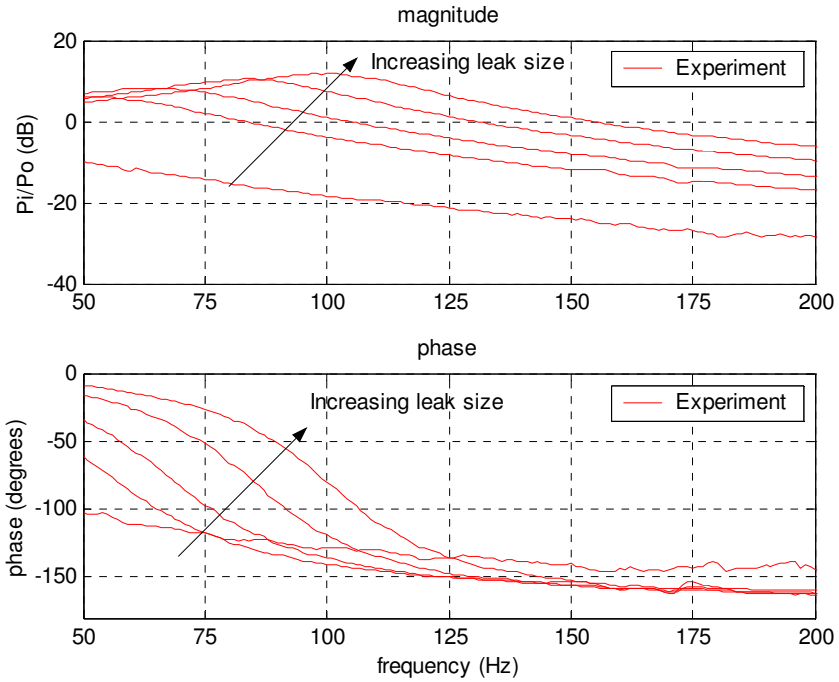

Figure 7.10 Driving point FRF of pressure Pi/Po from experiments

The magnitude of pressure ratio P_i/P_o is plotted versus leak diameter in Figure 7.11. The resonant frequencies are plotted versus leak diameter in Figure 7.12.

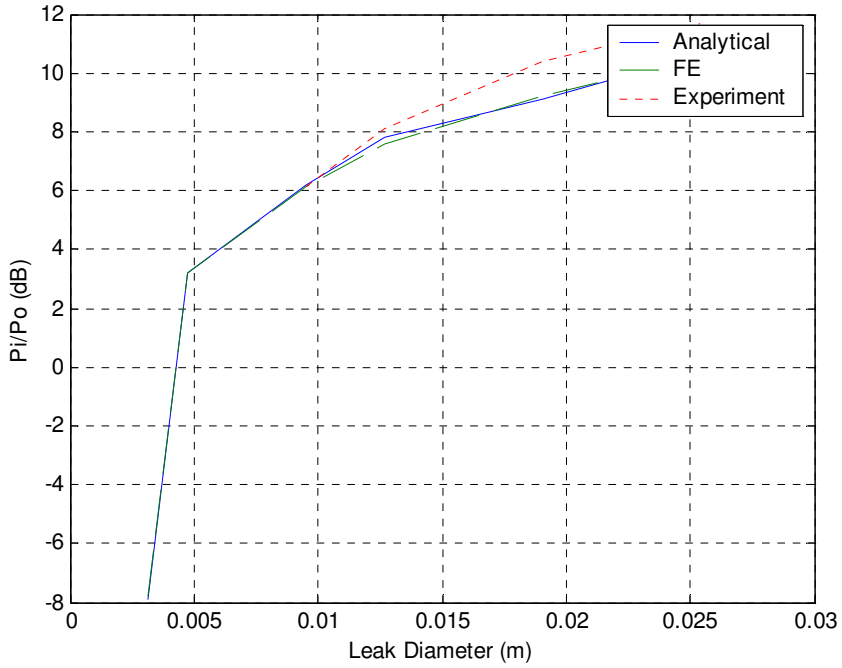

Figure 7.11 P_i/P_o versus leak diameter

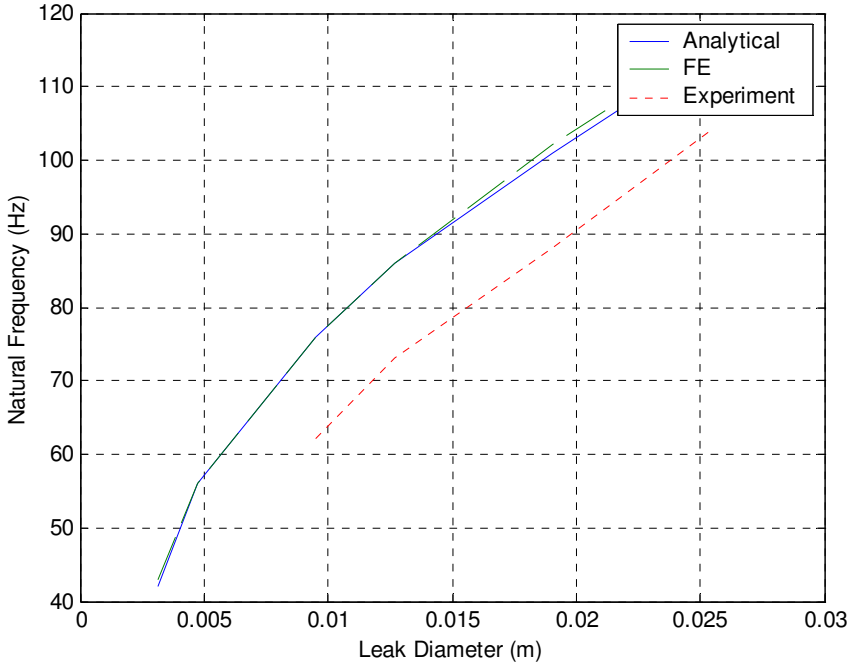

Figure 7.12 Natural Frequency versus leak diameter

It can be observed from the above plots that FE, analytical and experimental results follow the same trend. The amplitude of the pressure ratio P_i/P_o, at resonance and the resonant frequency, increase with the increase in the leak diameter or leak area. The

increase in leak area increases the net force acting on the leak area, which increases the stiffness of the air spring. The increased stiffness of the air spring results in an increase in the inner pressure amplitude of the earcup. This phenomenon is also verified by equation 7.16 [1] derived for Helmholtz resonator in Kinsler and Frey.

$$P_i = \frac{\rho_o c^2 A_l}{\forall_{cup}} x \qquad (Pa) \tag{7.16}$$

As seen in Equation 7.16, the internal pressure of the cup is a function of the volume ($\forall$) of the cup, the leak area (A_l) and the distance the slug of fluid travels (x).

The primary reason for the increase in resonant frequency is the increase in the stiffness of the air spring. However, it is plausible that the thermo viscous damping which is the main damping mechanism in this model, decreases with the increase in leak area, thus allowing the slug of air to move freely. For the smaller leak area the thermo-viscous damping is more and it tends to shift the resonant peak towards left i.e. lower resonant frequency.

The FE results are compared with the experimental results for the given leak sizes in Figure 7.13 (a, b, c, d & e).

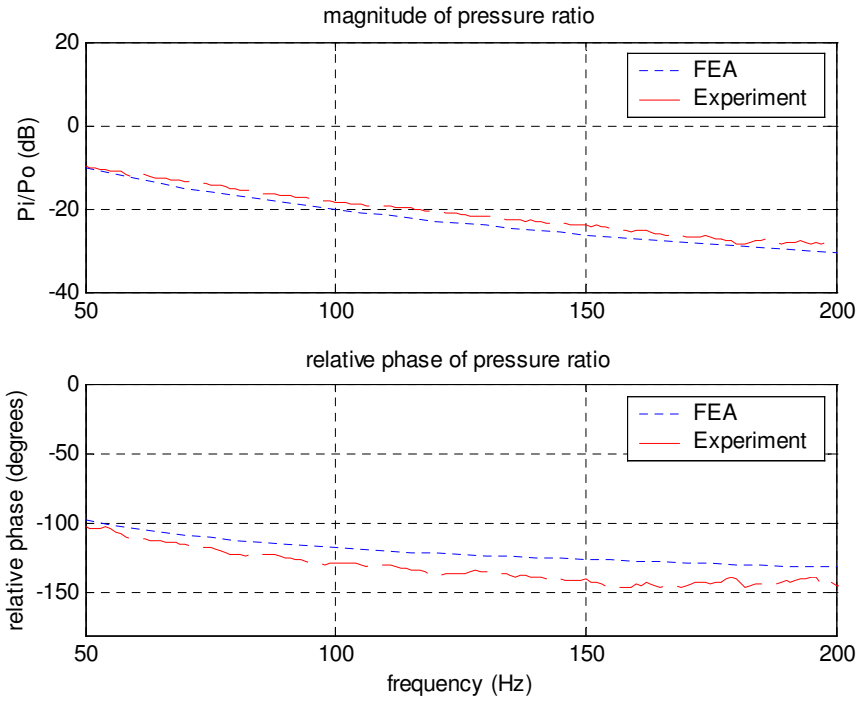

Figure 7.13 (a) Driving Point FRF for 1/8" Leak

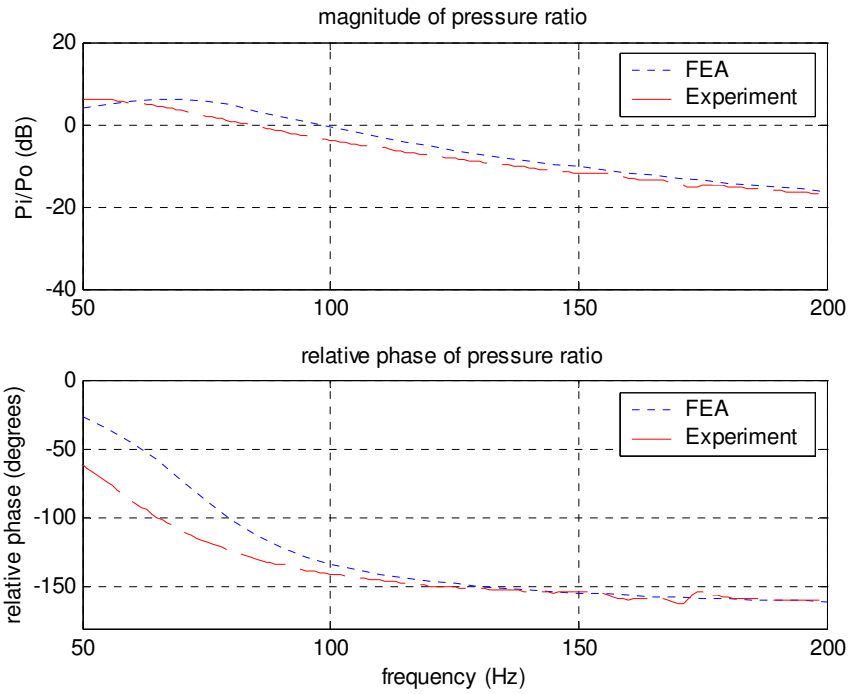

Figure 7.13 (b) Driving Point FRF for 3/8" Leak

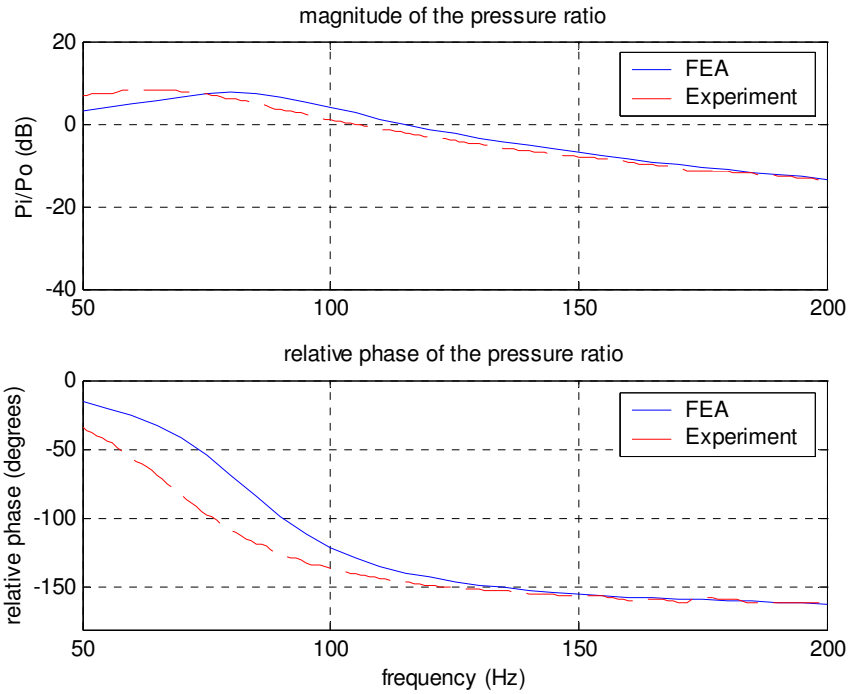

Figure 7.13 (c) Driving Point FRF for 1/2" Leak

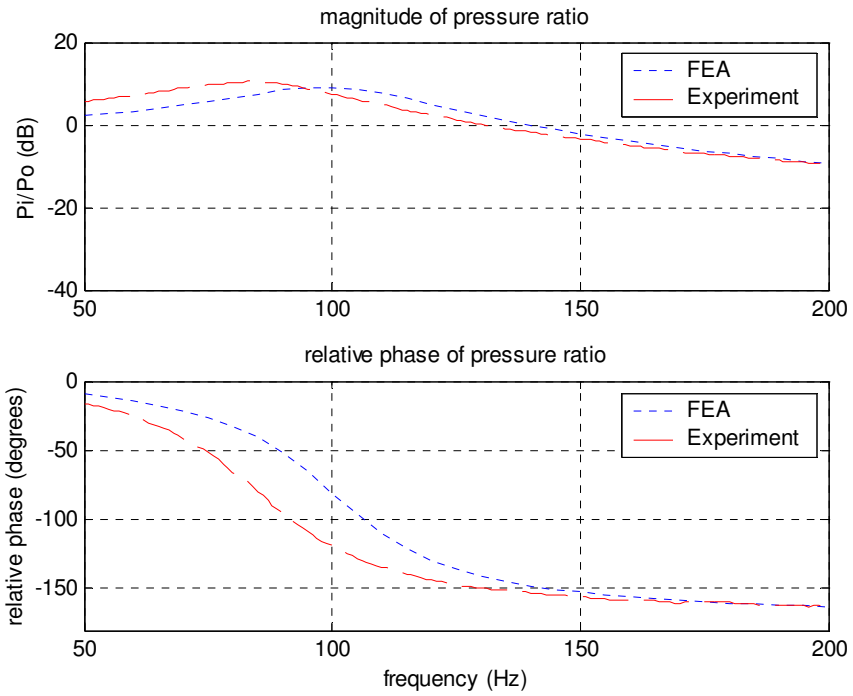

Figure 7.13 (d) Driving Point FRF for 3/4" Leak

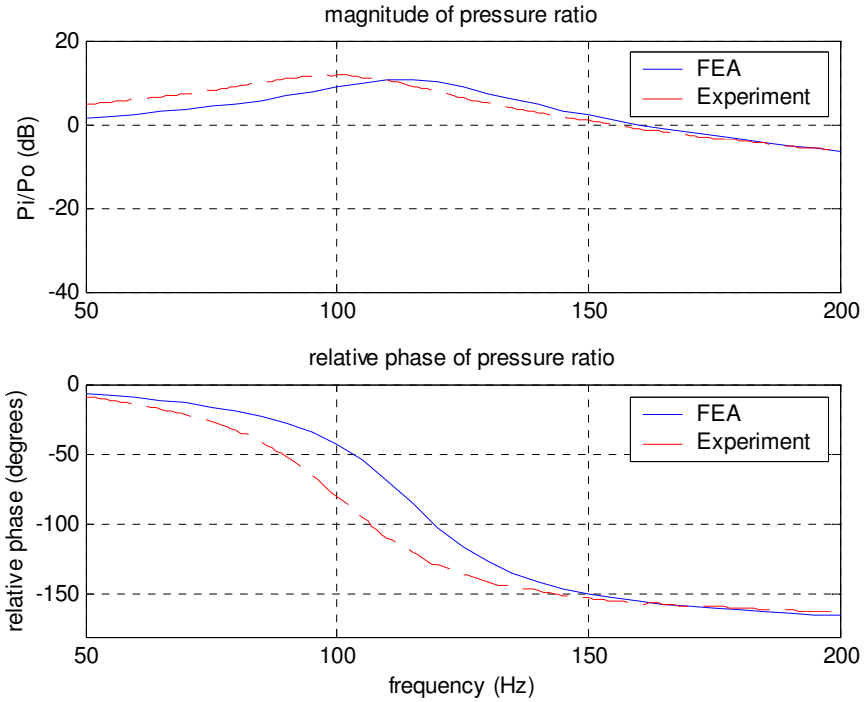

Figure 7.13 (e) Driving Point FRF for 1" Leak

The FE results correlate well with the experimental results for the respective leak sizes. The resonant frequencies and maximum pressure amplitude obtained from experiments and FE analysis are compared in Table 7.4.

Table 7.5 Helmholtz Resonance and Pressure Amplitude for Different Leak Sizes

Leak Size	Natural Frequency			Pressure Amplitude		
(in)	Experiment (Hz)	FE(Hz)	% difference	Experiment (dB)	FE (dB)	% difference
1/8"	-	-		-	-	
3/8"	62	76	22	6.1	6.1	0
½"	73	86	17	8.1	7.6	6
¾"	88	102	16	10.4	9.2	1.1
1"	104	116	13	11.7	10.5	10

The percentage difference calculated in the above table is given by,

$$\%\ difference = \frac{FEA\ value - Experimental\_value}{Experimental\_value} * 100$$

In all the plotted leak cases the difference of the maximum pressure amplitude between the FE results and the experimental results is less than 2 dB. However, it is interesting to note that in all leak cases the resonant frequency peak obtained from FE analysis is shifted 12-14 Hz higher than the experimental curve peak. This is also obvious from the phase plots for the respective leak cases. Once the analysis passes the resonant frequency the experimental and FE curves lie on top of each other.

Although 12-14 Hz shift in resonant frequency is not large considering the whole frequency range from 0 to 200 Hz, but it is important to know the reason for this shift and minimize this difference. The material properties used for air are published values, but the possibility of difference in the medium cannot be ruled out. The dimensions of the earcup's inner fluid volume, leak lengths and the leak areas in the FE model are kept the same as in the experimental setup. The FE model for the leak analysis consists of acoustic elements, there is no solid element present in the model and hence there is no interaction between the fluid and structure. The implied interaction between the fluid and structure is a perfect reflection of acoustic energy i.e. no losses. In the FE model the pressure comes from a single acoustic source and is radiated out of the domain without any reflections into the system.

The experiments for this analysis were not performed in an anechoic chamber and hence there may be reflection of acoustic energy from objects that are present in the surroundings of the test setup and the objects that are part of test setup. The reflected acoustic energy acts as several acoustic sources, which may affect the magnitude and phase of the pressure response. In essence, a better comparison between FE and experimental results is possible if the FE models are coordinated well with the experiments.

7.6 Fluid Structure Coupled Analysis

In the previous section the focus of the analysis was to analyze the isolated leak effects. However, in the actual earcup seal system the modes are coupled and the dynamics of the viscoelastic seal plays as important role in the lower frequency response of the earcup. As mentioned earlier in this thesis, there are two known phenomena, which are believed to be responsible for the performance of the circumaural ear defenders in the lower frequency range. These include the Helmholtz resonator and the piston mode. Since these modes are found very close in the lower frequency range they may have an impact on each other. It is therefore necessary to perform a fluid-structure coupled analysis of the earcup/seal system.

The lower frequency leak analysis is performed for the fluid structure coupled FE models, which include the earcup and the seal. The FE model developed to perform the analysis is shown in Figure 7.14. The inner fluid volume of the earcup is connected to the ambient environment through a leak. The earcup/seal structure is coupled with the fluid domain i.e. fluid elements at the fluid structure interface have displacement DOF which are coupled with the structure displacements.

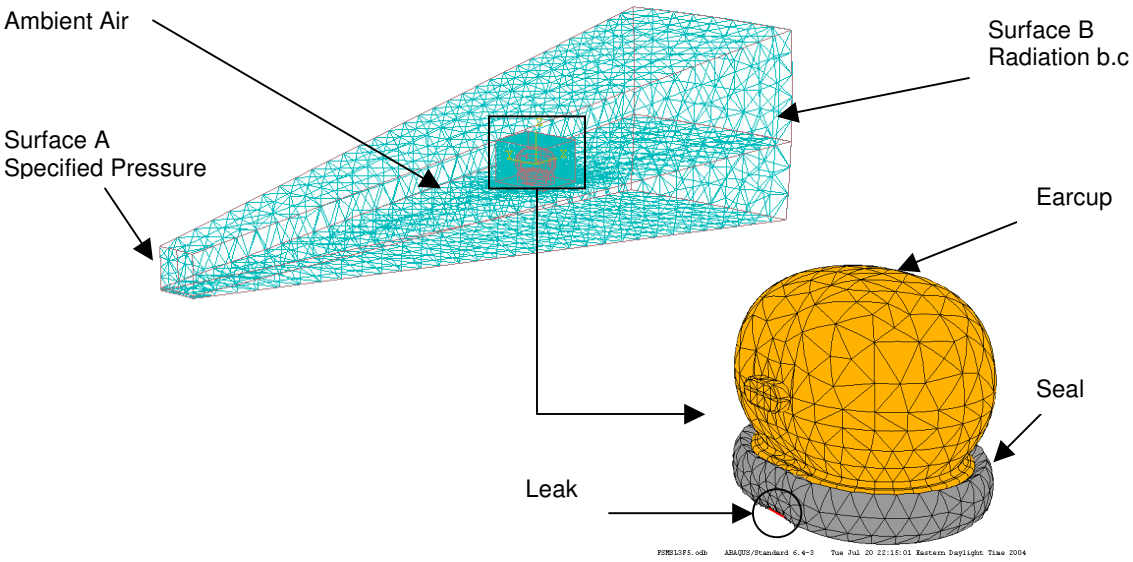

Figure 7.14 Acoustic structure coupled model including leak

Analysis and Results

The analysis consists of two steps, in the first step a static analysis is performed to account for the headband force on the earcup/seal system. The deformed shape due to the preload is shown in Figure 7.15.

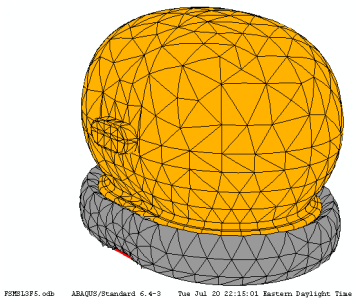

Figure 7.15 Deformed shape of the earcup/seal system due to preload

In the second step, harmonic acoustic pressure is specified at surface A (Figure 7.14), the radiation boundary conditions are specified at surface B. The pressure waves traveling in the fluid domain excites the earcup as well as the fluid mass present in the leak which connects to the inner fluid volume of the earcup.

The coupled field analysis was performed on the earcup seal system for three different leak size, the contour from the FE results is shown in Figure 7.16.

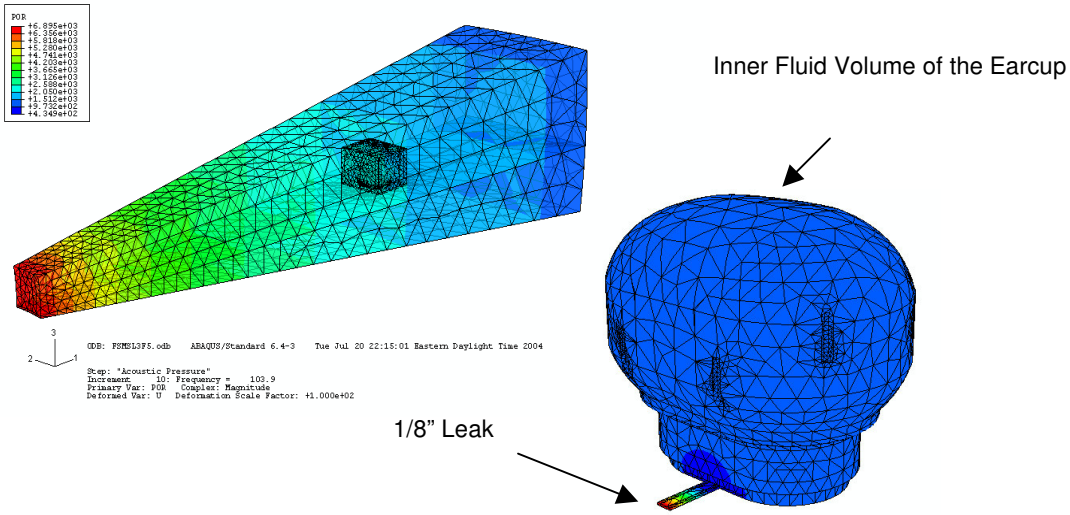

Figure 7.16 FE contour pressure plot for coupled analysis

The contour plot shows the pressure distribution in the external fluid domain, the leak and the inner fluid volume of the cup. It can be observed from Figure 7.16, that the pressure distribution inside the cup is uniform for the lower frequency analysis.

Coupled Analytical Model

The analytical solution to the coupled mode problem is provided by Dr. Kenji Homma of Adaptive Technologies Inc. The coordinate system for the coupled analytical model is shown in Figure 7.17.

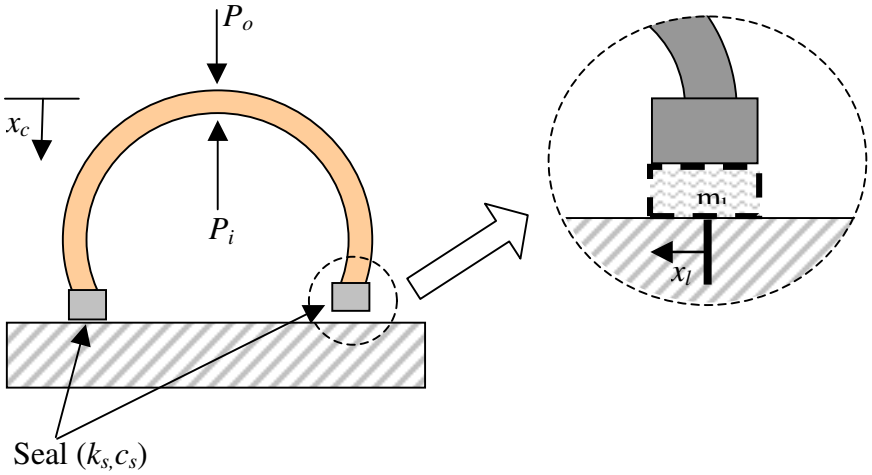

Figure 7.17 Coordinate system for coupled analytical model

The pressure inside the cup is a function of the change of volume within the enclosure. Accounting for this change in volume, and applying the ideal gas law can find an expression for the inner pressure in terms of x_l and x_c.

$$P_i = \frac{\rho c^2 A_c}{\forall_{cup}} x_c + \frac{\rho c^2 A_l}{\forall_{cup}} x_l \tag{7.17}$$

where,

A_c = effective cup surface area

A_l = leak opening area

x_l = leak displacement coordinate

x_c = cup displacement coordinate

The analysis of the coupled system is simplified by transforming the equations into vector form. Equation 7.17 can be represented in matrix form as,

$$P_i = \frac{\rho c^2}{\forall_{cup}} \cdot a^T \cdot \vec{x} \tag{7.18}$$

where,

$$a = \begin{bmatrix} A_c \\ A_l \end{bmatrix}, \qquad \vec{x} = \begin{bmatrix} x_c \\ x_l \end{bmatrix}$$

The external pressure exerts a force on the cup that can be quantified by the displacement of the system. This displacement is a function of the stiffness of the system.

$$k \cdot \vec{x} = a \cdot P_o \tag{7.19}$$

where,

$$k = \begin{bmatrix} m_c s^2 + c_s s + (k_s + k a_c) & \frac{\rho c^2 A_l A_c}{\forall} \\ \frac{\rho c^2 A_l A_c}{\forall} & m_l s^2 + c_l s + k a_l \end{bmatrix}$$

$s = j\omega$

c_s = seal damping coefficient

c_l = damping coefficient for leakage

k_s = seal stiffness

ka_c = air spring stiffness as seen by the cup

ka_l = air spring stiffness as seen by the leak

The expressions for the air stiffness are defined as:

$$ka_c = \frac{\rho c^2 A_c^2}{\forall}$$

$$ka_l = \frac{\rho c^2 A_l^2}{\forall}$$

Equation 7.18 and Equation 7.19 can be combined to create a transfer function between the interior and exterior pressure of the cup.

$$\frac{P_i}{P_o} = \frac{\rho c^2}{\forall_{cup}} \vec{a}^T \bar{k}^{-1} \vec{a} \qquad (7.20)$$

Equation 7.20 is used to obtain the pressure ratio for the coupled piston and Helmholtz resonator mode.

Comparison FE versus Analytical

Harmonic pressure analysis was performed for the leak diameters of 1/8'', 3/16'' and 3/8''. These leak sizes are chosen because they are close to the leaks that occur in the actual earcup seal system. The pressure ratio of the reference pressure outside the cup and the pressure inside the earcup P_i/P_o is plotted versus frequency in Figure 7.17, Figure 7.18 and Figure 7.19 respectively. Figure 7.17 shows the frequency response for the pressure ratio P_i/P_o for the smallest leak size of 1/8". The magnitude of the pressure ratio is within 4 db up to near 150 Hz. It is important to note that the FEA study predicts a smaller pressure ratio with a mean error of -2.17 dB. The FEA phase prediction exhibits the same trend as the analytical solution. The maximum phase difference with the analytical result is approximately 15 degrees and occurs at 90 Hz. The mean error is defined as,

$$\text{Mean Error} = \frac{\sum\{\text{FEA value at n data points} - \text{Analytical value at n data points}\}}{\text{No. of data points}}$$

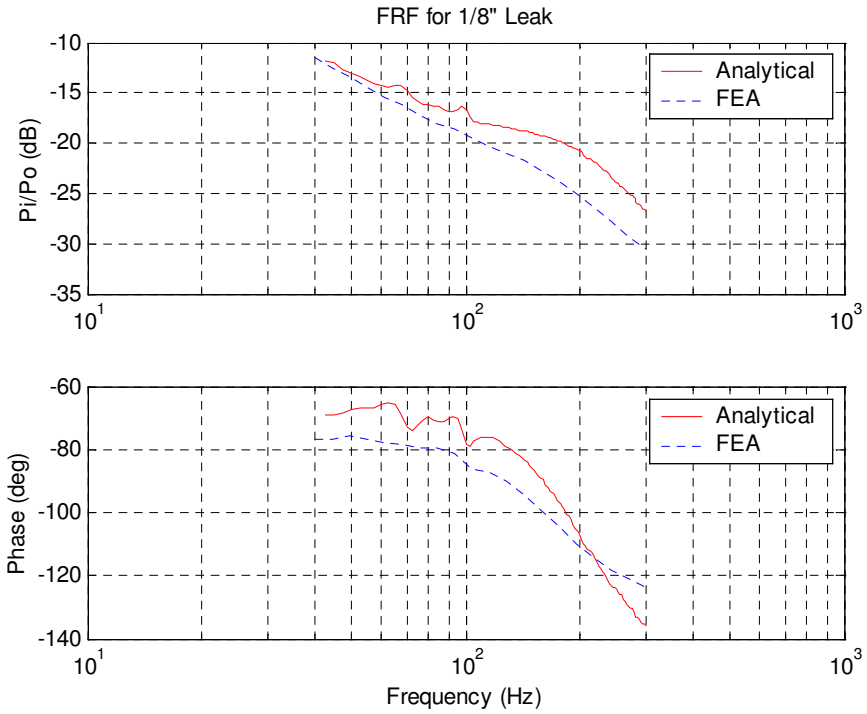

Figure 7.17 Driving point FRF for pressure response (P_i/P_o) for the 1/8" leak

The larger 3/16” diameter leak case shown in Figure 7.18 shows better agreement with the analytical result in both magnitude and phase. The magnitude and phase trends of the FEA and analytical model are highly correlated. The maximum difference in pressure ratio magnitude over the frequency range is about 4 db near 200 Hz. FE predicts a low value of pressure ratio than the analytical with the mean error of -1.67 dB. The phase response of the pressure ratio is further out of phase than the analytical model with a maximum difference of 10 degrees.

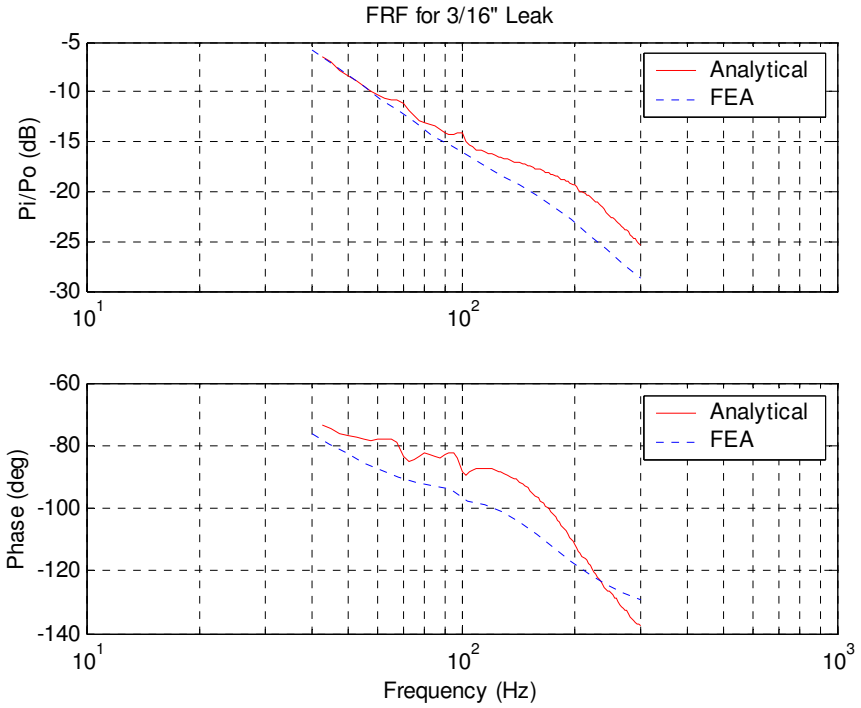

Figure 7.18 Driving point FRF for pressure response (P_i/P_o) for the 3/16” leak

The FE results show good agreement with the 2DOF analytical model for the largest leak size shown in Figure 7.19. The results correlate to within 2 dB in magnitude and 10 degrees in phase. The mean error is 0.88 dB. The FEA error are 4 dB for the smaller leak sizes, Figures 7.17 and 7.18, the difference in results are 4dB. Comparison of the P_i/P_o for the three leak sizes shown in Figure 7.20 conforms to the prior inference for P_i/P_o versus leak size i.e. the amplitude of pressure ratio P_i/P_o and the resonant frequency increase with the increase in the leak area.

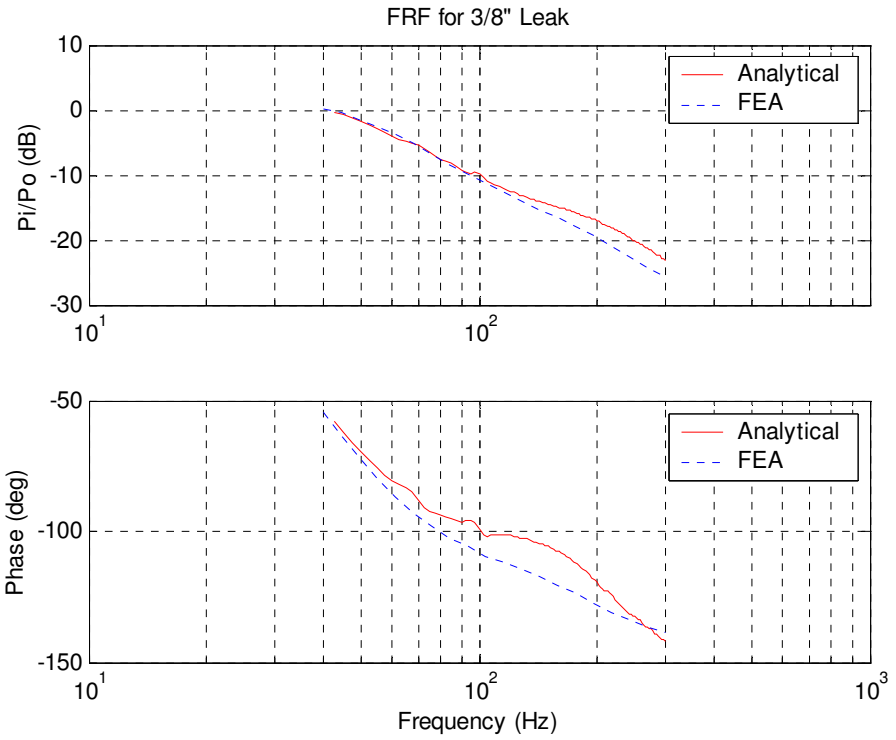

Figure 7.19 Driving point FRF for pressure response (P_i/P_o) for the 3/8" leak

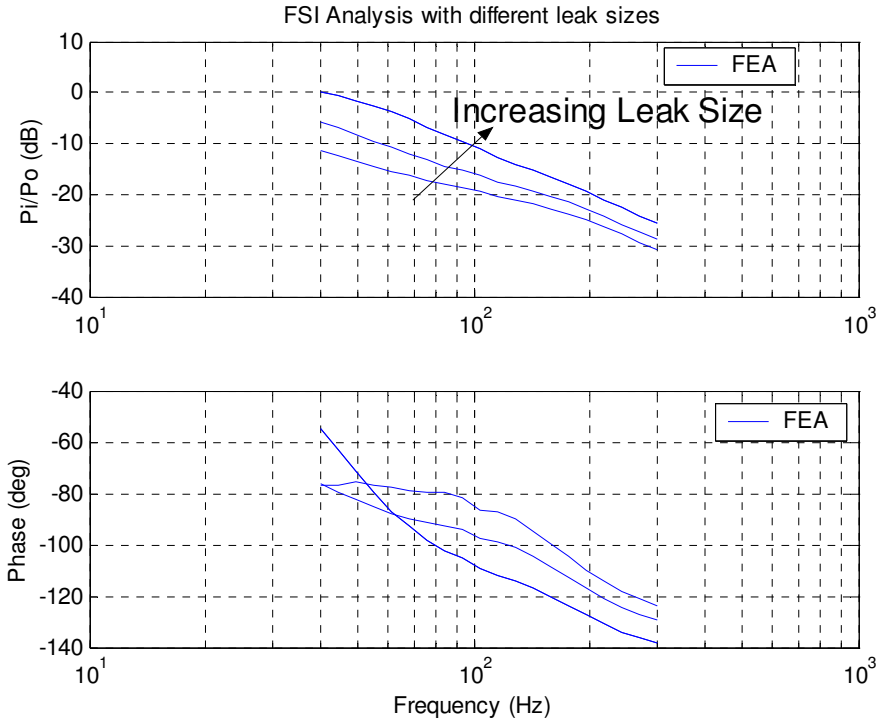

Figure 7.20 Comparison of pressure ratio (Pi/Po) for Fluid Structure Interaction (FSI) analysis for three different leak sizes

However, it is interesting to note that the amplitude of Pi/Po for the earcup/seal system is less than the amplitude of Pi/Po for the rigid earcup. This may be due to the observation that some energy in the system goes into lifting the cup, which gets damped out in the seal, also some energy goes into flexing the cup. For the rigid cup there is no loss of energy, therefore the strength of reflected waves has significant impact on P_i/P_o.

Eliminating Leak

For the purpose of investigating the maximum attenuation at low frequency, a no leak analysis is performed with the fluid structure coupled model. This analysis is similar to the previous leak analysis except that there is no leak that connects the external fluid domain to the internal fluid domain. The only pressure created within the earcup is due to the motion of the earcup/seal system and transmission through the material. The cup flexure modes do not occur between 0 Hz and 200 Hz.

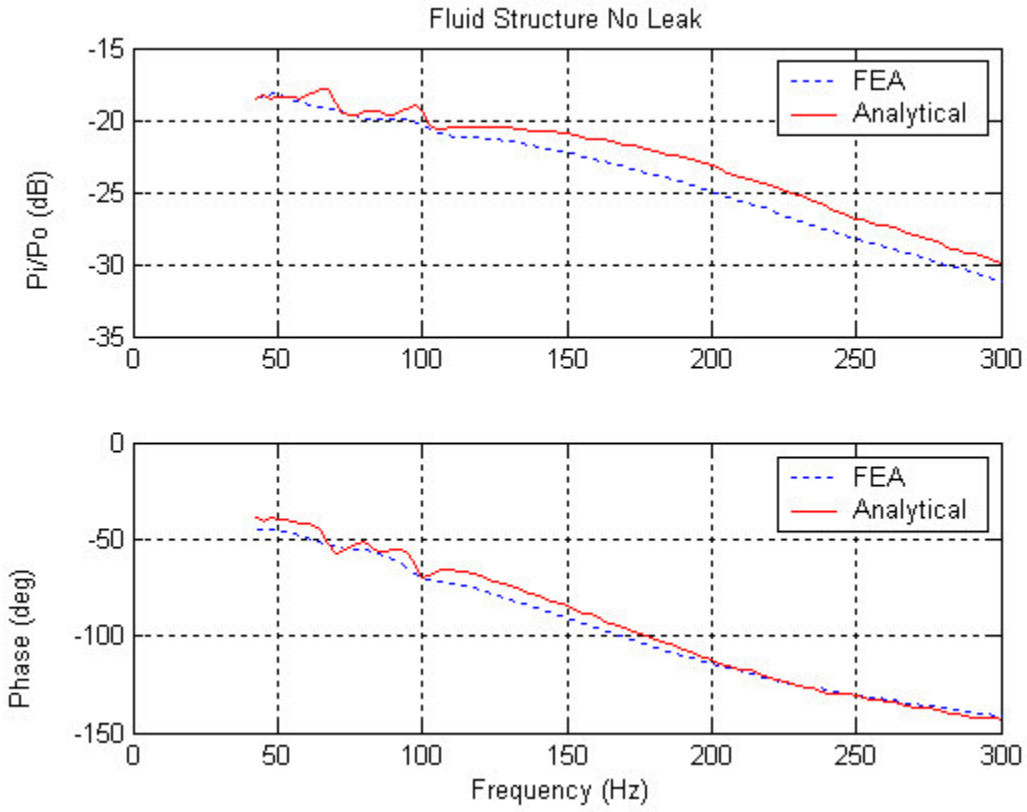

Figure 7.21 Comparison of pressure ratio (Pi/Po) for no leak case

The above plot compares the FE results for the no leak case with the analytical results. . The results correlate to within 2dB in magnitude and 5 degrees in phase. The mean error is –1.5 dB. The maximum amplitude P_i/P_o for the no leak case is –18 dB, where as the smallest leak size has maximum amplitude Pi/Po of –12 dB. It can be inferred from this result, that eliminating the leak could improve the attenuation by 6 dB.

Performance Ratio

One of the most important factors in the FE analysis is the analysis time; the analysis time for the three cases of analysis is tabulated in Table 7.5. It can be noticed that the analysis time is substantially less with use of SGI Altix system.

Table 7.6 Analysis Run Time for FE Models.

Case	No. of Element	Dell Workstation 450 (Run time/Frequency)	SGI Altix 3300 (Run time/Frequency)
Structural Model	12,000	60 sec	-
Acoustic Model	45,000	300 sec	50 sec
Acoustic-Structure Coupled Model	55,000	1000 sec	200 sec

Chapter 8
Conclusion

8.1 Summary of Thesis

The primary goal of this research is to identify, model and explore the physical phenomena that are primarily responsible for the poor performance of circumaural ear defenders at low frequencies (0 Hz – 300 Hz).

Through prior research literature and the experiments performed on the earcup/seal system, it is observed that there are four mechanisms that are primarily responsible for the poor performance of circumaural ear defenders. These mechanisms are,

1. Air leaks, which influence the attenuation in a broad frequency range.
2. Earcup vibration which causes the circumaural earmuffs to work as a mass-spring system generally below 1000 Hz, resulting from the earmuff's inability to fit rigidly against the head.
3. Sound penetration of the earcup and the cushion that limits sound attenuation at frequencies above 1000 Hz.
4. Bone and tissue conduction into the outer, middle and inner ear, which limit's the sound attenuation at frequencies above 1500 Hz.

It is believed that two of these four mechanisms, air leaks and earcup vibration, are responsible for the modes that occur at frequencies below 300 Hz. These modes are recognized as the *Helmholtz mode* and the *Seal Piston mode.*

Due to the presence of leaks, between the earcup seal and the head, the earcup is believed to behave as a Helmholtz resonator at lower frequencies. When a slug of air present in the leak is excited by an ambient pressure source, it starts to vibrate between the inner fluid volume of the earcup and the ambient air, causing a volume change. If an

ideal gas is assumed, the volume change is proportional to the pressure change in the ear cup. The volume change can be enough to cause amplification of noise within the earcup above the ambient pressure.

The seal piston mode occurs when the ambient noise field excites the earcup, such that it starts to vibrate like a piston against the earcup seal. In this case the earcup acts as a rigid mass and the seal as a spring. The compression of the earcup against the seal causes a change in the inner fluid volume and thus causing pressure amplification.

The objective of this research is to model the above-mentioned physical phenomenon. For this purpose, the large volume earcup with soft gel undercut seal is employed in this research. Isolated study of each physical phenomenon is performed and the effects of different parameters on the attenuation are explored. The coupling between the fluid and structure enlightens the fact that the fluid and structure modes have an impact on each other. Therefore, a coupled fluid-structure analysis is also performed.

The analysis of the earcup/seal system involves the structural modeling, acoustics leak modeling and fluid-structure coupled modeling. A simple representation of the Helmholtz and the seal piston mode can be modeled analytically by the single degree of freedom equation that estimates the acoustic pressure response of the earcup/seal system in the lower frequency. The criterion selected to analyze the performance of the earcup is the acoustic pressure ratio P_i/P_o, where P_i is the internal acoustic pressure of the earcup and P_o is the reference acoustic pressure at the external surface of the earcup/seal system. The pressure ratio P_i/P_o, provides normalized amplitude of pressure response inside the earcup.

Although, the analytical models provide a good approximation for the pressure response inside the earcup, these formulations are based on single degree of freedom system with lumped mass assumptions. The actual earcup/seal system is a multi degree of freedom system with mass distributed over the volume of the earcup and the seal. It was therefore necessary to adopt a modeling and analysis tool, which better represents the physics involve in the analysis of the earcup.

A better representation of the earcup/seal system and the physics involved in the analysis of the above mentioned phenomena is achieved by employing the Finite Elements Methods. The FE modeling of the earcup/seal system involves the structural modeling, the acoustic modeling and the fluid structure coupled modeling. The FE analysis consist of the following steps,

4. Build the geometry for the required analysis.
5. Mesh the geometry with appropriate elements to represent the spatial domain.
6. Input material properties data into the software environment.
7. Apply loads and the boundary conditions.
8. Solve the problem.
9. Extract and interpret the FE results.

The geometry of the earcup/seal system was imported into the FE software environment. A very large effort was put into the earcup geometry to make it ready for meshing. Meshing 3-D parts with solid elements requires a great deal of "partitioning" of the CAD geometry definition. The original IGES ear cup definition received from ATI was reworked to remove small lines and define sub volumes so the earcup could be meshed. This was not enough; additional effort was put into the solid geometry to make it efficient for meshing. Meshing controls were placed on individual lines of the new "clean ear cup geometry" to control and produce a very effective meshing scheme for the earcup. As a result the earcup mesh was reduced to 12,000 elements from over 110,000 elements. The reduction in the number of elements is important for an efficient FE analysis because it directly effects the analysis solution times.

The earcup consists of polycarbonate material for which the material properties data was readily available. However, the seal consists of viscoelastic material, which has frequency dependant storage and loss moduli. Enormous efforts were made to come up with a material model, which is adequate for the lower frequency range analysis. Material properties extractions models were created from SDOF and MDOF model. However, insufficient data restricted the utility of these material models. The material properties used in the FE models were extracted from the complex stiffness data that was obtained from experiments.

The geometry of the acoustic leak model was imported into ABAQUS. It consisted of an external air domain, the internal fluid volume of the earcup and the leak volume that connects the internal fluid volume of the earcup to the external fluid domain. The leak sizes were selected to match the experiments i.e. (1", 3/4", 1/2",3/8", 3/16" and 1/8 ").

There were two FE modeling issues in modeling the external domain, the creation of infinite domain and representation of acoustic source. In ABAQUS, applying radiation conditions at the boundary of the acoustic medium creates an infinite acoustic medium. The ABAQUS theory manual [3] recommends modeling a layer of the acoustic medium using finite elements, to a thickness of 1/3 to a full wavelength, out to a "radiating" boundary surface for the lowest frequency to be used in the analysis. The lowest frequency of interest for this analysis was 50 Hz; in order to get accurate results from the FE analysis, the radius of the acoustic medium has to be 1/3 of the lowest wavelength, which in this case is 2.5 m. The radiation boundary condition is then imposed on this surface to allow the acoustic waves to pass through and not reflect back into the computational domain.

The acoustic source was represented as a point source emitting spherical pressure waves. The acoustic pressure could be specified at a node, but creates a singularity in the FE model, which requires a heavy mesh around that particular node to inject acoustic energy from that node into the entire fluid domain. In order to avoid this numerical problem an acoustic pressure was specified over an area so that the intensity of the spherical source remains the same as for the point source.

Some partitioning was performed on the geometry of the acoustic leak model to reduce the number of elements from 90,000 to 45,000 3-D quadratic acoustic elements. This model takes 50 sec to solve for each frequency on the SGI Altix machine.

For lower frequency analysis, damping is calculated from thermoviscous damping model. These damping values are entered in ABAQUS as a volumetric drag term.

The geometry of the fluid structure coupled model is imported into the FE software environment. The modeling issues related to the coupled modeling are similar to those associated with the structural and acoustic modeling. However, defining the fluid-structure coupling is the key to the coupled fluid-structure analysis of the earcup/seal

system. In ABAQUS, a surface-based procedure is used to enforce this coupling. This method requires that the structural and acoustic meshes use separate nodes. The user defines surfaces on the structural and fluid geometries and defines the interaction between the two meshes using the *TIE option. The *TIE command replaces the adjacent fluid and structure elements with the interface elements. The nodes of the interface element possess both acoustic and structure degrees of freedom i.e. the pressure as well as the displacement degrees of freedom.

The initial coupled FE model was consisted of more than 140,000 elements. The geometries of the internal and external fluid domain were partitioned and meshing controls were specified on lines in order to reduce the mesh size to 55,000 elements. This model takes 200 sec to solve for each frequency on the SGI Altix machine.

Modal analysis was performed on the earcup structure in order to locate the earcup elastic modes. The first elastic mode was found at 1076 Hz frequency. This result means that the earcup elastic modes do not significantly affect the pressure response at frequencies below 300 Hz.

Modal analysis was performed on the earcup/seal system. It was found that the seal piston mode occurs at 206 Hz. The seal piston structural modes have a strong influence on pressure response at frequencies below 300 Hz.

Modal analysis was performed on the earcup internal fluid volume in order to locate the earcup internal acoustic modes. The first internal acoustic mode was found at 2201 Hz. As a result the earcup internal acoustic modes do not significantly affect the pressure response at frequency below 300 Hz.

Frequency response analysis was performed to analyze the affects of leak size on the pressure response inside the earcup. The results show that the leak has a dominant impact on the acoustic response at lower frequencies. The dimensions of the leak govern the resonant amplitude of pressure inside the earcup, as well as the resonant frequency. It was observed that both the resonant amplitude of the pressure ratio and the resonant frequency increase as the leak size is increased.

Frequency response analysis was performed to analyze the affects of leak size and the seal piston mode on the pressure response inside the earcup. The results obtained from the coupled analysis also exhibit the same trend of pressure inside the earcup as for

the acoustic only leak analysis. The amplitude of the pressure ratio and the resonant frequency were shown to increase as the leak size increased. However, the overall amplitude of response for the coupled analysis that also includes the seal, was lower than what was observed for the acoustic only leak case or the rigid cup case.

Frequency response analysis was performed to analyze the affects of the seal piston mode on the pressure response inside the earcup. It was observed that eliminating the leak from the earcup/seal system increased the over all attenuation of pressure by 6 dB. This means that the coupling of the Helmholtz mode and the piston mode can cause a 6 dB loss in hearing protection.

8.2 Conclusion of Research

The significance of this research is the use of FE modeling technique for the analysis of circumaural ear defenders. The FE modeling has proved to be very useful for the investigation of phenomena responsible for the performance of the circumaural ear defenders at lower frequency range. The analysis results not only provide information about the structural and internal acoustic mode shapes of the earcup/seal system but also provide the pressure response (0 Hz – 300 Hz) due to excitation through an ambient pressure wave. The findings of this research are,

- The piston mode for the earcup/seal system occurs at 206 Hz and is responsible for poorer performance of the circumaural ear defenders.
- The Helmholtz resonator mode occurs at low frequency (below 300 Hz) due to the presence of acoustic leaks
- The amplitude pressure ratio P_i/P_o and the resonant frequency associated with the Helmholtz resonator mode increase with the increase in the leak size.
- The amplitude of pressure ratio P_i/P_o for the earcup/seal system is less than the amplitude of P_i/P_o for the rigid earcup case.
- The coupled model for the smallest leak size i.e. $1/8^{th}$ predicts the maximum amplitude of P_i/P_o is –12 dB.
- Eliminating the leak improves the attenuation of the earcup/seal system by 6 dB.
- For the mid frequency range there are resonances due to earcup's structural modes and the internal acoustic modes that occur due to the formation of standing waves in the internal fluid volume of the earcup.

8.3 Recommendations for Future Work

The current research has led to a better understanding of phenomena that are responsible for the lower frequency acoustic response of the earcup, but a lot has to be done to develop a earcup seal system which will attenuate the sound pressure more effectively.

Although, the FE models developed in this research correlate well with the analytical and experimental results, but there is a need to coordinate the FE modeling efforts with the experimental testing. A better correlation between FE and experimental results can be achieved by coordinating test and model development realize practical test and model conditions

The FE software issues regarding the lower frequency acoustic and structure modeling are resolved. One of the most important factors in FE modeling is to get the appropriate material properties into the FE model. The material properties for earcup were readily available but the most challenging work regarding the FE modeling in this research work is to get the appropriate material properties for the viscoelastic seal material. The material model used in this research is good enough for lower frequency range, but a proper system identification process is required to come up with the material model that is appropriate for lower frequency as well as the mid frequency range.

References

[1] L.E. Kinsler, A.R. Frey, A.B. Coppens, J.V. Sanders, *Fundamentals of Acoustics*, 4th ed., John Wiley & Sons Inc. New York, 2000.

[2] F. Fahy, *Sound and Structural Vibration*, Academic Press, 1985.

[3] "ABAQUS Theory Manual" ver 6.4, ©ABAQUS, Inc. 2003

[4] Von Gierke, H.E., and Warren, D.R., "Protection of Ear From Noise: Limiting Fators," *Benox Report*, 1953 contract N6 orl-020 Task Order 44, University of Chicago.

[5] G.J. Thiessen, E.A.G. Shaw, "Ear Defenders for Noise Protection," *Aviation Medicine*, pp 810-814, November 1958.

[6] Zwislocki, J., "In search of bone conduction threshold in a free sound field," *The Journal of the Acoustical Society of America*, 29(7), 795-804, 1957.

[7] G.J. Thiessen, E.A.G. Shaw, "Acoustics of Circumaural Earphones," *The Journal of the Acoustical Society of America*, vol. 34, pp 1233-1246, September 1962.

[8] Berger, E.H., "Laboratory Attenuation of Earmuffs and Earplugs Both Singly and in Combination," *American Industrial Hygiene Association Journal,* 44(5) 321-329, 1983.

[9] Goff R.J., Blank W.J., "A field evaluation of muff-type hearing protection devices," *Sound and Vibration Journal,* 18(10), 16-22, 1984.

[10] R. Pääkkönen, "Effects of cup, Cushion, Band Force, Foam Lining, and Various Design Parameters on the Attenuation of Earmuffs," *Noise Control Engineering Journal*, vol. 38, n2, pp 59-65, 1992.

[11] T.W. Rimmer, M.J. Ellenbecker, "Feasibility Assessment of a New Method for Measurement of Hearing Protector Attenuation: Bone Conduction Loudness Balance," *Applied Occupational and Environmental Hygiene Journal*, pp 69-75 E.H, January 1997.

[12] Berger, R.W. Kieper, Dan Gauger, "Hearing Protection: Surpassing the Limits to Attenuation Imposed by the Bone-Conduction Pathways*," The Journal of the Acoustical Society of America*, vol. 114, n4, pp 1955-1967, 2003.

[13] R.S. Birch, S. N. Gerges, E. F. Vergara, "Design of a Pulse Generator and Shock Tube for Measuring Hearing Protector Attenuation of High-Amplitude Impulsive Noise," *Journal of Applied Acoustics*, vol. 64, pp 269-286, 2003.

[14] W. J. Murphy, E. H. Berger, A. Behar, J. G. Casali, C. Dixon-Ernst, E. F. Krieg, B. T. Mozo, J. D. Royster, L. H. Royster, S. D. Simon, C. Stephenson, "Development of a New Standard Laboratory Protocol for Estimation of the Field Attenuation of Hearing Protection Devices: Sample Size Necessary to Provide Acceptable Reproducibility," *The Journal of the Acoustical Society of America*, vol. 115, n1, pp 311-323, January 2004.

[15] D.J. Nefske, J.A. Wolf, Jr. and L. J. Howell, "Structural Acoustic Finite Element Analysis of The Automobile Compartment: A Review of Current Practice", *Journal of Sound and Vibration*, 80(2), 247-266, 1982.

[16] O.C. Zienkiewicz and P. Bettess, *Numerical Methods in offshore Engineering* Chap. 5, John Wiley and Sons Ltd, 1978.

[17] L.Kiefling, G.C. Feng., " Fluid Structure Finite Element Vibrational Analysis", *AIAA Journal*, vol. 14 no. 2, 1976.

[18] Jonathan D. Sides, "Low Frequency Modeling and Experimental Validation of Passive Noise Attenuation in Ear Defenders." Masters Thesis, Virginia Polytechnic Institute and State University, Blacksburg, VA, 2004

Appendix A
FE Software Verification Studies

A1. Transmission Loss Study

The purpose of this study is to calculate transmission losses, for the case of plane acoustic wave traveling in one medium (water) encounters another medium (steel plate) of some thickness 'L' and then transmitted to a third medium (water). When an acoustic wave traveling in one medium encounters the boundary of a second medium reflected and transmitted waves are generated. If the amplitude of the pressure of the incident wave is P_i and that of transmitted pressure is P_t then the transmission coefficient T is the ratio of transmitted pressure to incident pressure, transmission coefficient is used to calculate transmission loss

The analysis is performed using ANSYS which is capable of performing both coupled & uncoupled acoustics analysis. However, we are interested in the coupled fluid structure analysis, which takes fluid structure interaction into account. The model consists of a water channel, at the center of which there is a steel plate which acts as a partition between the two fluid (water) mediums. A pressure wave is generated on the left side of the channel; the pressure incident on the partition & the transmitted pressure is obtained from the analysis. These pressures are used to calculate transmission coefficient and transmission loss. The results are also verified by analytical solution

Problem Description

In this problem we have channel carrying water which is separated by a steel plate as shown in Figure A1.1. A plane pressure wave of pressure 1 Pa is generated in the left portion of the channel at a distance of 1.5m from the partition. Analysis is to be done for partition thickness of 0.015m & 0.05m, in order to determine the effects of the stiffness of the partition on transmission loss.

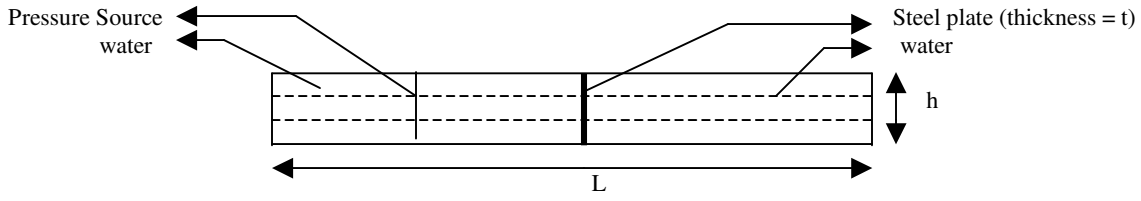

Figure A1.1 Schematic diagram of channel containing water partitioned by a steel plate.

Geometry

L = 6m
t = 0.015m (for first run)
t = 0.05m (for second run)
h = 0.2m
Press = 1 Pa

Material Properties

Steel

Density = 7700 Kg/m^3
Young's Modulus = 19.5e^{10} Pa
Poisson's Ratio = 0.29
Speed of Sound in Steel = 5050 m/sec

Water

Density = 1000 Kg/m^3
Speed of Sound in Water = 1481 m/sec

Modeling

The system is modeled in ANSYS to carry out the acoustics analysis. Seven areas are created as shown in Figure A1.2 (a, b and c). Solid plane 42 elements are used to mesh Area 7 which represents a partition (steel plate). Areas 2 & 6 are adjacent to area 7 and are meshed with Fluid 29 elements with key option '0' i.e. structure present option. Fig 1.2 c shows meshed areas 2, 6 & 7 the boundary between Plane 42 elements and Fluid 129 elements is marked as the Fluid Structure Interface (FSI).

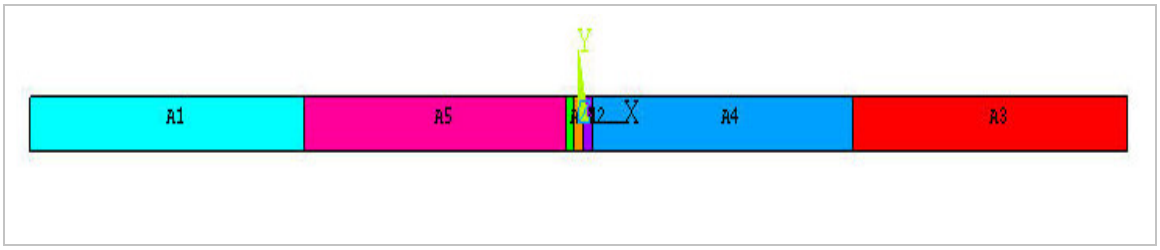

Figure A1.2 a: seven areas each represented by different color.

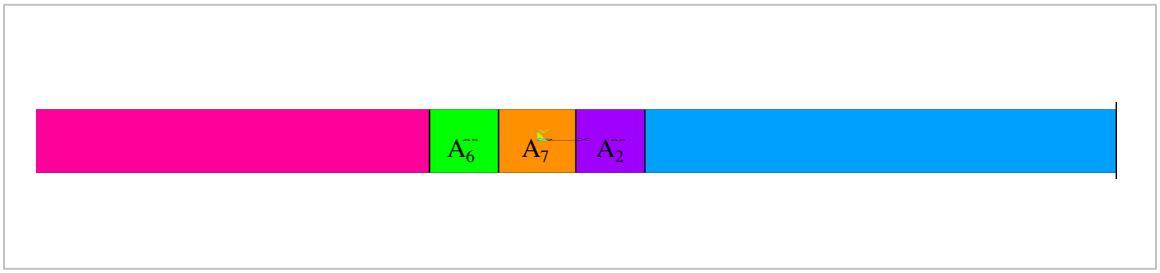

Figure A1.2 b: zoomed view of areas 2, 6 & 7

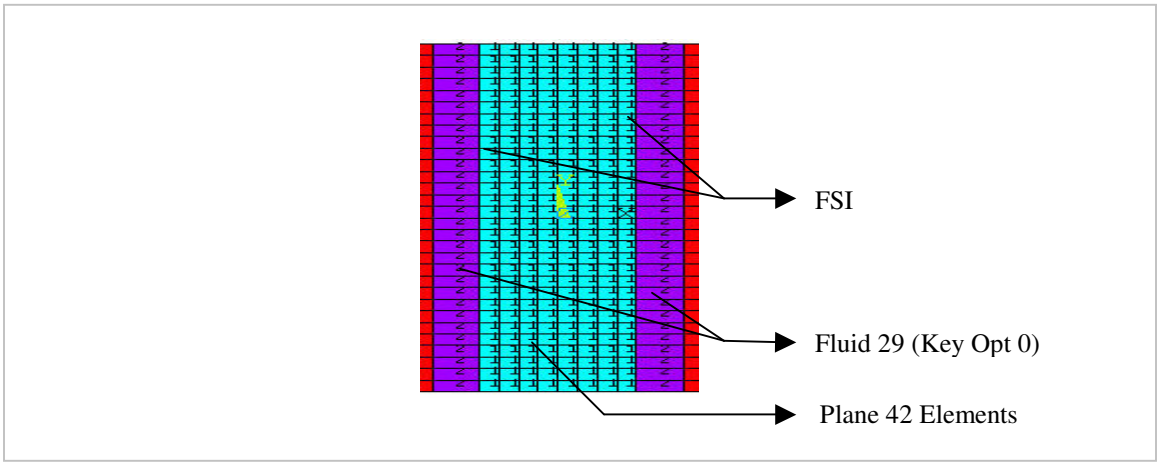

Figure A1.2 c meshed areas 2, 6 & 7

Areas 1, 3, 4 & 5 in Figure A1.2 a are meshed with Fluid 29 elements with key option '1' i.e. structure absent option. At the ends of the channel Fluid 129 (infinite acoustic elements) are created. The meshed areas 3 & 4 & the infinite acoustics elements are shown in Figure A1.3.

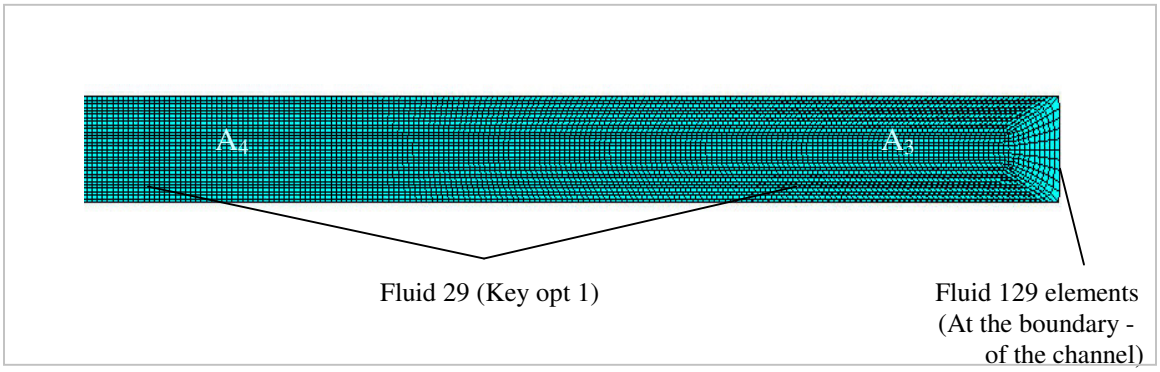

Figure A1.3 Meshed areas 3 & 4. Infinite acoustic elements at the boundary of the channel

Loads & Boundary Conditions

A plane pressure wave of 1 Pa at 2000 Hz is generated towards the left of the channel which is acting normal on the steel partition the partition is constrained so that it can not move in x & y direction. Infinite acoustic elements at both ends of the channel provide an absorbing boundary condition so that an outgoing pressure wave reaching the boundary of the model is absorbed with minimal reflection into the fluid domain. Figure A1.4 shows a comprehensive model with all elements, loads & boundary conditions.

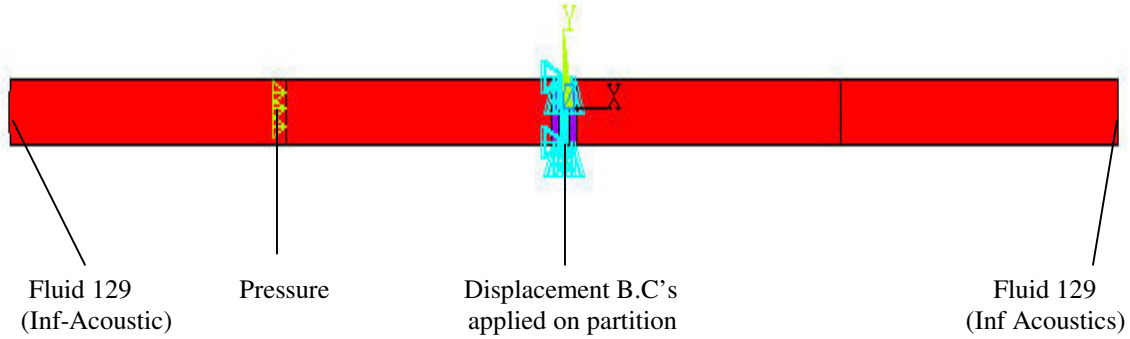

Figure A1.4 Comprehensive view of the model & B.C's

Analysis Solution Process

Harmonic Analysis is performed on the model for three different thicknesses of the steel partition and three different thicknesses of the fluid structure interface. The pressure incident on the partition and the pressure transmitted through the partition are obtained from FEA results and are used to calculate transmission coefficient and the transmission loss by using following relations,

Transmission Coefficient: $T = P_t / P_i$ (A1.1)

Transmission Loss: $TL = 10 \, Log \, (1/T)$

where,

P_i = Amplitude of incident pressure
P_t = Amplitude of transmitted pressure

For analytical solution, the expression used to calculate transmission coefficient is,

$$T = \frac{4n}{\left[(\omega m - s/\omega) / \rho_2 c_2 \right] + \left[\omega_o m \eta / \rho_2 c_2 + n + 1 \right]^2} \quad \text{(A1.2)}$$

where,

ρ is the density of the fluid medium.
c is the velocity of sound in fluid medium.
s is stiffness of the partition.
η is the loss factor.
m is the mass per unit area of the partition.
n is the ratio of acoustic impedance.

Results

Figure A1.5 below compares the current ANSYS FEA transmission loss computations to the expected transmission loss values according to Equation 1.0 cited earlier. Work is ongoing to identify reasons for the differences in the two results; however, it should be stated that the trend is very good and the approach seems very encouraging. It is well known that precise boundary conditions of a panel subject to an incident pressure field will have a significant influence on the TL values. Equation 1.0 is based on "infinite" panel dimensions where the boundary conditions have not been taken into account. It is precisely this type of limitation in the analytical-based solutions that call for exploration of the FEA solution methodologies being investigated in this Phase I program.

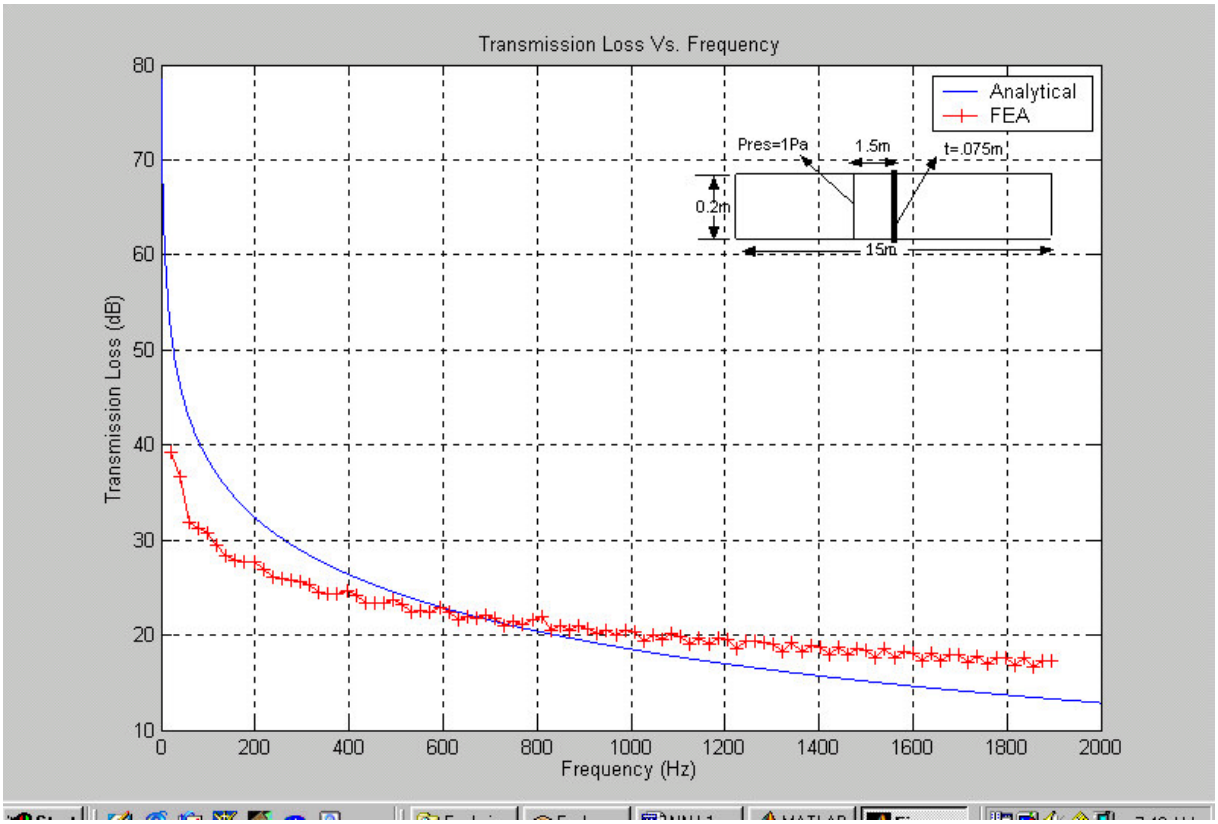

Figure A1.5: Comparison of current ANSYS TL calculations for a plane wave incident on a 0.015 m steel panel in a heavy (water) fluid; comparison to analytical TL from Equation 1.0

A2. Coupled Acoustic Structure Study

The objective of the FEA validation problem presented next is to verify the accuracy of ANSYS modeling algorithms in predicting the response of a fluid-structure coupled field analysis. The reason for performing this analysis is that ear cups are surrounded by an acoustic medium (air), and the interaction between certain cup materials and the fluid may alter the natural frequencies of the ear cup from its in-vacuo values. Modal analysis is then performed with ANSYS to find the natural frequencies of a fluid loaded structure. The other phenomenon investigated during the analysis is the pressure-velocity coupling generated in the fluid due to a prescribed velocity of a piston. Harmonic analysis is performed with ANSYS to investigate the pressure generated due to a harmonic velocity. The problem selected for the analysis is a spring mounted piston sliding in a thin cylindrical tube containing water, terminated by a rigid end cap.

FEA Modeling Solution

The system is modeled in ANSYS as a 2-D axi-symmetric model. The reason to for this approach is that a 2-D axi-symmetric representation can be used to represent most of the physics associated with the actual 3-D system. This approach minimizes the computing resources required to investigate the model. The Figure below shows the schematic of the FE model.

Mesh Information

Piston: Solid, axisymmetric elements, (ANSYS Plane 42).

FSI: Fluid, axisymmetric elements, structure present. (ANSYS Fluid 29)
Ux, Uy and dynamic pressure degrees of freedom.

Water: Fluid, axisymmetric, structure absent. (ANSYS Fluid 29)
Dynamic pressure degree of freedom

Loads and Boundary Conditions

The boundary conditions are applied to perform the modal analysis with ANSYS. The piston is constrained to move only in y-direction. The bottom nodes of the spring

elements are constrained not to move. The boundary between solid and fluid elements is marked as a fluid structure interface (FSI) Figure A2.1.

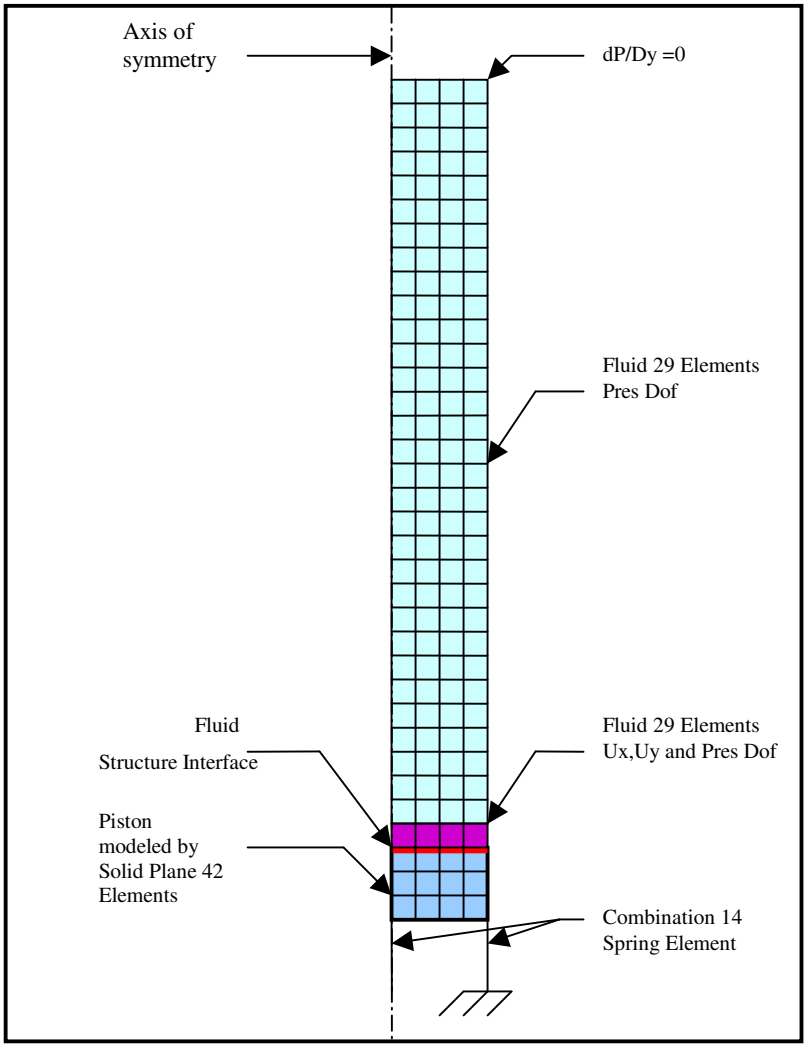

Figure A 2.1 Schematic diagram of the FEA Model.

Water was chosen as the fluid for this problem, in order to exaggerate the effects of fluid loading. This problem is considered for the analysis because the analytical solution to this classical problem is well known. The FEA results will then be compared with the analytical results. The boundary conditions applied to the model, the modal analysis, and the harmonic analysis are evident from the figure (continuity of velocity at the piston face and zero velocity at the closed end of the tube). The geometric dimensions of the tube, material properties and the physical properties are given below:

Table A 2.1 Properties for FSI Problem

Geometric Properties	Steel Material Properties	Water Properties	Physical Properties
L = length of tube = 20 m	Density = 7700 kg/m^3	Density = 1000 kg/m^3	Mass of the piston = 12.252 kg
d = diameter of tube = 0.2m	Young's Modulus = 19.5e^{10} Pa	Phase Speed in Water = 1481 m/sec	Stiffness of the Spring = 4836978 N/m
h = height of piston = 0.05m	Poisson's Ratio = 0.29		
	Phase Speed in Steel = 5050 m/sec		

Effects of Fluid Loading on Structure's Natural Frequency

In order to determine the effects of fluid loading on the spring piston's natural frequency, the in-vacuo natural frequencies and the fluid structure coupled natural frequencies are obtained by performing a modal analysis with ANSYS. The results will then be compared with the analytical solution shown below.

Analytical Solution

The appropriate equation for simple harmonic motion of a fluid loaded piston is given by,

$$\tilde{F} = j\omega\xi\left(\pi r^2\right)\left(\bar{z}_a + \bar{z}_p\right) \qquad \text{(A2.1)}$$

where,

$\tilde{F}$ = force

r = radius of piston

ξ = line displacement

$\bar{z}_a$ = acoustic impedance of a column of fluid

$\bar{z}_p$ = impedance of in-vacuo piston

The natural frequency of the coupled system corresponds to the condition $\tilde{F} = 0$, i.e. the total impedance vanishes. Hence,

$$\cot(kl) = \left(\beta^{-1}\right)\left(\frac{kl}{k_o l}\right)\left[1 - \left(\frac{k_o l}{kl}\right)^2\right] \qquad \text{(A2.2)}$$

The term on the left hand side of the Equation 1 is the eigen frequency function. The term on the right consists of β, kl and kol where, β is the ratio of characteristic specific acoustic impedance of the fluid to the magnitude of the impedance of the piston mass per unit area at the in-vacuo natural frequency , kl is the normalized wave number at any frequency and kol is the normalized wave number at in-vacuo natural frequency ω_o.

$$\beta = \frac{\rho_o c A}{M \omega_o}$$

ρ_o = mean fluid density

A = cross-section area of piston

ω_o = in-vacuo natural frequency of the structure = $\sqrt{\frac{K}{M}}$

K = stiffness of the spring

M = mass of the rigid piston

k_o = wave number = ω_o / c

c = the speed of sound in fluid

l = the length of the tube

The peaks in Figure A2.2 below correspond to the wave numbers at the natural frequency. The natural frequencies are obtained by using the relation $k = \omega / c$.

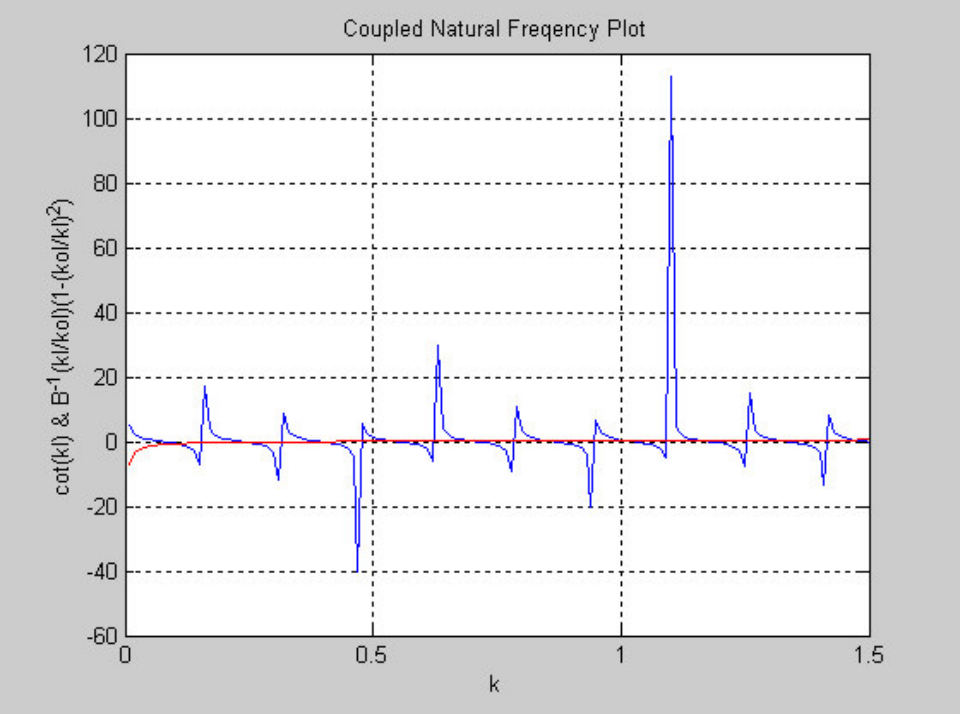

Figure A2.2 Plot of cot(kl)= β-1(kl/kol)(1-(kol/kl)2) vs. k

Results

The results obtained by FEA analysis are tabulated below. It can be seen from Table A2.2 that the fluid structure interaction has significant effects on the natural frequencies of the spring piston system as expected, and that the FEA calculation is valid as shown next.

Table A2.2 Coupled Natural Frequencies FEA versus Analytical

No.	Coupled Natural Frequency FEA(Hz)	Coupled Natural Frequency Analytical(Hz)	% Difference Coupled Natural Frequency
1	25.3	25.0	1.2
2	57.9	57.7	0.3
3	92.9	92.9	0. 0
4	128.6	128.6	0.0
5	164.6	164.6	0.0
6	200.8	200.8	0.0
7	237.0	237.0	0.0
8	273.3	273.3	0.0
9	309.7	309.7	0.0
10	346.1	346.1	0.0

Frequency Response Problem

The velocity pressure coupling is now investigated by performing harmonic analysis with ANSYS and the results are compared with the analytical solution for the harmonic plane wave.

Analytical Solution

The pressure gradient of the fluid is given by Euler Equation,

$$\frac{\partial P}{\partial x} = -\rho\omega^2 U_y \tag{A2.3}$$

where,

$\frac{\partial P}{\partial x}$ = pressure gradient

ρ = mean fluid density

ω = the forcing frequency

U_y = prescribed displacement

The complex form of the harmonic solution for the acoustic pressure of a plane wave is

$$P = Ae^{j(\omega t - kx)} + Be^{j(\omega t + kx)} \tag{A2.4}$$

and after differentiation with respect to *x,*

$$\frac{\partial P}{\partial x} = (-ik)Ae^{j(\omega t - kx)} + (ik)Be^{j(\omega t + kx)}$$

Factoring out $e^{\omega t}$ for steady state acoustics, $\frac{\partial P}{\partial x}$ can be written as,

$$\frac{\partial P}{\partial x} = (-ik)Ae^{-jkx} + (ik)Be^{+jkx} \tag{A2.5}$$

Two boundary conditions are obtained from Equation 2 for *x=0 and x=L.*

$$\frac{\partial P}{\partial x} = -\rho\omega^2 D \quad @\ x=0 \quad \text{(driver/piston end)}$$

$$\frac{\partial P}{\partial x} = 0 \quad @\ x=L \quad \text{(closed end of the tube)}$$

These two boundary conditions give two equations and two unknowns (A and B) when applied to Equation 5. The values of A and B are substituted in Equation 3 to obtain the values of the pressure at a particular location *x*. The pressure at any location *x* is given by,

$$P = 2C\cos kx + 2D\sin kx \qquad \text{(A2.6)}$$

where C and D are constant coefficients, *k* is the wave number.

FE Modeling of Harmonic Response

The FE model used to perform the harmonic analysis is the same model used for the modal analysis except for the prescribed displacement at the structure (piston) elements (refer back to Figure A2.1).

Loads and Boundary Conditions

A prescribed displacement of the piston oscillating at a specified frequency is used to perform the harmonic analysis. The piston displacement is a prescribed axial displacement of 2 x 10-11meters. The forcing frequency ranges from 0-500 Hz with a frequency resolution of 1 Hz.

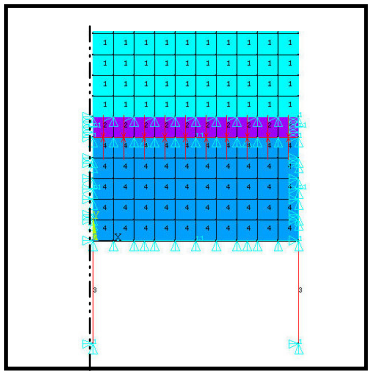

Figure A2.3 Boundary conditions for harmonic analysis

Results

The pressure generated due to the prescribed displacement is determined at the driver end (piston end) and at the closed end where the velocity is zero. The results obtained by FEA and analytical solutions are plotted in the following FRF plots. Figure A2.3 (a & b) shows the plots of the impedance frequency response function at the piston end and the impedance frequency response function at the closed end respectively versus the frequency. These plots indicate the excellent agreement between the frequency response function predictions using ANSYS. The peak values at each resonance are not identical because no attempt was made to calibrate damping values between the two solution approaches.

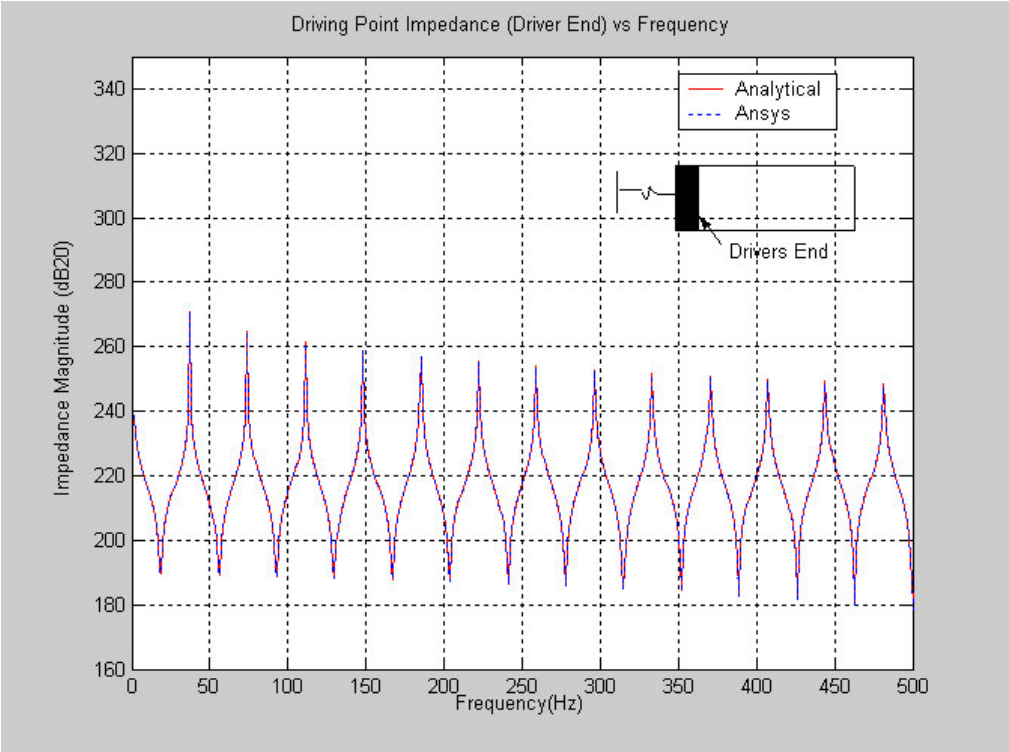

Figure A2.4 (a) Driving point impedance vs. frequency, prescribed displacement of 2e- 11m

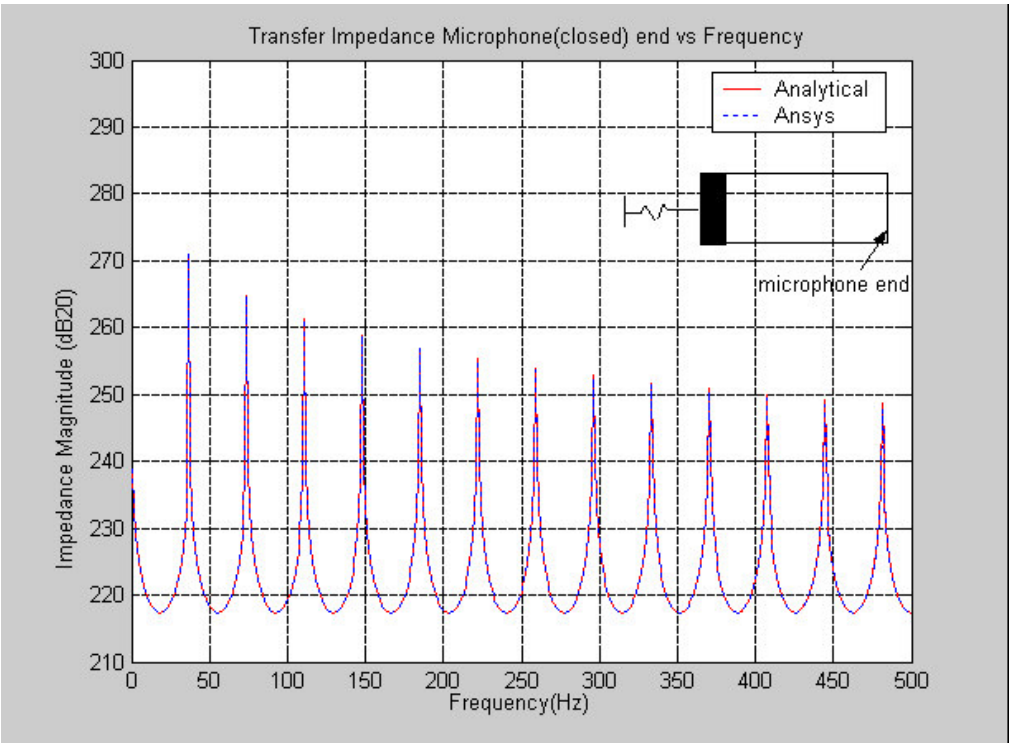

Figure A2.4 (b): Transfer impedance vs. frequency, prescribed displacement of 2e-11m

The peaks in the above plots correspond to the resonance. It can be seen that the peak amplitude at resonance is decreased as the frequency is increased this is due to the fact that at higher frequencies the pressure amplitude gets lower.

FEA Conclusions of Validation Problems

Since the FE results obtained from the modal analysis and the harmonic analysis performed with ANSYS compared well with the analytical solution it could be concluded that FEA using ANSYS is valid for performing acoustics coupled field analysis of any structure. The in-vacuo and the acoustics natural frequencies of the ear cup can be obtained by performing modal analysis with ANSYS. Similarly, the pressure generated inside the ear cup due to the vibration of the cup material could be predicted by performing harmonic analysis with ANSYS. These essential results confirm the ability of the FEA modeling to accurately assess the transmission loss, fluid-structure interaction, and harmonic analysis.

APPENDIX B

Material Properties Data

B1. Viscoelastic Material Data For ABAQUS

m_1, m_2, m_3, m_4, Frequency (Hz)

```
2.4650E+001,-2.4030E+001,2.4650E+001,-2.4030E+001,4.3750E+001
2.3678E+001,-2.4652E+001,2.3678E+001,-2.4652E+001,5.0000E+001
2.6695E+001,-2.6676E+001,2.6695E+001,-2.6676E+001,5.6250E+001
2.8451E+001,-2.7341E+001,2.8451E+001,-2.7341E+001,6.2500E+001
3.0593E+001,-2.7830E+001,3.0593E+001,-2.7830E+001,6.8750E+001
3.2710E+001,-2.9427E+001,3.2710E+001,-2.9427E+001,7.5000E+001
3.4150E+001,-3.2392E+001,3.4150E+001,-3.2392E+001,8.1250E+001
3.5470E+001,-3.2878E+001,3.5470E+001,-3.2878E+001,8.7500E+001
3.6513E+001,-3.1722E+001,3.6513E+001,-3.1722E+001,9.3750E+001
4.0252E+001,-2.9872E+001,4.0252E+001,-2.9872E+001,1.0000E+002
4.4221E+001,-3.2512E+001,4.4221E+001,-3.2512E+001,1.0625E+002
4.5089E+001,-3.4902E+001,4.5089E+001,-3.4902E+001,1.1250E+002
4.5935E+001,-3.5707E+001,4.5935E+001,-3.5707E+001,1.1875E+002
4.6808E+001,-3.6528E+001,4.6808E+001,-3.6528E+001,1.2500E+002
4.8589E+001,-3.7338E+001,4.8589E+001,-3.7338E+001,1.3125E+002
5.0585E+001,-3.7944E+001,5.0585E+001,-3.7944E+001,1.3750E+002
5.2020E+001,-3.8594E+001,5.2020E+001,-3.8594E+001,1.4375E+002
5.3224E+001,-3.8737E+001,5.3224E+001,-3.8737E+001,1.5000E+002
5.5439E+001,-3.9624E+001,5.5439E+001,-3.9624E+001,1.5625E+002
5.7078E+001,-4.0226E+001,5.7078E+001,-4.0226E+001,1.6250E+002
5.8349E+001,-4.0473E+001,5.8349E+001,-4.0473E+001,1.6875E+002
5.9674E+001,-4.1535E+001,5.9674E+001,-4.1535E+001,1.7500E+002
6.0915E+001,-4.1797E+001,6.0915E+001,-4.1797E+001,1.8125E+002
6.2315E+001,-4.2473E+001,6.2315E+001,-4.2473E+001,1.8750E+002
6.3467E+001,-4.2975E+001,6.3467E+001,-4.2975E+001,1.9375E+002
6.5324E+001,-4.3192E+001,6.5324E+001,-4.3192E+001,2.0000E+002
6.6882E+001,-4.3579E+001,6.6882E+001,-4.3579E+001,2.0625E+002
6.8325E+001,-4.4203E+001,6.8325E+001,-4.4203E+001,2.1250E+002
6.9808E+001,-4.4775E+001,6.9808E+001,-4.4775E+001,2.1875E+002
7.1146E+001,-4.4591E+001,7.1146E+001,-4.4591E+001,2.2500E+002
7.2957E+001,-4.5208E+001,7.2957E+001,-4.5208E+001,2.3125E+002
7.4851E+001,-4.5882E+001,7.4851E+001,-4.5882E+001,2.3750E+002
7.6192E+001,-4.5998E+001,7.6192E+001,-4.5998E+001,2.4375E+002
7.7299E+001,-4.5896E+001,7.7299E+001,-4.5896E+001,2.5000E+002
7.9536E+001,-4.7197E+001,7.9536E+001,-4.7197E+001,2.5625E+002
8.0935E+001,-4.8847E+001,8.0935E+001,-4.8847E+001,2.6250E+002
8.1691E+001,-4.9317E+001,8.1691E+001,-4.9317E+001,2.6875E+002
8.2422E+001,-4.8904E+001,8.2422E+001,-4.8904E+001,2.7500E+002
8.3787E+001,-4.9497E+001,8.3787E+001,-4.9497E+001,2.8125E+002
8.4937E+001,-4.9861E+001,8.4937E+001,-4.9861E+001,2.8750E+002
8.6020E+001,-4.9409E+001,8.6020E+001,-4.9409E+001,2.9375E+002
8.7081E+001,-4.9394E+001,8.7081E+001,-4.9394E+001,3.0000E+002
```

B2. Leak Damping Data

Damping (Kg/sec) , Frequency(Hz)

```
9.8278E+002,4.3750E+001
1.0506E+003,5.0000E+001
1.1144E+003,5.6250E+001
1.1746E+003,6.2500E+001
1.2320E+003,6.8750E+001
1.2868E+003,7.5000E+001
1.3393E+003,8.1250E+001
1.3899E+003,8.7500E+001
1.4386E+003,9.3750E+001
1.4858E+003,1.0000E+002
1.5316E+003,1.0625E+002
1.5760E+003,1.1250E+002
1.6191E+003,1.1875E+002
1.6612E+003,1.2500E+002
1.7022E+003,1.3125E+002
1.7423E+003,1.3750E+002
1.7814E+003,1.4375E+002
1.8198E+003,1.5000E+002
1.8573E+003,1.5625E+002
1.8941E+003,1.6250E+002
1.9301E+003,1.6875E+002
1.9656E+003,1.7500E+002
2.0004E+003,1.8125E+002
2.0346E+003,1.8750E+002
2.0682E+003,1.9375E+002
2.1013E+003,2.0000E+002
2.1339E+003,2.0625E+002
2.1659E+003,2.1250E+002
2.1976E+003,2.1875E+002
2.2287E+003,2.2500E+002
2.2595E+003,2.3125E+002
2.2898E+003,2.3750E+002
2.3197E+003,2.4375E+002
2.3493E+003,2.5000E+002
2.3785E+003,2.5625E+002
2.4073E+003,2.6250E+002
2.4358E+003,2.6875E+002
2.4640E+003,2.7500E+002
2.4918E+003,2.8125E+002
2.5193E+003,2.8750E+002
2.5466E+003,2.9375E+002
2.5735E+003,3.0000E+002
```